Draft Report

Groundwater Modeling Summary

Haile Gold Mine Project

Environmental Impact Statement

Lancaster County, South Carolina

U. S. Army Corps of Engineers
Charleston District, Regulatory Division

Prepared by
Cardno ENTRIX, Inc.

November 2013

U.S. Army Corps of Engineers
Charleston District

Table of Contents

Page

List of Appendices

Section 4 Appendices

Section 6 Appendices

Section 7 Appendices

List of Tables

Note: All tables are found at the end of the text

Tables-

List of Figures

Note: All figures are found at the end of the text

Figures-

List of Figures (Continued)

Figures-

List of Terms and Acronyms

AMEC model	groundwater model developed by AMEC
APT	aquifer performance test
bls	below land surface
CPS	Coastal Plains Sand
CFR	Code of Federal Regulations
cm/sec	centimeters per second
CWA	Clean Water Act
DA	Department of the Army
depressurization	drawing down or lowering the groundwater level or hydraulic head
ERC	Ecological Resource Consultants, Inc.
EIS	environmental impact statement
ft/day	feet per day
gpm	gallons per minute
Haile	Haile Gold Mine, Inc.
HMC	Haile Mining Company
K	hydraulic conductivity
Kz	hydraulic conductivity (vertical)
Kx	hydraulic conductivity (horizontal)
mgd	million gallons per day
msl	mean sea level
NEPA	National Environmental Policy Act
NRMSE	normalized root mean squared error
NW-SE	northwest-southeast
offsite	outside the proposed Haile Gold Mine Project boundary
onsite	inside the proposed Haile Gold Mine Project boundary
PEST	parameter estimation tool
proposed Project	proposed Haile Gold Mine Project
RMSE	root mean squared error
RQD	rock quality designation
SCM	site conceptual model

the Site	Haile Gold Mine site
SP	self potential
SW-NE	southwest-northeast
SWS model	groundwater model developed by Schlumberger Water Services
SRMSE	scaled root mean squared error
VWP	vibrating wire piezometer
USACE	U.S. Army Corps of Engineers, Charleston District
USGS	U.S. Geological Survey

EXECUTIVE SUMMARY

Haile Gold Mine, Inc. (Haile) has proposed to reactivate mining operations at the Haile Gold Mine site (the Site) near Kershaw, South Carolina. Two previous iterations of groundwater flow models were developed in an effort to predict the extent of potential impacts on the natural hydrologic systems from the proposed Haile Gold Mine Project (the proposed Project). The Schlumberger Water Services model (SWS model) was developed in 2011, and the AMEC model was developed in 2012.

During the early stages of development of the Environmental Impact Study (EIS) for the proposed Project, extensive meetings and discussions involving Haile, the U.S. Army Corps of Engineers, Charleston District (USACE), and other state and federal agencies addressed the groundwater models, their underlying data, their adequacy, their use in predicting groundwater changes from mining, and their subsequent use in determining impacts on groundwater-dependent resources for the impact analysis in the EIS. Ultimately, it was decided that additional data collection and model development would be needed to develop a groundwater model with an appropriate level of accuracy and reliability for the intended uses. The work was performed collaboratively by Haile, the USACE, and other state and federal agencies to expedite data collection and analysis, and to foster consensus on the revisions of the model.

Additional field investigations conducted in 2013 indicated that subsurface hydraulic conditions differed from the previous site conceptual model (SCM) and that the SCM should be revised to more accurately reflect site conditions. The groundwater model was modified to better reflect the revised SCM and to more accurately predict the response of the aquifers to the proposed mine. The purpose of this report is to document the revision and update of the groundwater flow model (the Cardno ENTRIX model) for the Site. This report summarizes the revised understanding of Site conditions, the revised SCM, the revised groundwater model (the Cardno ENTRIX model), and the results of the predictive runs to simulate the potential impacts of the mine on the aquifers. This report provides modeling results of the effects of pumping to dewater the mine area. It does not include predictions of refilling the mine after mine closure.

The hydrology of the Haile Gold Mine site is controlled by the geology of the bedrock and saprolite units surrounding the proposed pits and facility operations. Because of the location of the identified gold deposits in the bedrock units, eight open-pit mines are proposed. The generalized stratigraphy for the Site includes the following principal geologic layers and lithologic units: bedrock, mafic and diabase dikes, saprolite, sap-rock, and Coastal Plains Sand (CPS).

The SCM for the previous groundwater models had assumed that the saprolite and sap-rock units formed a confining unit with low vertical hydraulic conductivity (K_z) that largely isolated the CPS unit from the underlying bedrock unit. However, the SWS model required bedrock hydraulic conductivity (K) values one to two orders of magnitude lower than the field data from slug tests and pumping tests in the bedrock. Consequently, the actual vertical conductivity was estimated to be 10 to 100 times higher than assumed in the SWS model. AMEC constructed several modified versions of the SWS model that used hydraulic conductivity values closer to the

field data but maintained the other aspects of the initial SCM. AMEC had difficulty calibrating their models to the measured field data.

In coordination with Cardno ENTRIX, Haile installed several new piezometers in 2013 to expand the field data array and conducted a pumping test at a new pumping well to better define the three-dimensional response of the aquifer system to pumping. Based on the additional data, a number of revisions were made to the SCM. In general, the saprolitic layers and the upper bedrock were found to have more groundwater flow than previously assumed by SWS and AMEC, and the lower bedrock (lower than approximately 400 feet below land surface [bls]) has lower groundwater flow than previously assumed. Notable findings include:

- The saprolite and sap-rock are not effective confining units to groundwater flow.
- Vertical flow through the saprolite, sap-rock, and upper bedrock is much faster than assumed in the SWS and AMEC models.
- Because they are poor confining units, vertical hydraulic gradients on the Site are much smaller than previously believed. That is, with less ability to confine different aquifer layers, the gradients that indicate differences between those layers are much less than previously assumed.
- The sap-rock layer and upper bedrock layers have substantial horizontal fractures.
- The lower bedrock is generally dense and tight, with occasional horizontal fractures.
- The sap-rock layer is a major flow zone and responsible for most production in wells.
- The hydraulic conductivity of the bedrock is higher at depths shallower than approximately 400 feet bls. At greater depths, the hydraulic conductivity is much lower. Significant horizontal variation in hydraulic conductivity of the bedrock is not apparent above and below approximately 400 feet bls.

The Cardno ENTRIX model was developed to better reflect the actual Site conditions, as expressed in the new SCM of the aquifer system. The revisions to the previous model included:

- Revised calibration points to eliminate data from faulty vibrating wire piezometers (VWPs) and to include new, more accurate piezometers and monitoring wells.
- The southern half of the model domain was eliminated downgradient of the mine where no aquifer data or calibration points were available. This modification did not affect the findings of the model nor the model's ability to predict environmental consequences from proposed mine dewatering.
- A specified flux boundary was added along the new southern boundary of the model to preserve regional groundwater flow.

- Because fewer layers were needed because of the smaller vertical gradients and low vertical confinement, the model layers were reduced from 13 to 7. This reduction better reflects the open communication between the shallow (less than 400 foot bls) groundwater zones.

- The vertical K of the CPS, saprolite, sap-rock, and upper bedrock was increased to reflect field data that indicated greater flow across these units.

- The horizontal K of the sap-rock and upper bedrock was increased.

- The dikes were removed as hydraulic features in the model.

- The recharge to the model was increased.

The revised groundwater model was calibrated to steady-state conditions using the Parameter Estimation (PEST) automated calibration tool. The model was calibrated to both hydraulic head and baseflow to streams. The response of the model to pumping was validated using the data from a 43-day pumping test conducted at PW-09-01 in 2010 and a 7-day bedrock aquifer test conducted in 2013.

Two versions of the Cardno ENTRIX model were created. Both models were calibrated to existing field data. The first model minimized statistical fitting errors; the second model had slightly higher statistical fitting errors but used aquifer parameters that more accurately reflected field data. The second Cardno ENTRIX model that more accurately reflected field data was designated as the primary model and was used for predictive runs to simulate mine impacts. The difference in model variations between the two models was less than 4 percent.

Mine impacts were predicted using the mine operation plan and the mine dewatering files prepared for the previous AMEC model. The calibrated model developed for this study was discretized into 23 stress periods, or periods of varying pumping rate, to simulate the proposed mine plan. The change in groundwater levels of each model layer was determined for the entire model domain for each time step. The maximum simulated areal extent of the cone of depression occurs in Mine Year 12. The 1-foot drawdown contour extends offsite to a maximum distance of approximately 5,000 feet beyond the southern, eastern, and western boundaries of the Site, and approximately 2,000 feet beyond the northern boundary. The cumulative pumping rates gradually increase from approximately 1.2 to 3.4 million gallons per day (mgd) from Mine Years 2 to 4. The average simulated pumping rates between Mine Years 5 through 12 ranged between approximately 2.5 mgd (Year 6) and 3.5 mgd (Year 8), with an average of 3.0 mgd.

The change in baseflow in 16 stream segments was determined for each mine year simulated. Model results suggest that 7 of the 16 reaches that were analyzed show a reduction in baseflow because of proposed dewatering at the site. Reach 16 represents most of the streams onsite; it showed the greatest change, with an overall baseflow reduction of 50 percent. Reaches 4 and 15, which represent the Camp Branch Creek segment north of the Site, showed an average baseflow reduction of 10 percent.

The findings of this report are that the Cardno ENTRIX model is an appropriate numerical representation of the hydrologic system that is adequately calibrated and validated to be used for predictive modeling analysis. The model simulates three-dimensional effects of mine dewatering, and the predictions can be used to support impact assessments. The modeling results for the predictive analysis will form the framework for evaluating mining impacts during the operating mine life and will provide approximate groundwater withdrawal volumes for mine water balance modeling. The modeling results will provide a platform for evaluating the potential effects of groundwater system alteration on groundwater and groundwater-dependent resources. Subsequent modeling efforts by others based on these modeling results will be used to analyze impacts during post-mining, reclamation, and post-closure periods. Considerations regarding use of the model for predictive groundwater analysis are provided herein.

1. INTRODUCTION

1.1 Background

Haile Gold Mine, Inc. (Haile), a subsidiary of Romarco Minerals, Inc., has proposed to reactivate mining operations at the Haile Gold Mine site (the Site), approximately 3 miles north of the town of Kershaw, in Lancaster County, South Carolina (Figure 1-1). Haile would expand the existing mine area for open-pit mining and would construct associated facilities to process ore and produce gold for sale.

On January 11, 2011, the U.S. Army Corps of Engineers, Charleston District (USACE) received from the Applicant an application for a Department of the Army (DA) permit for the proposed mine. The permit requested authorization for placement of fill material in waters of the United States[1] pursuant to Section 404 of the Clean Water Act (CWA). The DA permit application was advertised in a Joint Public Notice (P/N# SAC 1992-24211-4IA) on January 28, 2011. On August 15, 2012, the Applicant submitted a revised DA permit application that included a revised mine plan and proposed a reduction from the originally proposed direct impacts on waters of the United States.

The USACE, as part of its ongoing DA permit review process, is currently developing an Environmental Impact Statement (EIS) in compliance with the National Environmental Policy Act (NEPA) and the USACE's regulations implementing NEPA at 33 Code of Federal Regulations (CFR) 325, Appendix B. The USACE announced its intent to prepare an EIS in the Federal Register on September 29, 2011. As part of its application, Haile submitted the results of geologic, groundwater, and hydrologic evaluations and reports—including two iterations of groundwater models that were designed to be used for mine planning and design, depressurization feasibility, water balance calculations, and permitting activities (AMEC 2012a).

The two previous iterations of groundwater flow models submitted by Haile were developed in an effort to predict the extent of potential impacts on the site-wide hydrogeologic system resulting from the proposed Haile Gold Mine Project (proposed Project). The Schlumberger Water Services model (SWS model) was developed in 2011, and the AMEC model was developed in 2012.

During the early stages of development of the Environmental Impact Study (EIS) for the proposed Project, extensive meetings and discussions involving Haile, the U.S. Army Corps of Engineers, Charleston District (USACE), and other state and federal agencies addressed the groundwater models, their underlying data, their adequacy, their use in predicting groundwater changes from mining, and their subsequent use in determining impacts on groundwater-dependent resources for the impact analysis in the EIS. Ultimately, it was decided that additional

1 The definition of "waters of the United States" can be found at http://water.epa.gov/lawsregs/guidance/wetlands/CWAwaters.cfm.

data collection and model development would be needed to develop a groundwater model with an appropriate level of accuracy and reliability for the intended uses.

Additional field investigations conducted in 2013 indicated that subsurface hydraulic conditions differed from the previous site conceptual model (SCM) and that the SCM should be revised to more accurately reflect site conditions. The groundwater model was modified to better reflect the revised SCM and to more accurately predict the response of the aquifers to the proposed mine.

1.2 Objectives and Report Organization

The primary objective of the work described in this document was to use existing and new information to develop a groundwater model with an appropriate level of accuracy and reliability for the intended uses of the model—particularly predictions of groundwater depressurization (drawdown) to support evaluating the potential effects of groundwater system alteration on groundwater and groundwater-dependent resources in the EIS. The purpose of this report is to document the revision and update of the groundwater flow model to create the Cardno ENTRIX model for the Site.

The report consists of seven chapters, as described below.

- Chapter 2 describes the initial understanding of the site-wide hydrogeologic system, when Haile submitted its DA permit application and groundwater model documentation. Chapter 2 addresses the understanding of the system before the additional field data collection and analysis were completed.

- Chapter 3 discusses the previous groundwater modeling and the SWS and AMEC groundwater models.

- Chapter 4 explains how the existing data were re-evaluated and how new groundwater and other supporting data were collected. The chapter explains how these data were interpreted to revise the SCM in order to redesign the groundwater model of the Site and address previously unresolved issues regarding the three-dimensional distribution of permeability in the bedrock, the vertical permeability of the saprolite and sap-rock units, and the hydraulic gradients between model layers.

- Chapter 5 describes the revisions made to improve and update the SCM based on the additional data collected during 2013 and associated analysis, and the improved understanding of the site-wide hydrogeologic system.

- Chapter 6 addresses development of the Cardno ENTRIX model, including modeling approach, development, calibration, testing, sensitivity analysis, and validation using the new aquifer test results.

- Chapter 7 describes the groundwater hydraulic simulations of mine operations, the general results and conclusions, and considerations in the use of model predictions.

1.3 Physical and Climatic Setting

The Site is located within the Piedmont physiographic province of the southeastern United States (Figure 1-2). The Piedmont physiographic province trends from southwest to northeast and is bounded by the Coastal Plain to the east and the southern Appalachian Mountains to the west. The southeastern Piedmont is characterized by gentle topography and rolling hills, dense networks of stream drainages, and red-brown saprolite soils.

The topography of the Site is the result of dissection by Haile Gold Mine Creek, a perennial stream that flows from northeast to southwest, and its intermittent tributaries that flow into the creek from the southeast and northwest. Slopes in the drainages are gentle to moderate (approximately 9 to 13 percent), and upland slopes above the drainages are gentle to nearly flat (up to 1 percent).

The drainage basin of Haile Gold Mine Creek, the primary drainage feature at the Site, is approximately 4.9 square miles. The basin is comprised of small drainage areas that divide the Site and drain into the southeast-flowing Little Lynches River that is approximately 1 mile southwest of the Site and drains to the Lynches River. The Site contains reclaimed and re-vegetated mine features and is wooded with both natural and logged pine and hardwood forests. Figure 1-3 is an aerial photo of the Site (2009) with the proposed facilities highlighted.

The climate of the Site is subtropical, with hot and humid summers and daytime temperatures averaging between 86 and 92°F. Precipitation is abundant throughout the year; the wettest months are March and July. The driest months are April, October, and November. Winters are mild and wet, and overnight temperatures often are below freezing. Precipitation is usually rainfall. Measurable snowfalls, which occur a few times each winter, usually total less than 6 inches and do not tend to accumulate on the ground.

1.4 Mining History at the Site

Gold was first discovered in 1827 near the Site by Colonel Benjamin Haile, Jr. in the gravels of Ledbetter Creek (now Haile Gold Mine Creek). This led to placer mining and prospecting until 1829, when lode deposits at the Haile-Bumalo pit site were found. Surface pit and underground work continued at the Haile-Bumalo site for many years. In 1837, a five-stamp mill was built on the Site (Newton et al. 1940). Gold production and pyrite-sulfur mining for gun powder continued through the Civil War. In 1882, a 20-stamp mill was constructed and operated continuously until 1908. During this 26-year period, mining operations expanded to include the Blauvelt, Bequelin, New Bequelin, and Chase Hill areas.

From mid-1937 to 1942, larger-scale mining was undertaken on the Site by the Haile Gold Mines Company. The property then consisted of owned or leased land totaling approximately 3,300 acres. Most of the main pits were mined to the 150-foot level, with some underground operations at Haile-Bumalo reaching the 350-foot level (Pardee and Park 1948). The mining operation was shut down by presidential decree (L208) in 1942 because of World War II. By this time, the Haile Mine had produced over $6.4 million worth of gold (in 1940 dollars) (Newton et al. 1940).

From 1951 to the present, the Mineral Mining Company (Kershaw, South Carolina) has mined Mineralite® from open pits around the Haile property. This industrial product is a mixture of sericite, kaolinite, quartz, and feldspar and is used in manufacturing insulators and paint base.

Between 1981 and 1985, the Piedmont Land and Exploration Company (later Piedmont Mining Company) explored the historic Haile Mine and surrounding properties. Piedmont mined the Haile deposits from 1985 to 1992, producing 85,000 ounces of gold from open-pit heap leach operations that processed oxide and transitional ores. New areas mined by Piedmont included the Gault Pit (next to Blauvelt), the 601 pits (by US Highway 601), and the Champion Pit. They also expanded the Chase Hill and Red Hill Pits and combined the Haile-Bumalo zone into one pit. They discovered the Snake deposit sulfide gold resource and mined its oxide cap. Piedmont extracted gold ores from a mineralized trend a mile long, from east to west. In June 1991, Amax signed an agreement to evaluate the site in order to determine whether it should enter a joint venture on the Haile property. During that evaluation period, core drilling that stopped north of the Haile-Bumalo area resulted in the discovery of the new sulfide resource at the Mill zone (under the old 1940s mill). With the satisfactory verification of Piedmont data, Amax and Piedmont entered into a Joint Venture agreement and established the Haile Mining Company (HMC) in May 1992.

From 1992 to 1994, HMC completed a program of exploration/development drilling, property evaluation, mineral resource estimation, and technical report preparation. During this period, the Ledbetter resource zone was discovered under a mine haul road. Because of unfavorable economic conditions at the time, Amax did not proceed with mining but began a reclamation program, still ongoing, to mitigate acid rock drainage conditions at the property. Kinross acquired Amax in 1998, assumed Amax's portion of the Haile joint venture, and later purchased Piedmont's interest.

Haile Gold Mine, Inc., a subsidiary of Romarco Minerals, Inc., acquired the Haile property from Kinross in October 2007 and began an additional drilling program in late 2007. Results of the drilling programs performed by Haile led to development of the Proposed Action being evaluated by the USACE in the EIS.

2. INITIAL SITE UNDERSTANDING

This chapter presents the initial understanding of the site-wide hydrogeologic system prior to additional field data collection and analysis that is described in Chapter 4. It should be noted that the SCM and the previously constructed groundwater models were revised considerably based on the additional data collection and modeling, as discussed in Chapters 5 and 6.

2.1 Geologic Setting

The Site is located in the Carolina Slate Belt within the Carolina terrane. The Carolina terrane consists of the Carolina Slate Belt, the Charlotte Belt, the Kiokee Belt, and the Kings Mountain Belt. This region is interpreted to be formed from a volcanic arc terrane that originated adjacent to the African continent and was later accreted to the North American craton during the mid- to late-Paleozoic (SWS 2010a).

The Site is located along a contact area between metamorphosed volcaniclastic and metamorphosed sedimentary rocks of Late Proterozoic or Early Cambrian age. The metamorphosed volcaniclastic and interbedded epiclastic lithologies are interpreted to be part of the Persimmon Fork Formation, and the metamorphosed sedimentary dominated sequence is associated with the Richtex Formation (SWS 2010a). The Persimmon Fork Formation was derived from volcanic material that contains a continuous range of compositions from basaltic to dacitic and a transitioning geochemical signature from tholeiitic to calc-alkaline (SWS 2010a), suggesting a mature arc setting on an older arc sequence or thinned continental crust. The Carolina terrane was metamorphosed to amphibolite grade conditions in the Charlotte and Kiokee Belts and to greenschist grade within the Carolina Slate Belt (SWS 2010a). The extent of deformation during the Alleghanian orogeny (320 to 270 Mega annum) within the Carolina terrane is localized to mylonitic zones with normal and dextral strike-slip sense of shear (SWS 2010a).

Post-tectonic granites were intruded within the Carolina terrane at the end of the Alleghanian orogeny. These granites have variably developed contact metamorphic aureoles. Alleghanian-aged granites are exposed to the northeast and west of the Site. Intermediate dikes of unknown age and Mesozoic diabase dikes intrude the Carolina terrane. While it is possible to determine that the intermediate dikes were emplaced post-deformation, their ages remain uncertain. The diabase dikes were interpreted to be produced when North America rifted from Africa during the Mesozoic Era.

Deep erosion and extensive weathering developed within the region, likely as a result of near-tropical, humid paleo-environmental conditions; and the intensity of this weathering event likely altered the original composition and textures of the bedrock. The resulting saprolite consists of kaolinite, quartz, and iron oxides. Weathering of the saprolite decreases with depth, and a transition to saprolite-rock (sap-rock) may be interpreted. Regional submersion during the Cretaceous Period resulted in the deposition of kaolinite-bearing sands above the saprolites in the region, leaving a layer of CPS above the saprolitic materials. Later episodes of continental uplift and ocean regression led to continued and ongoing erosion throughout the region, producing the resulting terrain and topography.

The generalized stratigraphy for the Site includes the following principal geologic layers and lithologic units: bedrock, mafic and diabase dikes, saprolite and sap-rock, and Cretaceous-aged CPS. A generalized stratigraphic section is presented in Figure 2-1. A site geology map was developed using exploration drilling data to depict the geologic interpretation at 300 feet below land surface (bls) (Figure 2-2). Hydrogeologic cross sections for the Site are presented in Figures 2-3 through 2-5.

2.1.1 Bedrock

The bedrock stratigraphy of the Site consists of the early Cambrian- to Pre-Cambrian-aged Richtex and Persimmon Fork Formations. Contacts for these metasedimentary and metavolcanic units are not exposed at the surface; therefore, structural conditions are interpreted based on core and drilling data. While interpretations of the age and formation associated with the metavolcanic and metasedimentary units vary, they are consistently interpreted to be part of the Richtex and Persimmon Fork Formations.

The Persimmon Fork and Richtex Formations generally strike northeast-southwest and dip moderately to the northwest at the Site. The Persimmon Fork and the Richtex Formations are known to be complexly folded with local shearing. Metamorphism has obscured some of the primary depositional or volcanic textures, making the exact geologic history difficult to interpret. These units are crosscut by northwest-trending diabase dikes. Saprolite of variable thickness has developed within the crystalline rock. The bedrock and saprolite are overlain by CPS sediments. Figure 2-1 is a generalized stratigraphic section reflecting the bedrock pattern under the CPS and saprolite.

The Richtex Formation at the Site is a metasedimentary unit and considered to be the primary host rock for mineralization. An alternate interpretation, which does not affect the overall Site characterization or impact analysis, is that the metasedimentary unit could be interbedded sediments associated with the upper part of the Persimmon Fork Formation. Regardless, the metasedimentary bedrock unit at the Site may be characterized by thin, alternating rhythmic bands of silt, clay, and sand, which are metamorphosed into a finely banded phyllitic metasiltstone. The metasedimentary bedrock unit is generally well foliated, and crenulation surfaces are common. When strongly mineralized, the metasiltstone is highly silicified and has a pale, steel gray color. The unit often contains strong metamorphic cleavage and is colored light gray, green, tan, or brown. Weathered portions of the unit are generally observed as very light gray or pink. Laminae and bedding often are folded and sometimes are disrupted by passive-slip shearing or dissolution. Mineral composition for this unit is quartz, white mica (up to 50 percent), pyrite (generally less than 10 percent), pyrrhotite, and chlorite—with lesser amounts of biotite and calcite. The unit contains lenses of wackestones, sandstones, and conglomerates that host clasts of volcanic rock or siltstone. The coarser clastic units are poorly sorted and less likely to be as strongly foliated as the siltstones. The coarser grained lithologies of the metasedimentary bedrock unit exhibit cleavage development and flattening of clasts.

The metavolcanic unit of the bedrock is generally associated with the Persimmon Fork Formation and includes felsic volcanic rocks that are rhyodacitic to andesitic in composition. Overprinting of primary textures by alteration, mineralization, metamorphism, and weathering events has made interpretation of this unit difficult. The metavolcanic bedrock unit is generally

buff, gray, white, or green and is distinctive due to the lack of bedding and the presence of feldspar clasts. Albite, quartz, white mica, biotite, and chlorite are the dominant mineralogy; and the unit locally contains calcite and epidote. The unit appears more massive than the adjacent metasediments but has a well developed, penetrative cleavage. This unit is also interpreted to contain variable amounts of sub-rounded albite grains in a quartz-mica matrix. Portions of this unit contain poorly sorted, rounded to angular volcanic clasts.

2.1.2 Mafic and Diabase Dikes

Numerous post-metamorphic lamprophyre dikes intrude the Richtex and Persimmon Fork Formation bedrock units. These dikes intrude the previous units; are medium- to fine-grained with porphyritic, spheroidal, or mottled texture; and are sometimes strongly altered. They occur in the vicinity and adjacent to the diabase dikes. The dikes are gray, buff, tan, and green, and can either trend with the foliation or run perpendicular to it. These dikes are not foliated and are post-tectonic; thus, they may be related to the Alleghanian intrusive activity or the Mesozoic rifting event.

A series of at least 12 nearly parallel diabase dikes has been interpreted from the Site data. The dikes are oriented in a northwest-trending direction across the Site and dip toward the west or are sub-vertical. The diabase dikes are basaltic in composition; medium to fine grained; dense; black, green, or brown in color; and magnetic. They can have talc vein fillings. They cross cut the mafic/lamprophyre dikes and other geologic units, post-dating deposition, alteration, and deformation of the bedrock. The dikes often exhibit abrupt terminations or changes in orientation. The typical thickness of the dikes varies from 15 to 100 feet, although some occur as numerous, closely spaced thin dikes. The largest observed spacing between the dikes is approximately 500 feet. The dikes were emplaced along post-mineralization extensional fractures, thus forming part of a regional dike system that extends across the South Carolina Piedmont. Large amounts of displacement are not seen across the diabase dikes, and some dike trends consist of sub-parallel sets of dikes.

2.1.3 Saprolite and Sap-Rock

A veneer of saprolite overlies the majority of the bedrock at the Site. This kaolin-rich clay material results from the in-place weathering of the bedrock. Typically, the saprolite does not exhibit structure. The material is generally dense, with color varying from white to red-brown. The reported thickness of the saprolite varies from 5 to 150 feet, with an average thickness of 55 feet. Saprolite development is usually thickest in near-surface occurrences of metavolcanic rocks and thinnest in the silicified metasedimentary lithologies.

The contact zone between the saprolite and bedrock is poorly defined; in some cases, weathered material may underlie apparently unweathered, competent bedrock. In some areas, the saprolite grades into sap-rock; sap-rock is more competent and retains the parent rock's relict structure. The sap-rock has experienced weathering or alteration and is suspected to be the primary zone of groundwater flow across the site.

2.1.4 Coastal Plains Sand

The CPS of the Cretaceous-aged Middendorf Formation are present on the Site along topographic highs and appear to have been eroded away in the low-lying areas. The available data suggest that the thickness of the CPS on the Site can be up to 75 feet, generally thinning to the west. The CPS unit has been interpreted to consist of three distinct layers:

- Upper layer (composed of tan-colored, clean, poorly graded quartz sand);
- Middle layer (composed of white to red quartz sand with clay and possibly silt); and
- Lower layer (composed of iron-oxide-cemented coarse gravel and sand [ferricrete], and contains fragments of quartz veins).

The ferricrete in the lower layer of the CPS consists of iron-oxide cemented quartz vein fragments and angular sand clasts. Ferricrete cementation is sometimes sub-parallel to bedding, indicating that it is related to groundwater fluid movement.

2.2 Groundwater Occurrence

The hydrogeologic properties of the geologic units of the Carolina Slate Belt have not been extensively studied, but detailed investigations have been conducted at a few sites. The hydraulic properties of the bedrock aquifer have been measured for mine-related investigations at the Site and at the Brewer and Ridgeway Mines. The Brewer and Ridgeway Mines are within the Carolina Slate Belt; the mines are located approximately 8 miles northeast and approximately 30 miles southwest of the Haile Gold Mine, respectively. Figure 1-2 shows the location of the two mines relative to the Site.

Because the Brewer and Ridgeway Mines are located in similar geologic settings, hydrogeologic properties of the major geologic units should be similar to those of the Site. The proposed mining activity at the Site would be considerably deeper than past mining activities at the Brewer and Ridgeway Mines, and excavation and dewatering would occur in deeper units. The properties of the saprolite and CPS were studied at the Site, but published data on those units for the Brewer and Ridgeway Mines were not available.

Three major hydrogeologic units are present in the Piedmont physiographic province of South Carolina: fractured crystalline bedrock, the overlying saprolite, and recent alluvial deposits including the CPS. The CPS aquifer is unconfined and generally is directly connected to surface water features. The groundwater table generally reflects topography, with depths to groundwater typically less than 30 feet. Where present, the saprolite unit partially separates the CPS aquifer from the underlying bedrock aquifer; however, work on the Site has indicated that the saprolite is not an effective confining unit on the Site. The bedrock aquifer has low intrinsic permeability, and water occurs only in fractures within the rock. The hydraulic conductivity of the three major hydrogeologic units at the three mine sites is summarized in Table 2-1.

2.2.1 Description of the Coastal Plains Sand Unit

The hydraulic properties of the three CPS units are described in the following sections.

2.2.2 Upper Coastal Plains Sand Unit

The initial hydraulic characteristics of the upper CPS at the Site were estimated from laboratory analysis of soil samples collected from test pits that were excavated as part of the previous site geotechnical investigation program conducted by others (Vector Engineering 2008). The hydraulic conductivity values ranged between 0.31 and 2.64 feet per day (ft/day) ($1.1x10^{-4}$ to $9.3x10^{-4}$ centimeters per second [cm/sec]). These values represent the hydraulic conductivity in the vertical direction (Kv) but are from disturbed samples that may not represent field conditions. Depending on the thickness and topography, the upper CPS may be saturated. The upper CPS is saturated in some locations at the Site. No data values were reported for the upper CPS unit at the Brewer or Ridgeway Mines.

2.2.3 Middle Coastal Plains Sand Unit

No hydraulic conductivity tests were reported for the middle CPS unit. Based on its lithology, its hydraulic properties are expected to be similar to those of the upper CPS unit.

2.2.4 Lower Coastal Plains Sand Unit

One hydraulic test was conducted on the lower CPS unit on the Site during previous investigations. The hydraulic conductivity value obtained from the falling head test was 1.73 ft/day ($6.1x10^{-4}$ cm/sec). No data values were reported for the lower CPS unit at the Brewer or Ridgeway Mines.

The bottom of the lower CPS unit is characterized as oxide-cemented coarse gravel and sand. The contact with the underlying saprolite is marked by a layer of red-brown ferricrete containing quartz vein fragments. The observed conditions indicate that rain water likely percolates down through the CPS and travels horizontally along this contact.

There are no hydraulic test data on the ferricrete layer. However, the permeability of this layer appears to be low, as indicated by seeps that occur at the base of the lower CPS unit. The seeps provide baseflow recharge to upper Haile Gold Mine Creek. Fracturing in the ferricrete layer is evident, and this presents a likely pathway for groundwater flow from the lower CPS to the underlying saprolite (Vector Engineering 2008).

2.2.5 Description of the Saprolite Unit

A thick layer of saprolite overlies the bedrock on the majority of the site. Monitoring wells completed within the saprolite on the Site were typically reported to be dry immediately after installation of the well but recharged over a period of 3–6 days (SWS 2011). Hydraulic conductivity values of the saprolite unit from the Site, based on in-situ constant and falling head and slug tests, ranged between 0.17 and 0.3 ft/day ($1.0x10^{-5}$ to $6.0x10^{-5}$ cm/sec), with an average value of 0.10 ft/day ($3.5x10^{-5}$ cm/sec) (SWS 2011). Hydraulic conductivity estimates from

pumping test data on the Site ranged from 0.15 to 1.39 ft/day ($5.3x10^{-5}$ to $4.9x10^{-4}$ cm/sec). No data values were reported for the saprolite unit at the Brewer or Ridgeway Mines.

2.2.6 Description of the Bedrock Aquifer

The water-bearing formation in the region is the Piedmont bedrock, which is collectively referred to in this report as the "bedrock aquifer" or the "crystalline bedrock aquifer." The bedrock aquifer has not been hydraulically characterized to an extent that allows for designation of distinct aquifers within the bedrock.

Groundwater yield from the bedrock system varies greatly, depending on the number of joints and fractures intersected by individual wells, and on the extent of the fracture system. The bedrock aquifer has low intrinsic permeability, and water occurs only in fractures within the rock. The fracture pattern that was mapped prior to mining at the Brewer Mine consisted of at least three major fracture sets crossing the site at orientations of roughly northeast, northwest, and north-northwest, with a nominal spacing of 100 to 300 feet between fractures (Black and Veatch 2010). The fracture pattern has not been systematically studied at the Haile site.

Previous reports suggested that test drilling on the Site indicated that fracturing is common and laterally extensive at the sap-rock/bedrock contact but that fracture density in the deeper, competent bedrock may vary over short distances (SWS 2011). The reports also suggest that field testing indicated the presence of three productive horizons in the bedrock aquifer: a widespread productive horizon between 200 and 400 feet deep due to leaching of mineral residues within fractures in competent rock below the saprolite unit, a second productive zone at depths of 600 to 800 feet that is present in many of the boreholes, and a third productive zone at depths of over 1,000 feet that is present in a few boreholes (SWS 2010b). Other investigations based on exploratory drilling and pumping tests indicated that there is no difference in the distribution of fractures or the hydraulic conductivity of the bedrock aquifer to depths of at least 1,000 feet (AMEC 2012b).

Because of the differing findings between Schlumberger Water Services and AMEC on the heterogeneity of hydraulic conditions in the bedrock, field data—including new piezometers, wells, and aquifer pumping tests—were gathered to better define this characteristic. The hydraulic conductivity of the bedrock on the Site was estimated from falling head slug tests, airlift tests, and pumping test data collected from existing bedrock monitoring wells, new bedrock monitoring wells, and a 10-day aquifer test completed on the test production well (PW-09-01). The hydraulic conductivity from the slug test data ranged from 0.15 to 73.7 ft/day ($5.3x10^{-5}$ cm/s to 0.026 cm/s), with variability being a function of fracture intensity along the completed intervals. The average hydraulic conductivity for the bedrock was estimated at 2.4 ft/day ($8.4x10^{-4}$ cm/s) (SWS 2011). The conductivity of the bedrock was calculated from the PW-09-01 pumping tests conducted in 2012 (AMEC 2012a). These values ranged from 0.60 to 0.85 ft/day ($2.1x10^{-4}$ to $3.0x10^{-4}$ cm/sec), with an average value of 0.68 ft/day ($2.4x10^{-4}$ cm/sec). Section 4.6 discusses the 2013 aquifer performance test.

The hydraulic conductivity of the bedrock aquifer at the Brewer Mine was estimated at 0.0005 to 0.11 ft/day ($1.8x10^{-7}$ to $3.9x10^{-5}$ cm/sec) (SWS 2010b) and was estimated at 1.5 to 6.8 ft/day ($5.3x10^{-4}$ to $2.3x10^{-3}$ cm/sec) at the Ridgeway Mine (SWS 2010b). These values demonstrate

that the hydraulic conductivity of the bedrock aquifer at the Site is consistent with the values at the other two mines, and that the hydraulic properties reported are typical for the bedrock aquifer.

2.3 Groundwater Hydrogeology

2.3.1 Groundwater Recharge and Discharge

Recharge to the groundwater system primarily is derived from rainfall (infiltration of precipitation). The recharge rate to the groundwater system is estimated to be equivalent to between 8 and 10 percent of the annual precipitation (ERC 2012). Regional aquifers discharge to streams in the area and thus provide a source of stream baseflow. The regional aquifers are recharged by infiltration of precipitation.

2.3.2 Groundwater Elevations and Hydraulic Gradients

Depths to groundwater tend to follow topography across the Site, generally shallower in topographically low areas and deeper in topographically high areas. Interpretation of the data suggests a general southwest groundwater flow direction following the drainage. Groundwater in both shallow and bedrock aquifers generally flows in the southwest direction.

Hydraulic gradients indicate pressure difference over a unit length and allow assessment of flow direction. Hydraulic gradients (horizontal or vertical) are calculated by taking the change in water elevation/pressure at two locations divided by the distance between the two locations. Groundwater flows from locations with high elevation/pressure to locations with lower elevation/pressure.

Vertical groundwater gradients prior to the start of the extended-duration pumping test were calculated for each of the multi-completion piezometers on the Site. Gradient results suggest a general downward gradient for most of the Site, indicating flow from the upper bedrock down to the lower bedrock. It has been speculated that the vertical gradients may have resulted from dewatering of the deep bedrock unit caused by air rotary drilling at locations on the Site during the period of measurement (SWS 2011).

Upward gradients were observed in two piezometers completed in the saprolite and in one piezometer completed in the bedrock zone. These piezometers generally are located along the valley, suggesting possible upland recharge influence and the occurrence of groundwater discharge along Haile Gold Mine Creek.

Horizontal gradients were calculated from the groundwater contour map that was based on earlier data and is presented in Figure 2-6. Horizontal gradients ranged from 0.0097 ft/ft in the Upper Haile Gold Mine Creek area, to 0.0206 ft/ft in the Lower Haile Gold Mine Creek area, to 0.0356 ft/ft in the North Fork Haile Gold Mine Creek area, and 0.0542 ft/ft in the south portion of the Site toward Ledbetter Reservoir. These gradients are typical for moderately permeable aquifer units.

2.3.3 Site-Scale Structures

The effects of site-scale structures on groundwater flow were evaluated using available hydrogeologic and geologic data and data obtained from the pumping tests completed to date. The primary observed structures are the diabase dikes. The chief mine geologist reports that no evidence of major faulting has been observed on the Site during exploration activities. Lamprophyre and diabase dikes are the dominant structural features at the Site. The lamprophyre dikes generally strike north-northwest, dipping 80 to 90 degrees. These dikes occur in the vicinity and adjacent to the diabase dikes. The 12 (approximate) regional diabase dikes are oriented approximately N20W to N40W and dip steeply to the west or near vertical.

These dikes have the potential to form groundwater flow barriers locally within the bedrock aquifer. Due to weathering of the dikes near the surface, however, it is unlikely that groundwater flow is impacted by the dikes near ground surface (within the saprolite and sap-rock zone). Anecdotal evidence from exploration drilling activities suggests that the bedrock in margins around the dikes has been altered to a brittle state and has increased fracture intensity. The fracture intensity adjacent to the dikes may create conduits of flow along the strike of the feature where fractured; where fracturing is less pronounced, the dikes may restrict groundwater flow (Golder Associates 2010). The consistent orientation of the dikes suggests that they were formed in response to a consistent structural stress field that post-dates the mineralization. This provides anecdotal evidence that a preferential orientation of fractures on the site could increase the bulk hydraulic conductivity of the bedrock aquifer and create preferential flow directions that would affect groundwater migration and the shape of the cone of depression from pumping.

2.3.4 Connectivity of Major Hydrogeologic Units

The initial site conceptual model was that a shallow groundwater system at the Site consisted of the CPS and the saprolite units that outcropped at the surface. This shallow system was assumed to be hydraulically separated from the deeper bedrock groundwater flow system. The shallow groundwater system, recharged solely by precipitation, flowed laterally toward the Little Lynches River. However, the 2013 Site investigation data suggests that the shallow and deep aquifers are, in fact, hydraulically connected.

2.3.4.1 Compartmentalization

It has been hypothesized that (1) localized compartmentalization of the groundwater system may be present because of the presence of the diabase dikes; (2) the fracture intensity adjacent to the dikes will drive the local groundwater flow direction and magnitude around them; and (3) the dikes may create conduits of flow along the strike of the feature where fractured; where fracturing is less pronounced, the dikes may restrict groundwater flow. This hypothesis was based on previous investigations (Golder Associates 2010). An additional aquifer testing was conducted as part of this investigation to test the concept of compartmentalization of the groundwater system at the Site (refer to Chapter 4).

2.3.4.2 Groundwater/Surface Water Interactions

Groundwater generally flows from recharge in the upland areas of a watershed to discharge areas that are typically surface waterbodies. Recharge is believed to occur over much of the Site, with discharge occurring to Haile Gold Mine Creek. Discharge to surface water provides the baseflow to Haile Gold Mine Creek and other surrounding creeks. The distribution of discharge to Haile Gold Mine Creek is variable along the run of the creek and is controlled by the hydraulic conductivity of the aquifer and its connection to surface waters. The magnitude of groundwater discharge from the bedrock aquifer to the surface water system is partially determined by the continuity of the saprolite layer and the vertical hydraulic conductivity of the unit. The thickness of the saprolite unit is known to vary across the Site and is absent in some locations.

3. PREVIOUS GROUNDWATER MODELING

3.1 Introduction

As noted, two previous iterations of groundwater flow models were developed in an effort to predict the extent of potential impacts on the site-wide hydrogeologic system from the proposed Project. The SWS model was developed in 2011. This model was later modified by AMEC in June 2012 to reflect the additional data collected at the Site between July 2010 and March 2012. The model construction and simulation details are described in earlier reports, including Schlumberger Water Services (2011) and AMEC (2012a, 2012b). Table 3-1 presents a general comparison of the two models. A brief description of these models is provided below.

3.2 SWS Model

Schlumberger Water Services developed one steady-state model and two transient models. The steady-state model was developed to simulate average pre-mining groundwater heads. The first transient model was developed as part of the model validation process and simulated a 42-day aquifer performance test (APT) conducted at the Site. The second transient model (which is not described in this report) was developed to simulate potential mining impacts caused by dewatering of the mine pits. Hydrogeologic data that were available through October 2010 were utilized in the model development process. The model was developed using the finite difference code MODFLOW-SURFACT, with the use of Visual MODFLOW as a pre- and post-processing graphical user interface.

3.2.1 Grid Setup

The model grid consisted of 13 layers. The upper two layers represented the CPS unit, Layers 3 and 4 represented the saprolite unit, Layers 5 and 6 represented the sap-rock unit, and Layers 7 through 13 represented the bedrock units. The model layer thickness and hydrogeologic units assigned to the model layers are summarized in Table 3-2.

The modeled area was spatially discretized into a rectangular finite-difference grid of 630,032 active cells covering approximately 432 square miles. The grid was oriented 36 degrees in the northwest direction. The cell spacing ranged from 100 feet by 100 feet in the Project area to 1,000 feet by 1,000 feet at the model boundary.

3.2.2 Boundary Conditions

The outer model boundary cells on three sides of the model (northwest, northeast, and southwest) were simulated as “no-flow” cells. Constant head boundary conditions were specified at the southeast model boundary to represent fluxes leaving the model to regional aquifers downgradient from the site. The constant head cells were assigned a value of 220 feet mean sea level (msl) for Layer 1 and 175 feet msl for Layers 2 to 13. Flow at this boundary was assumed to be mostly lateral. The difference between the elevation of the constant head boundaries between Layer 1 and the rest of the model appears to have been an attempt to create a strong vertical gradient in the model that was observed in the VWP data. These data subsequently were found to be unreliable.

The model simulated rivers and drains as internal boundaries using the MODFLOW River Package and Drain Package, respectively. The River Package, which was used to simulate inflow and outflow from rivers and streams, was developed based on elevations obtained from a U.S. Geological Survey (USGS) digital elevation model. The Drain Package was used to simulate seepages occurring along the contact of the CPS and saprolite. The heads in the drain cells were specified 1.0 feet above the bottom of the model cell.

3.2.3 Aquifer Properties

The hydraulic coefficients used in the model to represent the major hydrogeologic units at the Site are summarized in Table 3-3. The model assumed a relatively low hydraulic conductivity value of 0.02 ft/day and 0.002 ft/day for the sap-rock and bedrock unit, respectively. The anisotropy ratio (horizontal hydraulic conductivity: vertical hydraulic conductivity) was generally assumed to be 1:1, except for the CPS unit. The anisotropy ratio of the CPS unit was assumed to be 10:1.

3.2.4 Calibration

The model initially was calibrated to average pre-mining groundwater levels (steady-state calibration) and then was validated against data collected during a 42-day APT conducted at the Site between August 16 and September 28, 2010 (transient calibration). The steady-state calibration process involved matching the model results to 45 average hydraulic head observations onsite and six observations offsite. Water level responses observed in 18 observation wells during the 42-day APT were used for transient calibration. Note that the models were calibrated only to groundwater heads and not to groundwater fluxes to surface water features.

The reported scaled root mean squared error (SRMSE) for the steady state calibration was 3.4 percent, which is typically an indication of good calibration. The transient model was unable to adequately match the water level changes observed in many of the observation wells used in the APT.

3.2.5 Model Limitations

The SWS model had several limitations and areas of concern. The calibrated model used hydraulic conductivity values in the bedrock that were much lower than the field values measured by slug tests and pumping test, which could potentially underestimate the radial extent of drawdown and depressurization pumping. The calibrated model was not able to adequately match the vertical gradients measured in the bedrock. The observed heads from several of the VWPs were shifted by tens of feet during the validation process in an attempt to validate the response of the model in order to match the observed response from the pumping test.

Thirteen of 51 calibration targets used in the steady-state calibration, and 16 of 18 calibration targets used in transient calibration were based on water level data collected using VWPs, which later were found to be unreliable based on results from field studies conducted subsequent to the SWS modeling study.

3.3 AMEC Model

AMEC revised the model developed by Schlumberger Water Services based on additional groundwater head and aquifer test data collected at the Site between July 2010 and March 2012. The AMEC model was completed in June 2012. The model used the same finite difference code used by Schlumberger Water Services (MODFLOW-SURFACT); however, the graphical user interface was changed from Visual MODFLOW to Groundwater Vistas. All major assumptions of the original SWS model, including assumptions pertaining to grid structure, model boundaries, recharge, and evapotranspiration, were retained in the AMEC model. Major changes made by AMEC are discussed below.

3.3.1 Simulation of Streams/Rivers

The original SWS model used the MODFLOW River Package to simulate the flows in the stream and river network distributed across the model domain. AMEC used the MODFLOW Stream Package to simulate streams in the vicinity of the mine pits. No modifications were made to the river cells located beyond the Site.

The MODFLOW River Package estimates flow of groundwater into or out of the aquifer based on the head/stage assigned to the river cell and the conductance specified for the river bed material. The stage in the river cell is compared to the simulated head in the aquifer. If the simulated aquifer head is higher than the assigned river stage, the river cell removes water from the aquifer and vice versa if the simulated head is lower than the assigned river stage. For models simulating mine dewatering, this approach potentially poses a problem because the river cells will act as unlimited source of recharge to the groundwater system (through losing river cells) when the aquifer heads are drawn below the river stage. The MODFLOW Stream Package calculates groundwater flow into or out of the aquifer in a similar manner to the MODFLOW River Package (based on stage and conductance term). The main difference between the packages is that the Stream Package has the capability of computing stage as well as flow for a surface waterbody and has the capability of routing the surface flows from upstream segments to downstream segments.

The Stream Package in the AMEC model was set up similarly to the SWS model's River Package. The inputs used in the AMEC Stream Package, which included stage elevation, streambed elevation, and conductance, are the same as used in the SWS model's River Package. Using this approach, the streams essentially were simulated as "sources," contributing water to the aquifer when the simulated aquifer head was below the stream stage. The functionality within the Stream Package that allows computations of stream stages was not used. The Stream Package was further modified for the Cardno ENTRIX model, as described in Chapter 6.

3.3.2 Model Layer Thickness

The SWS model specified varying top and bottom elevations for Layers 1 through 9 and constant elevations for Layers 10 through 13. The AMEC model retained the topographic variations of the near-surface layers but specified a constant thickness for Layers 6 through 13.

3.3.3 Model Parameters

The SWS model calibration process placed greater emphasis on matching the static water levels than on the results from APTs performed at the Site. The model achieved calibration by using bedrock hydraulic conductivity values that were one or two orders of magnitude lower than those suggested by the Site APTs. AMEC carried out a series of model runs in an attempt to develop models that represented a balance between results from Site testing while simulating the observed hydraulic heads. This approach resulted in three models that were referred to as the "Lower Bound Model," "Base Case Model," and "Upper Bound Model." The major differences between the three models were the hydraulic conductivity values specified in the bedrock layers. It was determined that the most representative hydraulic conductivity value based on Site data was 0.3 ft/day. The Lower Bound Model used horizontal hydraulic conductivity values of 0.002 ft/day for all the bedrock layers (Layers 7 to 13). This model was similar to the SWS steady-state model except for the minor grid refinement and use of the Stream Package. The Base Case Model used horizontal hydraulic conductivity values of 0.3 ft/day for the upper bedrock layers (Layers 7 to 9), and 0.03 ft/day for the lower bedrock layers (Layers 10 to 13). Additional high-conductivity zones arbitrarily were added in the model along the Lower Haile Gold Mine Creek and around well PW-09-01, the pumping well for the APT, to yield acceptable calibration. The Base Case Model also simulated the dikes outside the PW-09-01 APT area as low-conductivity zones (0.03 ft/day). The Upper Bound Model used the geometric mean of hydraulic conductivity estimates from the 2012 aquifer test (0.3 ft/day for upper bedrock units and 0.03 ft/day for lower bedrock units) and placed greater emphasis on field data and less emphasis on calibration statistics. Dikes were not exclusively modeled in the Upper Bound Model; however, the high-conductivity zones around well PW-09-01 were retained from the Base Case Model.

3.3.4 Calibration

The AMEC steady-state model was calibrated to the same hydraulic head data sets used to calibrate the SWS model. AMEC also developed a transient model to simulate the 42-day APT on well PW-09-01. The reported root mean squared errors (RMSEs) for the Lower Bound, Base Case, and Upper Bound steady-state models were 12.8 feet, 16.5 feet, and 19 feet, respectively. The reported scaled standard deviation values for the Lower Bound, Base Case, and Upper Bound steady-state models were 3.3 percent, 4.2 percent, and 4.8 percent, respectively. The transient validation results suggested that the model could not reasonably match the APT responses in many of the observation wells.

3.3.5 Model Limitations

Twenty five percent of the head targets used for the steady-state model calibration were recorded using VWPs that were later proved to be faulty. The majority of the transient validation matches also were based on water levels measured using VWPs. Furthermore, AMEC used high-conductivity zones around the pumping well for the transient validation. This zonation scheme was applied mainly around the pumping well and artificially created preferential flow paths between the pumping well and the monitoring wells. Also absent in the calibration and validation process for the AMEC model was the incorporation of surface flow data within and outside of the Site boundary.

4. ADDITIONAL DATA COLLECTION AND ANALYSIS

The calibration efforts of the previous groundwater models described in SWS (2011) and AMEC (2012a, 2012b) pointed to the need for additional information to better define Site conditions and test the validity of the head data from the VWPs. The analysis involved re-evaluating some existing site data and collecting new data to refine the SCM. The work was performed collaboratively by Haile, the USACE, Cardno ENTRIX, and state and federal agencies to expedite data collections and analysis, and to foster consensus on the revisions of the SCM.

The previous analysis of data from the Site left unresolved issues regarding the three-dimensional distribution of permeability in the bedrock, the vertical permeability of the saprolite and sap-rock units, and the hydraulic gradients between model layers. Existing data were re-examined and new data were collected to resolve these questions. Existing bedrock core data were re-evaluated to extract information on the distribution of fractures that could be used to estimate the distribution and density of fractures in the bedrock and form opinions on the distribution of permeable features in the bedrock. Existing boreholes were pumped to obtain estimates of the hydraulic conductivity of the aquifer units the wells were completed in. New piezometer nests were installed adjacent to the VWPs to confirm the head data provided by the VWPs. A second pumping well was installed with nested piezometers to act as multi-level monitoring wells for an additional APT. Additional shallow monitoring wells were installed to provide better definition of the shallow water table on the Site.

A limiting factor for model calibration was the absence of long periods of groundwater elevation data and surface water flow data from the Site and surrounding areas. The available data were re-evaluated to construct estimates of average values that could be used as calibration targets. Water level data from existing private wells near the proposed pit areas were used to better define the water levels in the aquifer and to provide additional calibration targets. Historical groundwater level data were examined to determine the natural range in water levels and to construct a set of water levels that more accurately represented average Site conditions for model calibration. Surface water flow data within the Site boundary and from adjacent basins were reviewed to establish reasonable estimates of flow for the stream reaches to serve as calibration targets.

This chapter provides a description of how the existing data were re-evaluated, how new data were collected, and how these data were interpreted to revise the SCM in order to redesign the groundwater model of the Site.

4.1 Single-Well Tests of Existing Boreholes

Single-well pumping tests were conducted on 17 existing boreholes on the Site to obtain additional data on the distribution of hydraulic conductivity of the aquifer system. Figure 4-1 shows the locations of the boreholes. Well specifications and curve fits are included in Appendix 4a.

Some wells were completed as piezometers, and some had long open-hole completions in bedrock. The pumping rate was limited by the diameter of the boreholes and the size of the pumping equipment that could be used; the rates ranged from 0.25 to 20 gallons per minute

(gpm). The wells generally were pumped for a period of a few hours while water level and pumping rate were recorded as a function of time. The data were analyzed using the AQTESOLV pumping test interpretation software to calculate the hydraulic conductivity of the aquifer and estimate the boundary conditions based on the type curve response. All of the wells were fit to a Theis solution for confined aquifers and then fit to the type curve that relatively closely fit the time-drawdown plot. In general, the Theis curve fits were poor, indicating that the aquifers were not fully confined systems. Most of the wells followed leaky artesian type curves (Hantush), with one well (BMW-5) plotting as a dual porosity- (Moench) type aquifer. The leaky artesian curve fits indicate that the fracture density in the bedrock aquifer around those wells is high enough to cause the aquifer to behave as a porous media equivalent. It also indicates that the bedrock receives vertical leakance through the overlying units and that the saprolite and sap-rock units are not effective confining units. The dual porosity curve fit at BMW-5 indicates that the bedrock aquifer in that location is dominated by a planar fracture and the fracture density is not high enough to cause the aquifer to behave as a porous media. The fact that most of the pumping test curves for the single-well and multi-well pumping tests fit the Hantush type curves, and that only a few wells fit fracture porosity type curves, indicates that the bedrock can be treated as an equivalent porous media on a Site-level scale. Small areas of the Site probably are dominated by one or more major fractures and do not behave as a porous media. However, these areas appear to be isolated and will not affect the performance of the model at the Site scale.

4.2 Vulcan Block Model

Observations of the fracture density in the bedrock were not collected during drilling of the existing borehole and piezometers on the Site. Consequently, it was not possible to determine the vertical and lateral distribution of hydraulically significant fractures in the bedrock and sap-rock aquifers. Haile geologists did conduct a detailed analysis of the bedrock core collected from the Site. As part of this analysis, they recorded the rock quality designation (RQD) of the bedrock and entered the data into a Vulcan three-dimensional mine model. RQD is typically used to determine the competency of rock for tunneling or excavations and is more focused on the structural load-bearing capacity of the rock. The competency of the rock is scored by noting the frequency and size of fractures per unit length of the core (intactness). The analysis does not distinguish between open, hydraulically connected fractures and clay-filled fractures that are less hydraulically connected. As such, RQD is not a direct measure of the hydraulic conductivity of the bedrock. However, zones of fractured rock are more likely to have higher hydraulic conductivity than dense unfractured rock. With this in mind, the RQD data were reviewed to determine whether discernible patterns in the distribution of fractures in the bedrock could be related to lateral or vertical trends in hydraulic conductivity in the bedrock aquifer.

Haile prepared a Vulcan block model of the geology and related data. The block model covers a 2,000-acre area within a rectangular domain, with an east-west orientation that includes the proposed pits and their immediate surroundings. The vertical extent of the model ranges from ground surface, to approximately 520 feet above msl, and to approximately 720 feet below msl. The model was developed using a comprehensive drill-hole database that was not provided as part of the model transmittal to the USACE.

The Vulcan block model was developed from the primary geologic features and lithology of the mine site identified from exploration drilling (the comprehensive drill-hole database) and other sources. CPS sediments and a saprolite rock layer exist near the topographic surface in the block model, while metavolcanic and metasedimentary rock make up the majority of the subsurface consolidated rock. Diabase dikes, with a northwest-to-southeast orientation perpendicular to strike, also are included in the model.

The Haile block model included "grade" or variable estimations for the RQD and air lift variables. The block model grade or variable estimation process is similar to modeling a quality variable to a grid surface but involves a three-dimensional estimation where blocks in the model become populated based on the variable data set collected from core samples plus the chosen estimation criteria and mathematical algorithm. Each physical block of the block model can contain the information for multiple variables (e.g., geologic, quality, or property). Haile used ordinary kriging to estimate the RQD and air lift variables in the block model.

Horizontal slices of the block model were developed at selected elevations to show the geology and RQD information proximate to the proposed mine pit locations. The following geologic units were depicted in the Vulcan model: CPS, saprolite, metavolcanic rock, metasedimentary rock, and diabase dikes. RQD data were depicted in 25-percent intervals: less than 25 percent equaled poor intactness, 25 to 50 percent equaled somewhat poor intactness, and 50 to100 percent equaled fair intactness.

Cross-section profiles were prepared to depict the stratigraphy and RQD information across the Site. The cross sections were oriented in line with the estimated regional strike and dip directions and include the exploration drill hole traces. Figure 4-2 is an example of the cross sections generated from the Vulcan model. The other cross sections and location map are included in Appendix 4b.

As part of the additional data collection and analysis effort, the Vulcan model was processed to map the distribution of RQD data in three dimensions. The results suggested that the bedrock above approximately 400 feet had lower RQD values and was more fractured and probably more permeable than the deeper bedrock. There were no other indications for lateral zonation of bedrock K based on RQD data.

4.3 Installation of Additional Production Wells and Piezometers

Ten nested piezometers were installed in early 2013 to provide supplemental hydrogeologic information. Three piezometer nests consisting of a total of 15 wells were drilled into the bedrock adjacent to the VWPs to verify the head measurements from the VWPs. Seven additional piezometers were drilled to support a second pumping well (PW-13-01) APT on the site for the 2013 bedrock aquifer test. PZ-4, PZ-5, PZ-6, and PZ-7 were completed in the CPS and saprolite layers. PZ8, PZ-9, and PZ-10 were completed in the bedrock. Figure 4-3 shows the locations of the piezometers. The well specifications, construction logs, and geophysical logs for the production well are included in Appendix 4c.

Geophysical well logs were run on all of the piezometers drilled in 2013 to obtain additional information on the fracture density in the aquifer. The logging suite consisted of self potential

(SP), gamma, borehole fluid conductivity, caliper, acoustic borehole imager, and heat pulse flow meter logs. The caliper and acoustic borehole imager logs indicated that the sap-rock and bedrock units above approximately 300 to 400 feet had higher concentrations of horizontal fractures than the deeper bedrock. The bedrock below approximately 300 to 400 feet generally contained only a few fractures in most wells. The well specifications, construction logs, and geophysical logs are included in Appendix 4d.

4.4 Evaluation of Data from Vibrating Wire Piezometers

The previous head measurements from a number of VWPs indicated that head differences of up to 50 feet were present in sensors completed in the bedrock at different depths in the same piezometer nests. The data indicated that strong vertical gradients existed in the bedrock aquifer, which implied recharge at different elevations and strong vertical confinement of distinct zones in the aquifer. The previous groundwater models were not able to reproduce these gradients, calling into question the validity of the field data. To resolve the issue, the three piezometer nests discussed above, consisting of a total of 15 wells, were drilled into the bedrock adjacent to the VWPs.

Water levels were monitored for several weeks following installation of the piezometers, and the water level data were compared to the data from the adjacent VWPs. Figure 4-4 shows the water levels for one of the piezometer/VWP pairs that illustrate the magnitude of variance observed. All of the head values for the VWP wells tested in 2013 were off by several feet to several tens of feet, indicating that the VWP data were not reliable and could not be used for calibration purposes. The water level plots for all six of the VWP/piezometer pairs are presented in Appendix 4e.

Attempts were made to shift the data from the VWPs vertically and laterally on plots of the water level data from the piezometers to determine whether some consistent offset value could be used to correct the VWP data or whether the relative change of water levels was consistent with the piezometer data and could still be used for model validation. Figure 4-5 shows an example of the variance between the VWP and piezometer data after the data have been shifted. VWP-10-03D appears to correlate fairly well with the data from PZ-13-02D for a few weeks in February and early March, but the water levels diverged by more than 10 feet in April. VWP-09-05D did not produce a compelling correlation with the water level data in PZ-13-01D, indicating that the data were not reliable. An additional well (VWP-10-02C) seems to have produced a reasonable correlation with PZ-13-03S, but only for part of the period of record. The data from the deeper point in the VWP nest (VWP-10-02D) did not correlate with PZ-13-03D. PZ-13-02S responded in an erratic manner, indicating a transducer problem that made the data unreliable. Only two of the six points showed any reasonable correlation in relative changes in water level over periods of several weeks of monitoring. However, the apparent correlation applied only after the WVP data were shifted by approximately 7 to 8 feet. The shifted water level plots are provided in Appendix 4f.

Based on these observations, it was concluded that (1) the data from the VWPs were not reliable; and (2) due to the poor results of the three locations tested, it was unlikely that additional testing would show that many more of the VWPs were reliable. The cause of the unreliable data from the VWPs was not determined.

The conclusion that the VWP data were not reliable and should be disregarded for model calibration resulted in the loss of 43 percent of all water level monitoring points on the Site, including 57 percent of the bedrock wells and 75 percent of the saprolite wells. Furthermore, it was concluded that the strong vertical gradients were a relic of the VWP data and were not actually present on the site. Previous calibration efforts that relied on this head data also were called into question, and the previous modeling efforts were discounted as a result. The loss of the VWP data also reduced the historical groundwater level data available for the Site that was needed for calibration of a groundwater model.

4.5 Additional Shallow Monitoring Wells and Off-Site Private Wells

During the 2013 aquifer investigation, it was determined that additional water level data from the shallow CPS and saprolite units onsite would be beneficial for calibration of the Cardno ENTRIX model and for long-term monitoring. It also was determined that data from the area around the Site would improve the calibration of the model. Haile elected to install 15 shallow monitoring wells in the CPS unit to fill in gaps in the existing coverage. Haile also provided water level and construction data from 24 private water wells adjacent to the Site for use as calibration targets. Tables 4-1 and 4-2 summarize the location and construction of the new shallow monitoring wells and the private wells used for calibration, respectively. The construction logs of the new shallow wells are included in Appendix 4g.

4.6 Additional Aquifer Performance Test

An additional APT, referred to as the "2013 bedrock aquifer test," was undertaken in March 2013 to supplement the data from two previous tests run at PW-09-01. A new pumping well (PW-13-01) was drilled in the southwest portion of the Site near wells PZ4 through PZ10, to conduct the test. The value of the data from the two previous APTs was degraded when the VWP data were found to be invalid. The loss of the VWP data left only one valid monitoring point in the radius of influence from the previous tests. An additional test with reliable monitoring points was deemed necessary to measure how the various layers of the aquifer responded to pumping stresses. The PW-09-01 site was deemed to be unfavorable for additional testing due to limitations that prevented installation of additional monitoring wells in the CPS unit. The location of PW-13-01 was selected for its proximity to a diabase dike and the presence of the CPS unit adjacent to the well. The new location allowed piezometers to be installed in the CPS, saprolite, and bedrock units. The new location also allowed a bedrock piezometer to be placed on the other side of a diabase dike from the pumping well to directly measure the degree to which the dike formed a hydraulic barrier in the aquifer.

PW-09-01 was constructed with slotted casing in the sap-rock layer and open borehole in the bedrock. This made it difficult to determine how much of the well production came from the bedrock versus the sap-rock. PW-13-01 was cased through the sap-rock layer to test production from the bedrock only. A suite of geophysical well logs consisting of SP, gamma, borehole fluid conductivity, caliper, acoustic borehole imager, and heat pulse flow meter logs was conducted on the well. The construction logs and geophysical well logs are included in Appendix 4h. A step drawdown test was conducted on PZ-13-01 to determine a sustainable pumping rate. The production of the well was found to drop quickly when a zone of horizontal fractures at a depth

of between 190 and 210 feet was dewatered. The sustainable rate was set at 50 gpm to avoid dewatering the fracture. Figure 4-6 shows locations of the piezometers constructed for the test.

Table 4-3 provides additional information on the pumping well and piezometers. The construction logs for the piezometers and PW-13-01 are included in Appendix 4c. The plot of the step drawdown test is included in Appendix 4h.

The geologic descriptions and construction details have been compiled into a graphical representation along two lines of cross section: southwest-northeast (SW-NE) (Figure 4-7) and northwest-southeast (NW-SE) (Figure 4-8). These cross sections provide a graphical representation of the distribution of the various lithologic units encountered during drilling. The presence of the cross-cutting diabase dikes was previously mapped by Haile using magnetometer survey techniques and was verified by site-specific coring conducted immediately prior to installation of the well and piezometers. A conceptual representation of this dike is shown in Figure 4-8, the localized SW-NE cross section between PZ-13-09 and PZ-13-10.

PW-13-01 was pumped at 50 gpm for 7 days. Wells PZ-13-04 and PZ-13-06, completed in the CPS unit, went dry within 2 days of pumping, indicating that the saprolite was not an effective confining unit in the area. The drawdown data in the monitoring wells did not show any barrier boundary responses that would be expected if the dikes were hydraulic barriers in the aquifer. As Figure 4.3 illustrates, two of the bedrock piezometers (PZ-13-08 and PZ-13-09) were located on the same side of the dikes as the pumping well, while one piezometer (PZ-13-10) was located on the other side of the dike. The well on the opposite side of the dike did not exhibit a delay or diminishment in the degree of drawdown as would be expected if the dike was a hydraulic barrier. This was consistent with the results of the 43-day test on PW-09-01, which did not show any impact on the measured drawdown in the aquifer based on the presence of the dikes in that portion of the site. Because there was no indication of a hydraulic barrier from the diabase dike, it was evident that the dikes are fractured to the degree that they do not hinder groundwater flow in the bedrock.

The drawdown data were analyzed using the AQTESOLV pumping test analysis software. PZ-13-04, PZ-13-05, and PZ-13-06 fit the Theis confined solution, although it is likely that PZ-13-04 and PZ-13-06 may have followed an unconfined drawdown curve if they had not gone dry a short time after pumping started. PZ-13-05 and PZ-13-07 were deeper and were completed in the saprolite. These wells did not go dry and followed an unconfined aquifer solution, indicating that the saprolite behaved more like an aquifer than a confining unit. PZ-13-08, PZ-13-09, and PZ13-10 were completed in the bedrock. PZ-13-09 and PZ-13-10 followed a leaky artesian curve, indicating that the bedrock aquifer was acting as a porous media and receiving significant vertical flow through the saprolite and sap-rock units. PZ-13-08 followed a Moench dual porosity fracture flow drawdown curve, indicating that small portions of the bedrock are probably dominated by discrete fractures and locally behave as a fracture flow aquifer.

4.7 Streamflow Data

A description of how streamflow data were developed from site data, stream models, and analog basins is provided in Section 6.3.3.1.

4.8 Analysis of Groundwater Data for Seasonal/Annual Variability

An analysis of groundwater level data was conducted to determine seasonal and annual variability in the data for the purpose of finding calibration targets. A description of how the groundwater head data were developed for model calibration is provided in Section 6.3.3.

5. REVISION OF THE SITE CONCEPTUAL MODEL

The SCM developed in the previous modeling studies (SWS 2011; AMEC 2012a, 2012b) was updated by building on historical knowledge and information presented in earlier reports, and by incorporating results from the field investigation conducted in early 2013. The previous Site testing results and SCM are summarized in Chapter 2. This chapter describes the major revisions to the previously developed SCM.

5.1 Changes to the Site Conceptual Model Based on Findings from the 2013 Site Investigation

As described in Chapter 4, the 7-day bedrock aquifer test was conducted in March 2013 to determine the hydraulic coefficients of the bedrock and understand the vertical flow and hydraulic connection between the shallow aquifers (CPS and saprolite) and the deeper bedrock aquifer. A suite of wells was installed in the CPS, saprolite, and the bedrock for testing. The bedrock aquifer well PW-13-01 was pumped at a rate of 50 gpm, and the changes in water levels were monitored in the bedrock and the shallow aquifer wells (refer to Chapter 4 for details of this test).

Data from the 2013 bedrock aquifer test and from the adjacent monitoring wells produced results that necessitated revision of the previously developed SCM. The following findings from the Site investigation were incorporated into the revised SCM:

- The VWP data that were an essential part of previous modeling efforts, including development of the previous SCM, were found to be unreliable—with errors up to 50 feet. There was no distinct trend in the offsets in measured water levels between the confirmatory monitor wells and VWPs.

- Substantial vertical leakage through the saprolite unit occurred during the 2013 bedrock aquifer test, drawing down the water level in the CPS unit by up to 7 feet within the first 48 hours of the test.

- The sap-rock layer and upper bedrock layers had substantial horizontal fractures.

- The sap-rock layer was a major flow zone responsible for most production in both pumping wells on the Site.

- Dikes in the area did not appear to compartmentalize or otherwise restrict groundwater flow across the dike during the aquifer test.

- The hydraulic conductivity of the upper portion of the bedrock was determined to be higher than previously estimated.

- The lower bedrock was generally dense and tight, with occasional horizontal fractures.

- The field data suggested no apparent discernible differences in hydraulic conductivity between the metavolcanic and metasedimentary bedrock.

- Vertical hydraulic gradients were found to be small within the bedrock aquifer based on review of nested bedrock piezometers.

5.2 Geologic Cross Sections of the Site

Geologic cross sections of the site were developed to further characterize the SCM. Geologic cross sections and well boring logs from previous hydrogeologic characterization reports (Woodward-Clyde Consultants 1994; SWS 2010b; AMEC 2012a, 2012b) were reviewed. The Schlumberger Water Services (2011) cross sections were created from the Vulcan model and were based on detailed geologic data gathered during exploration drilling and geologic mapping. Although this dataset was not originally intended to provide a basis for hydrogeologic characterization, the dataset contained a higher density of areal coverage than the relatively sparse lithologic records contained in the available boring logs of monitor wells reviewed. In addition, the Vulcan model rock types had been standardized whereas the nomenclature and rock type descriptions used in the monitor well boring logs were inconsistent.

As described in Chapter 4, the geologic descriptions and construction details prepared by Haile geologists of eight boreholes were compiled into a graphical representation along two lines of cross section. The cross sections are oriented SW-NE and NW-SE, as shown in Figures 4-7 and 4-8, respectively. These cross sections provide a graphical representation of the distribution of the various lithologic units encountered during drilling. The presence of the cross-cutting diabase dikes was previously mapped by Haile using magnetometer survey techniques and was verified by site-specific coring conducted immediately prior to installation of the well and piezometers. A conceptual representation of this dike is shown on the localized SW-NE cross section (Figure 4-7).

Figure 5-1 is a cross-sectional representation of the updated SCM that is based on previously documented surficial geology, drill core and boring logs, and interpreted structural relationships. The discontinuous CPS unit is the youngest strata represented and is thickest in the upland portions of the Site. The underlying saprolite and sap-rock units are represented as underlying the entire Site. The two primary bedrock units represented are metavolcanic and metasediment; for the groundwater flow model, these units are effectively undifferentiated hydraulically. The cross-cutting diabase and alkaline dikes are represented in roughly the configurations that have been shown by previous geologic maps. The extent of penetration of these dikes into the sap-rock and saprolite is unknown; however, the alkaline dikes are believed to be younger than the diabase dikes and are older than the CPS.

5.3 Implications of the Revised Site Conceptual Model for Groundwater Modeling

The model design used the updated SCM based on additional information gathered during the 2013 site testing. The aquifer parameters that were changed in the model design include vertical hydraulic conductivity of the shallow aquifers (CPS, saprolite, and sap-rock) and horizontal hydraulic conductivity of the uppermost bedrock layers. Overall, the vertical conductivity values of the shallow aquifers and the horizontal hydraulic conductivity of the upper bedrock were increased in the numerical model by up to an order of magnitude.

6. GROUNDWATER MODEL REVISIONS

6.1 Introduction

The Cardno ENTRIX model, a three-dimensional numerical groundwater flow model, was developed to simulate potential impacts on the site-wide hydrogeologic system from proposed dewatering (depressurization) of the mine pits. The SWS and AMEC models previously developed for the Site were used as a base model for the Cardno ENTRIX model. Details of the construction of the base model were previously documented (SWS 2011; AMEC 2012a, 2012b). The following is a description of how the base model was modified to meet the objectives of this study.

6.2 Modeling Approach

The model was structurally modified to match the SCM design described in Chapter 5. The modifications included changing the grid discretization, boundary conditions, and aquifer parameters. Next, the modified steady-state model was calibrated to average heads observed in 76 wells and baseflow estimated in 16 stream/river reaches within the model domain. The calibration parameters included hydraulic conductivity (horizontal and vertical) of all model layers and groundwater recharge. The calibrated steady-state model was then used to develop two transient models; one transient model was developed to validate the 40-day APT conducted by Schlumberger Water Services in 2010 (i.e., after excluding water level elevation data from VWPs), and the second transient model was developed to validate the 7-day 2013 bedrock aquifer test. The validation process involved adjusting the storage coefficients of the model layers until the model satisfactorily simulated the APT. The final step involved using the calibrated and validated model to simulate potential impacts caused by pit depressurization at the Site for a 14-year period.

6.3 Steady-State Model

Cardno ENTRIX modified the finite difference grid structure, boundary conditions, and aquifer properties of the base model as described below.

6.3.1 Model Discretization

The base model, which consisted of 13 layers and spatially covered approximately 432 square miles, was modified by reducing the number of layers to seven and the area of active model domain to approximately 310 square miles. Approximately 122 square miles of the southern portion of the base model was removed. The rationale for reducing the size of the model was to remove portions that did not affect the mine impact predictions, as described in Section 6.3.2. Figure 6-1 is a map showing the model domain.

The primary hydrogeologic units represented by the base model included the CPS (Layers 1 and 2), saprolite (Layers 3 and 4), sap-rock (Layers 5 and 6), and bedrock (Layers 7 through 13). The base model was designed to reproduce apparently high vertical gradients in the aquifer system; these were based on erroneous head data from the VWPs. After it was established that the actual gradients were much smaller, the number of vertical layers needed to reproduce the vertical flow in the system was reduced to seven. Layer 1 represented the CPS, Layer 2

represented the saprolite, Layer 3 represented the sap-rock, and Layers 4 through 7 represented the bedrock. The overall thickness of the primary hydrogeological units used in the model was not modified from the base model. This was accomplished by combining into one layer the multiple model layers used in the base model to represent a single hydrogeological unit. The restructuring of model layers resulted in faster model runs and yielded better calibration results compared to the 13-layer base model. No changes were made to the horizontal cell spacing in the model. The cell spacing in the center of the model at the Site was 100 feet by 100 feet; the cell spacing incrementally increased toward the boundaries of the model. Table 6-1 compares the model layering and hydrogeological representation between the AMEC and Cardno ENTRIX models.

6.3.2 Boundary Conditions

For the base model, the external boundaries at the eastern, western, and northern sides of the model were simulated using "no-flow" cells. The external boundary at the southern side was represented by "constant head" cells, which simulated flow leaving the model domain to the regional aquifers. For this study, the eastern, western, and northern boundary conditions were retained from the base model. However, the southern boundary cells were simulated as a "specified flux" boundary. The simulated groundwater heads in the base model were analyzed and flux values assigned based on the gradient across the selected southern model boundary cells. The location of the southern boundary cells was determined by trial-and-error runs of the base model. This process effectively truncated the model at approximately 5 miles south of the Site boundary by deactivating cells further south. It was noted that the hydrologic features simulated south of the revised southern boundary had minimal effects on model results within the core of the model. The conversion of the southern boundary from constant head to specified flux removed a potential for infinite sources of groundwater recharge that can be created by constant head cells under transient simulations.

The internal boundary conditions of the base model were revised utilizing MODFLOW River, Stream, and Drain Packages to represent rivers, streams, and drains, respectively. The same packages were used in the Cardno ENTRIX model; however, the river and stream cells were modified so that the stage elevations specified in each of these cells were set equal to their respective bottom elevation values. This step was necessary to prevent the river and stream cells from acting as infinite water "sources" that fed the aquifer underneath for the mine depressurization simulations (discussed in Chapter 7). The base model used drain cells to simulate the discharge from seeps and springs occurring along the contact between the CPS and the saprolite. The drain cells were specified with a head value that was 1.0 foot above the bottom of the model cell. These drain cells were removed from the Cardno ENTRIX model because the referenced seepage was not physically validated in the field. Figure 6-1 displays the model boundary conditions.

6.3.3 Model Calibration

Model calibration is the process of adjusting model parameters to produce simulated heads and fluxes that match field-measured values within a pre-established acceptable range of error. In this study, the steady-state model was calibrated to average water levels observed in 76 wells and estimated baseflow rates in 16 reaches within the model domain. The 76 "target" wells used in

the calibration process were subdivided into the following four categories: (1) recently installed shallow wells; (2) domestic wells; (3) onsite test wells; and (4) a USGS well. The recently installed shallow wells included 14 wells that were installed in the CPS and saprolite units in June 2013 (note that 15 wells were actually installed but one of them was consistently dry). At the time of revised model development, weekly water levels were available from these wells for July 2013. Average water levels observed in these wells in July were used as calibration targets. Water level data from 20 domestic wells also were available for calibration. Available data indicated that water levels were recorded only twice in these wells; once in January 2012 and once in June 2013. The average of these values was used for calibration. In addition, water level data from 43 onsite test wells were used for calibration. Of these 43 wells, water level data for a 4-year period from 2008 to 2012 were recorded for 29 wells, and one reading was measured in April 2013 for the remaining 14 wells. For the 29 wells with historical data, typically only from two to four water level readings were available for each year during the period of record, and these measurements were taken sporadically. The average water levels observed during this period in the 29 wells with historical data were used as calibration targets. Water levels in these wells fluctuated during the period of record; most of the variance was between 3.7 feet (one standard deviation) and 7.4 feet (two standard deviations) of the average water levels (Figure 6-2). Water levels in the remaining 14 onsite test wells were measured only once in April 2013, and these values also were included as calibration targets. Finally, the average water level reported in one offsite USGS well also was included as a calibration target. Table 6-2 shows the selected head targets.

6.3.3.1 Baseflow/Flux Targets

A set of 16 baseflow targets was developed for the calibration process. Initially, the river and stream cells in the model were grouped into 14 reaches, and Ecological Resource Consultants, Inc. (ERC) was requested to provide baseflow estimates for these reaches. Later in the calibration process, the Camp Branch Creek that was represented as one reach in ERC analysis was split into two, and an additional reach was added—for a total of 16 reaches. ERC used available streamflow data from the nearby USGS Hanging Rock Creek gage (USGS # 02131472) and performed a basin proration analysis to estimate baseflow at the selected locations. The basin proration analysis involved calculating the ratio between the drainage area of a selected reach and the drainage area of the Hanging Rock Creek gage, and applying this ratio of the estimated baseflow at Hanging Rock Creek to obtain baseflow at the selected reach. ERC delineated the drainage areas of selected reaches based on a USGS topographical map with 5-foot contour intervals of Kershaw and Lancaster Counties, South Carolina. Figure 6-3 shows the reach designations for the river and stream cells. Table 6.3 provides baseflow targets for the 16 reaches used in model calibration. Appendix 6a provides details of the ERC analysis.

6.3.3.2 Calibration Process

The model was calibrated using PEST, a state-of-the-art automated parameter estimation software developed by Watermark Numerical Computing (2002). Specifically, the pilot point functionality in PEST was used to create a heterogeneous hydraulic conductivity field, but at the same time using the regularization routines to impose a level of homogeneity. This combination allowed for much greater flexibility in deriving a unique solution given the limited amount of field data. Using this method, initial values and upper and lower bounds of horizontal and

vertical hydraulic conductivities were specified. Bounds of minimum and maximum values constrain the numerical values that PEST can estimate for each pilot point. Approximately 400 pilot points were used to create horizontal and vertical hydraulic conductivity fields. Two zones of recharge, one representing groundwater recharge to the CPS and the other representing groundwater recharge to the saprolite, also were included as calibration parameters. The head targets were assigned a weight of 1.0, and the baseflow targets were assigned a weight of 0.5. During the calibration process, the horizontal and vertical hydraulic conductivities and the recharge values were allowed to fluctuate within the designated bounds. The upper and lower bounds considered for the parameters in the calibration process were based on Site testing data and are provided in Table 6-4. The estimated conductivity and recharge values that minimized the difference in simulated and observed heads and fluxes were determined by the model, and were specified in each cell.

Numerous PEST simulations were carried out with different ranges of model parameters. The primary goal in the calibration process was to obtain a calibration with a normalized root mean squared error (NRMSE) of less than 10 percent while maintaining an acceptable range in hydraulic coefficient values. In theory, an NRMSE value of less than 10 percent represents an acceptable calibration. The NRSME is calculated using the following equation:

$$\text{NRMSE} = \text{RMS} / (X_{obs})_{max} - (X_{obs})_{min}, \text{ where RMS} = (1/n \sum_{i=1}^{n} R_i)^{0.5}$$

RMS = root mean squared error, R_i = calibration residual (difference between calculated results and the observed results) and X_{obs} = observed head.

Two PEST runs produced acceptable calibration statistics. The calibration statistics for the first run (designated as Model 1) demonstrated that the model-predicted water levels agreed closely with observed water levels. The NRMSE for the head calibration was 4.5 percent and flux calibration was 5.4 percent, which are indications of a good calibration. The calibration statistics for the second run (designated as Model 2) also yielded an acceptable NRMSE of 8.0 percent for head targets and 3.1 percent for flux targets. Because the parameterization of hydraulic coefficients achieved in Model 2 was more comparable with previous site testing results, Model 2 was selected for impact analyses (discussed in Chapter 7). Calibration statistics for Models 1 and 2 are provided in Table 6-5.

It is important to understand that all numerical models are approximations that represent a series of compromises between numerical solutions and field observations. Groundwater studies almost never have as many field observations as desired, and there are always margins of error in field observations that cannot be fully quantified. Therefore, basing the selection of groundwater models solely on the minimization of statistical error measurements ignores the limitations of the data density and sampling errors. While Model 2 did not provide the lowest statistical error terms for the head data, it was chosen as the most representative model because it more accurately reflected the field measurements from the Site.

6.3.3.3 Calibrated Parameters

The recharge values that yielded the best model in Model 2 were 8.2 inches/year for the saprolite unit and 12.1 inches/year for the CPS unit. The calibrated hydraulic conductivity values for each model cell for Models 1 and 2 are shown in Appendix 6b. Table 6-6 provides a summary of calibrated hydraulic coefficients. Figure 6-4 shows water table elevations simulated by Model 2.

6.3.4 Sensitivity Analysis

The purpose of the sensitivity analysis was to quantify the uncertainty in the model caused by uncertainty in estimates of calibrated aquifer parameters. The sensitivity of selected model parameters was analyzed, including horizontal and vertical hydraulic conductivities and groundwater recharge to model output, as indicated in the sum of squared residuals.

The most sensitive model parameters are horizontal conductivities in Layers 4 and 5 (which represent the upper bedrock) and vertical hydraulic conductivities in Layers 2 and 3 (which represent saprolite and sap-rock, respectively). Changes to these parameters within the range of observed variability influence the simulated head values at target locations, simulated stream fluxes, and the general groundwater flow within the model domain. Groundwater recharge into the CPS unit also was noted to be sensitive. The remaining parameters analyzed were noted to be relatively less sensitive to model output. Figures 6-5, 6-6, and 6-7 show the results of the sensitivity analysis.

6.3.5 Groundwater Budget

Mass balance summaries showing the groundwater budget components are provided in Table 6-7. As shown in the table, the percentage discrepancy of groundwater flow in and out of the model is 1.0E-4 percent, indicating that the flows from and to "sources" and "sinks" simulated in the model balance each other and do not result in artificial mounding or depletion of the simulated heads or fluxes. No unexplained sources or sinks of water were needed to balance the model.

6.4 Model Validation: Transient Effects Evaluated with Pumping Test Data

The calibrated steady-state model was validated to drawdown data collected during two APTs conducted onsite. The first APT was the 40-day test conducted by Schlumberger Water Services in well PW-09-01 in August 2010. The second APT was the 7-day bedrock aquifer test conducted in March 2013.

6.4.1 Transient Validation 1 (40-Day APT)

The steady-state models were validated by simulating the decline in groundwater heads observed during the 40-day APT when well PW-09-01 was pumped at a rate of 195 gpm. The validation process involved adjusting the storage coefficients of the seven model layers until the simulated decline in heads due to groundwater withdrawals reasonably matched the change in heads observed during the test. The previous transient validation efforts by Schlumberger Water Services and AMEC used groundwater heads observed in 18 monitor wells during this APT using VWPs. The VWPs were installed at depths ranging from elevations 380 feet above msl to

500 feet below msl. As explained in Chapter 4, results from all but one of these VWPs were found to be unreliable and were discarded for validation of the model. For the transient validation, only groundwater head data from observation well BMW-09-04 were used. The pumping well PW-09-01 was simulated using the MODFLOW Well Package. Well cells were placed in Layer 3 (sap-rock) and Layer 4 (bedrock). Seventy percent of the pumpage was simulated from Layer 3, and 30 percent of the pumpage was simulated from Layer 4. This split in pumpage rate was considered reasonable because previous well testing data indicated that the production capacity of wells that are open to both the sap-rock and bedrock were between approximately three and four times higher than the production capacity of wells that were open only to the bedrock. One model observation well was placed in Layer 3 to simulate head responses in Well BMW-09-04.

The calibration hydrograph of well BMW-09-04 is provided in Appendix 6c. Table 6-5 shows the calibrated storage coefficients. The shape and magnitude of the simulated hydrograph match reasonably well with the shape and magnitude of the observed water level decline during the 40-day APT. The calibration hydrograph suggests that the observed head gradually declined from 470 to 385 feet above msl, while the simulated head gradually declined from 470 to 412 feet above msl. This provides assurance that the model can be used as a useful predictive tool, capable of simulating the magnitude and rate of expansion of the cone of depression caused by Site depressurization within the aquifers of interest.

6.4.2 Transient Validation 2 (7-Day APT)

The steady-state model was validated a second time by simulating the 7-day 2013 bedrock aquifer test. Seven observation wells were used for this APT: two wells each completed in the CPS and saprolite units, and three wells completed in the bedrock. The pumping well PW-13-01 was simulated to withdraw 50 gpm from the bedrock (Layer 4).

Calibration hydrographs of the seven observation wells are provided in Appendix 6c. The adequacy of transient calibration was evaluated by comparing the shape and magnitude of simulated and observed drawdown in the observation wells. In general, the shape of the modeled hydrograph response curves matched the observed shape of drawdown curves in the monitoring wells. The simulated drawdown in the CPS and saprolite unit was less than the observed drawdown by approximately 3 feet (PZ-13-04) to approximately 12 feet (PZ-13-07). The simulated drawdown in two of the bedrock observation wells (PZ-13-08 and PZ-13-10) was higher than the observed drawdown by an average of approximately 20 feet. The magnitude difference between observed versus simulated drawdown in bedrock well PZ-13-09 was minimal. Overall, the model was able to adequately simulate the water level responses observed in the field during the 7-day 2013 bedrock aquifer test, providing additional confidence in using the model as a predictive tool to simulate potential impacts from mine depressurization (discussed in Chapter 7).

7. GROUNDWATER HYDRAULIC SIMULATIONS OF MINE OPERATIONS

The Cardno ENTRIX model—calibrated and validated as discussed in Chapter 6—was used to run predictive simulations of mine pit depressurization during mining operations in order to evaluate potential changes in groundwater heads and flows. The objectives of the simulations were to evaluate (1) groundwater withdrawal rates required to depressurize groundwater levels to desired depths during pit dewatering; (2) the extent and magnitude of resulting groundwater drawdowns; and (3) the subsequent effects on near0surface groundwater regimes and stream baseflow in selected river and stream reaches.

This chapter describes the groundwater hydraulic simulations of mine operations, including how the mine operations were simulated, generally presents the results, and discusses considerations in the use of model predictions. Detailed results and interpretation of the simulations are not provided here, as they are to be used in further environmental analyses in support of the EIS and will be presented elsewhere. Note that the simulations reported here include only Mine Years 0 through 14. The effects of the cessation of mine drawdown and groundwater rebound and of pit refilling are not part of this simulation. The results of these post-mining simulations are to be developed by Haile.

7.1 Mine Operation Plan Summary

The mine operation plan has been presented in earlier reports, including *Depressurization and Dewatering Study* (SWS 2011) and *Addendum to Depressurization and Dewatering Feasibility Study* (AMEC 2012a). For ease of review, the proposed mine plan also is presented in Appendix 7a of this report. Drawings in the plan show the layout of facilities and the sequence of pit topography during Mine Years 0 through 14. Note that the first mining year is referred to as “Year 0” because it represents a pre-production year planned primarily for stripping of the overburden, although some depressurization would occur.

7.2 Model Setup

The calibrated model developed for the depressurization study was discretized into 23 stress periods to simulate the proposed mine plan during mining, similar to the structure for the previous modeling efforts. Stress periods 1 through 12 simulated Mine Years 0 through 2 with 90-day time periods; stress periods 13 through 22 simulated Mine Years 3 through 12; and stress period 23 simulated a 2-year period after the active mining period, when dewatering is proposed to meet water supply demands at the site. Table 7-1 provides a breakdown of the model stress periods.

The MODFLOW Drain Package was used to simulate proposed dewatering at the site. The representation of the mine plan using the Drain Package was developed solely by Haile for the purpose of this analysis; it was used with minor modifications, as described below. The desired groundwater levels in the open pits during depressurization/dewatering were specified in the Drain Package, and the package calculated the quantity of water that needed to be removed from the drain cells to achieve the desired groundwater levels. The Drain Package was imported into the calibrated model. The layer numbers in the drain cells were revised to account for restructuring the grid from 13 layers (in the original model) to 7 layers. No other changes were

made to the Drain Package, including no changes to the specified stage—the key input parameter that determines how much groundwater flows into the open pits during dewatering. Generally, the drain elevations were set to be 5 feet below the desired mine pit elevations.

7.3 Groundwater Withdrawal Rates

The mass balance summary generated by the model was reviewed after each stress period to determine the groundwater withdrawal (pumping) rates required to suppress groundwater levels to depths specified in the mine plan. The pumping rates were calculated as the average volume of water exiting through the drain cells per day. Figure 7-1 shows the simulated cumulative groundwater withdrawal rates during Mine Years 0 through 14.

Results indicated that the cumulative initial rates during the pre-production year (Year 0) ranged from approximately 0.75 to 1.75 mgd, with an average of approximately 1.0 mgd. The cumulative pumping rates gradually increased from approximately 1.2 to 3.4 mgd from Mine Years 2 to 4. The average simulated pumping rates from Mine Years 5 through 12 ranged from approximately 2.5 mgd (Year 6) to 3.5 mgd (Year 8), with an average of 3.0 mgd.

7.4 Simulated Drawdown of Groundwater Levels

Groundwater drawdowns resulting from dewatering were calculated by comparing the simulated water table elevation during mining to the average pre-mining water table elevation generated by the calibrated steady-state model (discussed in Chapter 6). The simulated drawdown isopleth maps for Mine Years 0 to 12 and Year 14 are provided in Appendix 7b.

Based on model results, the maximum simulated drawdown during Mine Years 0 to 2 occurred in the Mill Zone Pit and ranged from 144 feet (Year 0) to 410 feet (Year 2). During Mine Years 3 to 6, the maximum simulated drawdown occurred in the Snake Pit and ranged from 373 feet (Year 3) to 553 feet (Year 4). During the last 6 years of mining (from Mine Years 7 to 12), the maximum simulated drawdown occurred in the Ledbetter Pit and ranged from 506 feet (Year 7) to 842 feet (Year 12). The maximum drawdown simulated for each mine year is tabulated in Table 7-2.

The simulated areal extent of the cone of depression was reviewed for each mine year. For the purpose of this study, the outer boundary of the cone of depression was set to be the simulated 1-foot drawdown contour. The rationale for selecting the 1-foot drawdown contour is discussed in Section 7.6. The maximum simulated areal extent of the cone of depression occurred in Mine Year 14 and simulated drawdowns are shown in Figure 7-2. The 1-foot drawdown contour extends offsite to a maximum distance of approximately 2 miles beyond the southern and eastern edges of the pits, approximately 1.5 miles beyond the western edges of the pits, and approximately 3 miles beyond the northern edges of the pits.

7.5 Simulated Stream Baseflow Impacts

To assess potential impacts on the groundwater contribution to streams and rivers (baseflow), the simulated baseflow during Mine Years 0 through 14 was compared to the pre-mining baseflow simulated by the calibrated steady-state model. The 16 river and stream reaches used in the baseflow calibration process of the steady-state model (Figure 6-3) were selected for the

baseflow analysis. Table 7-3 shows the simulated baseflow into the selected reaches during Mine Years 0 to 14. Figure 7-3 is a bar chart showing percentage reduction in simulated baseflow to the selected reaches.

Model results suggested that 7 of the 16 reaches that were analyzed show a reduction in baseflow due to proposed dewatering at the site. Reach 16, which represents most of the streams onsite, showed the highest impact, with an overall baseflow reduction of 50 percent. Reaches 4 and 15, representing the Camp Branch Creek segment north of the Site, showed an average baseflow reduction of 10 percent. The other affected reaches include Reaches 5 and 13 (which showed an overall baseflow reduction of 4 percent) and Reaches 3 and 8 (which showed an overall baseflow reduction of 1 percent). Note that Reaches 13 and 8 are located immediately south of the Site, Reach 3 is located immediately north of the Site, and Reach 5 is located on the Site (Figure 6-3).

7.6 Summary of Findings and Considerations in the Use of Model Predictions

The Cardno ENTRIX model is shown in this report to be an appropriate numerical representation of the hydrogeologic system of the Haile Gold Mine Site and is adequately calibrated and validated to be used for predictive modeling analysis. The model simulates three-dimensional effects of mine dewatering, and the predictions can be used to support impact assessments. The model and predictive analysis reported here will form the framework for evaluating mining impacts during the operating mine life. They are suitable for approximating groundwater withdrawal volumes for mine water balance modeling, and for other environmental analyses to evaluate potential effects on groundwater-dependent resources. Subsequent modeling efforts by others based on these modeling results will be used to analyze impacts during reclamation and post-closure periods.

Groundwater models such as MODFLOW SURFACT (the code used for model simulations) have limitations in simulating flow through the unsaturated zone, including meteorological parameters such as air temperature, humidity, solar radiation, and vegetation types. These limits are common to many groundwater modeling exercises and, if recognized and considered, do not unduly hamper their value. The strength of the model developed here is not in predicting absolute groundwater elevations and flows, but rather in estimating the relative change that would be expected to occur as a result of groundwater depressurization. These relative changes will be most relied upon during impact analyses.

The range of groundwater heads simulated in the model is approximately 225 feet. The RMSE of the steady-state model suggested that the model was capable of generating a hydraulic head field with an approximate accuracy of 92 percent. Furthermore, the model represents a regional area of over 300 square miles, and the smallest finite difference grid size is 100 feet by 100 feet. Consequently, measureable groundwater level changes are unlikely to be detected in areas of predicted groundwater drawdowns of less than 1.0 foot.

Two models were developed through this work. The second model (the Cardno ENTRIX model) was selected as the best representation of the hydrogeologic system of the Haile Gold Mine Site. Although the first model minimized the estimated model errors, basing the selection of the best groundwater model solely on the minimization of statistical error measurements ignores limitations of data density and sampling errors. The second model did not provide the lowest

statistical error terms for the head data; however, it was chosen as the most representative model because it more accurately reflected the field measurements from the Site.

The models developed herein relied heavily on the hydrogeologic data collected in the Project area. PEST primarily was used to determine the hydraulic coefficients that best calibrated the model to groundwater heads observed onsite. Although baseflow targets were included in the calibration process, the baseflow values were less accurate estimates. Because limited offsite data were available, the model is likely to be more reliable in predicting onsite groundwater heads and fluxes than predicting offsite heads and fluxes. The range of hydraulic conductivity values derived in the PEST calibration process was based on available Site testing data. Finally, it is important to recognize that the groundwater model predictions are likely to be most accurate in areas of the model domain closest to calibration points and less accurate the farther the distance from calibration points.

The model used the Drain Package to simulate mine dewatering. This was necessary because Haile has not provided a mine dewatering plan; the mine operation was simulated as specified by Haile. While this may be reasonable representation of the pit depressurization process for modeling purposes, simulating depressurization of the groundwater would be more realistic if it were based on a mine dewatering system. A mine dewatering system would generally consist of a series of wells at some distance from the pit walls, the operation of which would draw groundwater down to a depth greater than the target elevation, dewatering to depths below the bottom of the pits. Because the wells would be farther away from the pit, a greater drawdown cone of depression would likely result.

The magnitude of the difference between the drain cell approximation and the dewatering well system would depend on the design of the dewatering system and could not be fully quantified until a dewatering system was designed and tested. While not quantifiable without specific well locations, the magnitude of the difference between the predictions made using the Drain Package and a mine dewatering system generally would be expected to be greatest near the dewatering wells and smallest farther from the wells. The difference in drawdown predicted by these two approaches near the edge of the cone of depression likely would be less than the predictive abilities of the current model. Haile is contemplating a Monitoring and Management Plan that could be used to quantify variances between predicted and actual drawdowns onsite.

8. REFERENCES

AMEC. 2012a. Haile Gold Mine. Addendum to the Depressurization and Dewatering Feasibility Study. June.

AMEC. 2012b. Haile Gold Mine. Addendum to the Baseline Hydrologic Characterization Report. June.

Ecological Resource Consultants, Inc. 2012. Haile Gold Mine Site-Wide Water Balance Report. Prepared from AMEC Environment and Infrastructure. June.

ERC. See Ecological Resource Consultants, Inc.

Golder Associates. 2010. Draft Report on Feasibility Level Pit Slope Evaluation. March.

Newton, E.D., D.B. Gregg, and M. McHenry. 1940. Operation of the Haile Gold Mine, Kershaw, S.C. (U.S. Bureau of Mines Information Circular 7111.)

Pardee, J.R. and C.F. Park, Jr. 1948. Gold Deposits of the Southern Piedmont. (U.S. Geological Survey Professional Paper 213.) 156 pp.

Schlumberger Water Services. 2010a. Haile Gold Mine. Baseline Hydrologic Characterization Report. November.

Schlumberger Water Services. 2010b. Haile Gold Mine. Depressurization and Dewatering Feasibility Study. December.

Schlumberger Water Services. 2011. Haile Gold Mine, Depressurization Study. Volume 1. January.

SWS. See Schlumberger Water Services.

Vector Engineering, Inc. 2008. Haile Gold Project Tailing Storage Facility. Waste Rock Storage Facility and Plant Site Preliminary Geotechnical Investigations Report. May.

Watermark Numerical Computing. 2002. PEST Model Independent Parameter Estimation Manual. Fourth edition. http://www2.epa.gov/sites/production/files/documents/PESTMAN.PDF.

Woodward-Clyde Consultants. 1994. Hydrologic Characterization Progress Report Haile Mining Co., Kershaw, South Carolina. February.

Tables

Table 2-1 Hydraulic Conductivity of the Major Hydrogeologic Units at the Haile, Ridgeway, and Brewer Mines (ft/day)

Aquifer	Haile Site (SWS 2010b)	Haile Site (AMEC 2012b)	Haile Site (WWC 1994)	Brewer Mine (B&V 2010)	Ridgeway Mine (ABC 1987)
Upper CPS	0.31–2.64	ND	ND	ND	ND
Lower CPS	1.73	ND	ND	ND	ND
Saprolite	0.03–0.17	0.15–1.39	ND	ND	ND
Bedrock	0.15–5.1	0.17–73.7	0.1–4.4	0.11–0.0005	1.53–6.8

ABC = Adrian Brown Consultants
B&V = Black and Veatch
CPS = Coastal Plains Sand
ND = no data
SWS = Schlumberger Water Services
WWC = Woodward-Clyde Consultants

Table 3-1 General Comparison of Previously Developed Models for the Site

Model Designation for This Report	Model Author	Year Completed	Number of Layers	Reported RMSE of Residual (ft)	General Model Summary
SWS model	SWS	2011	13	12.8	SWS model: 13 layers, saprolite and sap layer assumed to be strong confining units, uniform hydraulic properties in bedrock, bedrock K value much lower than field data, could not reproduce vertical gradients in bedrock.
Base Case model	AMEC	2012	13	12.8	The Base Case model: representing a balance between simulating the observed steepness of the bedrock hydraulic gradient while retaining hydraulic conductivity estimates from the aquifer tests,
Lower Bound model	AMEC	2012	13	16.5	The Lower Bound model using assumptions of lower regional bedrock hydraulic conductivity that places greater emphasis on matching the observed hydraulic gradient at the Site, while de-emphasizing results from the aquifer test.
Upper Bound model	AMEC	2012	13	19	The Upper Bound model using the geometric mean hydraulic conductivity estimate from the 2012 aquifer test for regional bedrock, which places a greater emphasis on retaining conditions observed during the test while de-emphasizing the simulated match to the hydraulic gradient observed at the Site.

RMSE = root mean squared error
SWS = Schlumberger Water Services

Table 3-2 Summary of Model Layer Structures of the SWS and AMEC Models

Model Layer	Model Layer Thickness (ft) of the SWS Model	Model Layer Thickness (ft) of the AMEC Model	Primary Hydrogeologic Unit of Previous Model, AMEC (2012)
1	2.5 – 141	2.5 – 141	Coastal Plains Sand
2	2.5 – 141	2.5 – 141	Coastal Plains Sand
3	2.5 – 91	2.5 – 91	Saprolite
4	2.5 – 91	2.5 – 91	Saprolite
5	75	75	Sap-rock
6	75	75	Sap-rock
7	133.3 – 343	225	Bedrock
8	133.3 – 343	275	Bedrock
9	133.3 – 343	300	Bedrock
10	500	500	Bedrock
11	500	500	Bedrock
12	500	500	Bedrock
13	1,000	1,000	Bedrock

SWS = Schlumberger Water Services

Table 3-3 Model Parameters Used in the SWS Model

Hydrogeologic Unit	Minimum Layer	Maximum Layer	Horizontal Conductivity (ft/day)	Anisotropy Ratio (Kx:Kz)	Specific Storage (1/ft)	Specific Yield
Coastal Plains Sand	1	2	20	10	2.00E-04	0.2
Saprolite	3	4	0.008	1	2.00E-06	0.08
Sap-rock	5	6	0.02	1	2.00E-06	0.02
Fractured bedrock	5	7	1	1	2.00E-06	0.04
Bedrock	7	13	0.002	1	2.00E-07	0.01

SWS = Schlumberger Water Services

Source: Modified from Table 5.3 in the SWS Modeling Report (2011).

Table 4-1 Location and Construction of the New Shallow Monitoring Wells Used for Model Calibration (PZ-13-10 thru PZ-13-25 Water Elevations)

Well ID	TOP Northing	TOP Easting	TOP Elevation (in ft)	Ground Elevation (in ft)	Total Well Depth (in ft)	Water Elevation (6/13/13 in ft)	Depth to Water (6/13/13 in ft)	Water Elevation (6/14/13 in ft)	Depth to Water (6/14/13 in ft)
PZ-13-11	586507.27	2139987.24	571.41	568.97	20.00	552.72	18.69	552.58	18.83
PZ-13-12	585909.01	2138844.36	565.19	562.49	22.00	552.54	12.65	552.34	12.85
PZ-13-13	581009.37	2143174.41	526.37	523.85	20.00	512.97	13.4	512.79	13.58
PZ-13-14	581682.78	2139806.14	544.39	542.43	20.00	530.96	13.43	530.85	13.54
PZ-13-15	578891.68	2139991.13	510.45	508.05	20.00	500.71	9.74	500.59	9.86
PZ-13-16	576068.27	2141567.20	516.47	514.28	25.00	490.27	26.2	490.27	26.2
PZ-13-17	576582.59	2145834.40	521.49	519.45	18.00	512.14	9.35	511.91	9.58
PZ-13-18	577142.70	2139867.32	513.70	510.62	80.00	499.89	13.81	499.97	13.73
PZ-13-19	574451.72	2140491.29	505.63	503.49	20.00	490.25	15.38	490.13	15.5
PZ-13-20	576766.82	2136252.92	532.45	529.89	28.00	510.32	22.13	510.2	22.25
PZ-13-21	573689.58	2138809.99	531.12	528.85	30.00	DRY	DRY	DRY	DRY
PZ-13-22	572745.25	2135793.06	451.92	450.21	100.00	441.57	10.35	416.99	34.93
PZ-13-23	570733.26	2135689.64	400.87	398.39	45.00	362.45	38.42	362.6	38.27
PZ-13-24	576178.05	2130578.78	446.12	444.21	44.00	409.18	36.94	414.44	31.68
PZ-13-25	575472.06	2133207.68	484.33	482.28	37.00	462.53	21.8	462.61	21.72

*TOP = Top of pipe (same as top of casing)
Coordinates in NAD27 SC Sate Plane North

* PZ, 13, 22, 23, and 24 were bailed on 6/13/13
0.22 inches of rain on 6/13/13 after readings

Table 4-2 Location and Construction of the Private Wells Used for Model Calibration

Address	Collar Northing	Collar Easting	Collar Elevation (in ft)	Ground Elevation (in ft)	Total Well Depth (in ft)	Water Elevation (in ft)	Depth to Water (in January 2012 in ft)
7668 Haile Gold Mine Road	575396.08	2144223.98	532.72	532.36	33.34	521.94	10.78
4334 Emest Scott Road	584811.91	2141839.21	548.34	550.18	11.93	0.00	DRY
4462 Ernest Scott Road	583907.40	2143094.85	548.24	547.83	28.98	526.11	22.13
4752 Ernest Scott Road	581372.53	2145559.16	522.31	522.12	17.28	508.20	14.11
7375 Snowy Owl Road	583152.70	2142102.29	536.80	536.71	95.76	518.56	18.24
4430 Duckwood	590986.50	2138504.81	577.15	576.82	11.68	565.59	11.56
4442 Duckwood	591092.14	2138733.67	578.66	578.45	23.54	565.94	12.72
4488 Emest Scott Road	583750.95	2143369.13	548.81	547.13	28.66	524.52	24.29
4557 Gold Mine Highway	583527.76	2138003.73	557.61	555.12	31.00	538.09	19.52
4595 Payne Road	578155.26	2151284.44	536.63	536.63	(unsafe)	508.40	28.23
4706 Ernest Scott Road	581444.24	2145153.41	520.90	520.64	25.10	509.59	11.31
4975 Payne Road	578048.09	2150978.92	546.02	547.69	68.51	531.44	14.58
5213 Emest Scott Road	576184.96	2148483.76	537.1D	536.52	46.10	497.96	39.14
5311 Emest Scott Road	575399.22	2148948.50	525..46	525.31	36.82	499.00	26.46
7085 Snowy Owl Road	581908.84	2139566.23	547.81	547.09	24.20	528.41	19.40
7119 Snowy Owl Road.	582374.49	2140271.97	539.05	537.73	~189	519.32	19.73
7155 Snowy Owl Road	582128.00	2140721.20	535.02	534.54	23.65	525.22	9.80
7392 Snowy Owl Road	582167.93	2141491.90	523.08	522.07	46.82	520.34	2.74
7596 Gold Mine Highway	583216.10	2137706.38	564.75	563.69	34.00	537.40	27.35
7686 Haile Gold Mine Road	575489.37	2144304.06	531.30	531.16	14.11	522.51	8.79
7692 Haile Gold Mine Road	575637.66	2144395.14	533.46	530.48	27.89	522.33	11.13
7723 Haile Gold Mine Road	576073.88	2144639.86	527.97	526.90	40.12	504.63	23.34
7758 Haile Gold Mine Road	576435.54	2145246.75	535.75	525.24	22.67	516.76	18.99
Hilton Mobile Home Park	583974.89	2138269.97	557.57	556.72	99.19	540.96	16.61

Table 4-3 Summary of New Pumping Well and Piezometers for the 2013 Bedrock Aquifer Test

Name	Target Stratigraphy	Proposed Screen Interval (ft bgs)	Proposed Distance from Pumping Well (ft)	Proposed Northing [a]	Proposed Easting [a]
PW-13-01[b]	Bedrock	125.5	NA	574628	2135146
PZ-13-04	Coastal Plains Sand	20–30	20–30	574593	2135097
PZ-13-05	Saprolite	50–60	20–30	574603	2135103
PZ-13-06	Coastal Plains Sand	20–30	30–50	574677	2135132
PZ-13-07	Saprolite	50–60	30–50	574685	2135145
PZ-13-08	Bedrock downgradient of dike	200–500	75–100	574452	2135314
PZ-13-09	Bedrock downgradient of dike	200–500	100–150	574680	2135230
PZ-13-10	Bedrock downgradient of dike	200–500	500	574803	2135462

bgs = below ground surface

[a] Northing and easting coordinates are in NAO 27 South Carolina State Plane.
[b] Piezometer designations PZ-13-01,-02, and -03 represent the vibrating wire confirmation piezometers at Haile Gold Mine.

Table 6-1 Comparison of Layering and Hydrogeological Representation of the AMEC and Cardno ENTRIX Models

Model Layer	Model Layer Thickness (ft) of Previous Model, AMEC (2012)	Primary Hydrogeologic Unit of Previous Model, AMEC (2012)	Model Layer Thickness (ft) of Cardno ENTRIX Model	Primary Hydrogeologic Unit of Cardno ENTRIX Model
1	2.5 – 141	CPS	5.0 – 282	CPS
2	2.5 – 141	CPS	5 – 182	Saprolite
3	2.5 – 91	Saprolite	150	Sap-rock
4	2.5 – 91	Saprolite	225	Bedrock
5	75	Sap-rock	275	Bedrock
6	75	Sap-rock	300	Bedrock
7	225	Bedrock	2,500	Bedrock
8	275	Bedrock	-	-
9	300	Bedrock	-	-
10	500	Bedrock	-	-
11	500	Bedrock	-	-
12	500	Bedrock	-	-
13	1,000	Bedrock	-	-

CPS = Coastal Plains Sand

Table 6-2 Head Target Values Used in Steady-State Calibration

Well ID	Easting	Northing	Primary Aquifer Source	Target Head (ft amsl)
PZ-13-11	2139987.24	586507.27	CPS	552.7
PZ-13-12	2138844.36	585909.02	CPS	552.5
PZ-13-13	2143174.41	581009.36	CPS	513.1
PZ-13-14	2139806.14	581682.78	CPS	531.1
PZ-13-15	2139991.13	578891.68	CPS	500.9
PZ-13-16	2141567.20	576068.27	CPS	490.4
PZ-13-17	2145834.40	576582.59	CPS	512.1
PZ-13-19	2140491.29	574451.72	CPS	490.2
PZ-13-20	2136252.92	576766.82	CPS	510.0
7668-HGM-Road	2144223.99	575396.08	CPS	524.2
4462-Ernest-Scott-Road	2143094.85	583907.40	CPS	527.1
4752-Ernest-Scott-Road	2145559.16	581372.54	CPS	509.5
4430-Duckwood	2138504.81	590986.50	CPS	567.9
4442-Duckwood	2138733.67	591092.14	CPS	568.4
4488-Ernest-Scott-Road	2143369.14	583750.95	CPS	525.7
4557-GM-Hwy	2138003.73	583527.76	CPS	540.0
4706-Ernest-Scott	2145153.41	581444.24	CPS	509.6
5213-Ernest-Scott-Road	2148483.76	576184.96	CPS	500.4
5311-Ernest-Scott-Road	2148948.50	575399.22	CPS	499.1
7085-Snowy-Owl	2139566.23	581908.84	CPS	530.0
7155-Snowy-Owl	2140721.20	582128.00	CPS	523.8
7596-GM-Hwy	2137706.38	583216.10	CPS	538.5
7686-HGM-Road	2144304.06	575489.37	CPS	524.3
7692-HGM-Road	2144395.14	575637.66	CPS	524.3
7723-HGM-Road	2144639.86	576073.88	CPS	504.5
7758-HGM-Road	2145246.75	576435.54	CPS	517.1
MW-10-06	2138707.30	590644.10	CPS	564.6
MW-10-07	2140174.00	588495.00	CPS	549.0
MW-10-08	2136504.80	588668.50	CPS	549.1
MW-10-10	2137652.00	584524.90	CPS	540.7

Table 6-2 Head Target Values Used in Steady-State Calibration

Well ID	Easting	Northing	Primary Aquifer Source	Target Head (ft amsl)
DMW-4	2138790.00	576603.00	CPS	489.5
DMW-7	2138170.00	576973.00	CPS	498.5
PZ-13-04	2135126.10	574591.10	CPS	506.7
PZ-13-06	2135174.60	574672.70	CPS	506.4
USGS_KER_367	2158312.00	569249.00	CPS	457.2
PZ-13-18	2139867.32	577142.70	Saprolite	500.2
7392-Snowy-Owl	2141483.87	582162.04	Saprolite	520.1
BMW-10-02	2136975.00	577294.00	Saprolite	495.1
BMW-10-03	2134438.00	575727.00	Saprolite	505.1
DMW-10	2139273.00	575348.40	Saprolite	445.3
DMW-6	2138967.00	575150.00	Saprolite	442.3
DMW-8	2138521.36	575266.59	Saprolite	438.1
DMW-9	2138852.83	575277.03	Saprolite	441.3
PZ-13-05	2135126.90	574596.40	Saprolite	506.7
PZ-13-07	2135184.80	574667.30	Saprolite	506.3
PZ-13-22	2135793.06	572745.25	Sap-rock	417.2
PZ-13-23	2135689.64	570733.26	Sap-rock	362.6
7375-Snowy-Owl-Road	2142102.29	583152.70	Sap-rock	519.6
Hilton-MH-Park	2138269.97	583974.89	Sap-rock	541.0
BMW-10-01	2141705.39	579514.60	Sap-rock	472.3
MW-10-05s	2134777.92	569382.98	Sap-rock	342.5
BMW-3	2141160.00	574877.00	Sap-rock	484.1
BMW-5	2137068.06	573804.74	Sap-rock	404.8
BMW-6	2139034.00	573903.00	Sap-rock	472.0
BMW-7	2137366.49	571810.94	Sap-rock	364.9
DMW-1	2137464.00	575477.00	Sap-rock	437.7
BMW-10-04	2136275.00	573073.00	Bedrock	401.2
BMW-10-05d	2134765.00	569406.00	Bedrock	343.8
BMW-1	2139452.00	574704.00	Bedrock	447.8
BMW-2	2136416.00	576229.01	Bedrock	479.1

Table 6-2 Head Target Values Used in Steady-State Calibration

Well ID	Easting	Northing	Primary Aquifer Source	Target Head (ft amsl)
PW-13-01	2135159.00	574609.70	Bedrock	503.2
PZ-13-01S	2140944.70	576051.50	Bedrock	463.0
PZ-13-02S	2136754.80	572919.30	Bedrock	382.3
PZ-13-03S	2140291.00	580375.20	Bedrock	507.6
PZ-13-08	2135326.70	574453.00	Bedrock	499.5
PZ-13-09	2135234.10	574662.00	Bedrock	504.8
PZ-13-10	2135464.00	574800.09	Bedrock	498.4
BMW-09-03	2137233.00	573285.00	Bedrock	390.5
PZ-13-02D	2136725.70	572915.70	Bedrock	386.3
PZ-13-03D	2140305.31	580397.70	Bedrock	502.6
BMW-09-01	2136803.00	575495.00	Bedrock	444.6
BMW09-02	2139356.00	573603.00	Bedrock	475.3
BMW09-04	2141112.00	576372.00	Bedrock	458.5
BMW09-05	2139193.00	576948.00	Bedrock	485.3
BMW09-06	2139863.50	574964.40	Bedrock	439.9
PZ-13-01D	2140965.70	576065.20	Bedrock	474.2

amsl = above mean sea level
CPS = Coastal Plains Sand

Table 6-3 Steady-State Baseflow Targets for the 16 Reaches Used for Calibration

Reach Number	Baseflow Target Value (cubic ft/day)
1	423,642
2	237,328
3	1,533,984
4	181,440
5	Not estimated
6	304,423
7	1,015,441
8	1,183,725
9	461,348
10	616,609
11	632,690
12	993,673
13	410,334
14	721,965
15	241,920
16	640,800

Table 6-4 Upper and Lower Bounds of Hydraulic Coefficients Specified in PEST

Geologic Unit	Model Layer	Kx Initial (ft/day)	Kx Range (ft/day)	Kz Initial (ft/day)	Kz Range (ft/day)	Recharge (inches/year)
Coastal Plains Sand	Layer 1	20	2 to 30	3	2 to 30	1 to 12
Saprolite	Layer 2	0.6	0.001 to 3	1	0.01 to 3	1 to 12
Sap rock	Layer 3	0.05	0.01 to 5	1	0.01 to 5	N/A
Upper bedrock	Layer 4	1	0.5 to 5	1	0.5 to 5	N/A
Lower bedrock	Layer 5	1	0.5 to 5	1	0.5 to 5	N/A
Lower bedrock	Layer 6	1	0.5 to 5	1	0.5 to 5	N/A

Table 6-5 Calibration Statistics of the Steady-State Models

Statistic	Heads		Baseflow	
	Model 1	Model 2	Model 1	Model 2
Residual mean	2.7	0.0	-7,442.7	1,544.3
Absolute residual mean	8.2	13.4	56,325.8	31,751.3
Residual standard deviation	9.9	18.1	75,064.8	43,378.7
Sum of squares	8.0E+03	2.5E+04	8.0E+10	2.6E+10
Root mean square error	10.3	18.1	72,900.5	41,936.2
Minimum residual	-16.5	-41.9	-169,330.8	-84,197.5
Maximum residual	31.4	44.9	138,233.7	97,175.7
Number of observations	76	76	15	15
Range in observations	226	226	1,352,544	1,352,544
Scaled residual standard deviation	0.04	0.08	0.06	0.03
Scaled absolute residual mean	0.04	0.06	0.04	0.02
Scaled root mean square error	**4.5%**	**8.0%**	**5.4%**	**3.1%**

Table 6-6 Calibrated Hydraulic Coefficient Range

Geological Unit	Model Layer	Kx Range (ft/day)	Kz Range (ft/day)	Ss (1/foot)	Sy (unitless)	R Zone 1 (inches/year)	R Zone 2 (inches/year)
CPS	Layer 1	1.8 – 30	2 – 3.7	1.10E-04	5.00E-02	8.2	12.1
Saprolite	Layer 2	0.001 – 3.1	0.008 – 3	2.05E-07	1.00E-02		
Saprock	Layer 3	0.008 – 5	0.007 – 5	1.00E-05	5.00E-02		
Bedrock	Layer 4	0.4 – 5.5	0.5 – 5	1.00E-05	5.00E-02		
Bedrock	Layer 5	0.4 – 5.6	0.5 – 4.3	1.00E-05	5.00E-02		
Bedrock	Layer 6	0.01	0.07	1.00E-05	5.00E-03		
Bedrock	Layer 7	0.01	0.01	1.00E-05	5.00E-03		

CPS = Coastal Plains Sand
Kx = horizontal conductivity
Kz = vertical conductivity
R = recharge
Sy = specific yield
Ss = specific storage

Table 6-7 Mass Balance Summary of the Final Steady-State Model

Flow Component	Model Inflows	Model Outflows
Flux boundary	58,449	-63,882
River	0	-11,467,602
Stream	1,477	-654,374
Recharge	12,125,772	0
Total	**12,185,699**	**-12,185,858**
Percentage error	0.0013%	-

Table 7-1 Model Stress Periods Vs. Mine Years

Stress Period	Period Length	Mine Year
1	90	End of Quarter 1, Year 0
2	91	End of Quarter 2, Year 0
3	92	End of Quarter 3, Year 0
4	92	End of Quarter 4, Year 0
5	90	End of Quarter 1, Year 1
6	91	End of Quarter 2, Year 1
7	92	End of Quarter 3, Year 1
8	92	End of Quarter 4, Year 1
9	90	End of Quarter 1, Year 2
10	91	End of Quarter 2, Year 2
11	92	End of Quarter 3, Year 2
12	92	End of Quarter 4, Year 2
13	365	End of Year 3
14	365	End of Year 4
15	365	End of Year 5
16	365	End of Year 6
17	365	End of Year 7
18	365	End of Year 8
19	365	End of Year 9
20	365	End of Year 10
21	365	End of Year 11
22	365	End of Year 12
23	730	End of Year 14

Table 7-2 Simulated Maximum Drawdown in Each Mine Year

Mine Year	Maximum Simulated Drawdown (ft)	Maximum Drawdown Location
Year 0	144	Mill Zone Pit
Year 1	280	Mill Zone Pit
Year 2	410	Mill Zone Pit
Year 3	373	Snake Pit
Year 4	553	Snake Pit
Year 5	375	Snake Pit
Year 6	375	Snake Pit
Year 7	506	Ledbetter Pit
Year 8	584	Ledbetter Pit
Year 9	639	Ledbetter Pit
Year 10	721	Ledbetter Pit
Year 11	808	Ledbetter Pit
Year 12	842	Ledbetter Pit
Year 14	842	Ledbetter Pit

Table 7-3 Simulated Baseflow in CFD to Selected Reaches During Pre-Mining and Mining Years

	Pre-Mining	Year 0	Year 1	Year2	Year 3	Year 4	Year5	Year 6	Year 7	Year 8	Year 9	Year 10	Year 11	Year 12	Year 14	Percentage Reduction
Reach 1	336,981	336,987	336,985	336,984	336,983	336,982	336,981	336,980	336,979	336,978	336,977	336,976	336,975	336,974	336,972	0%
Reach 2	252,816	252,794	252,790	252,780	252,763	252,742	252,721	252,701	252,682	252,662	252,641	252,620	252,597	252,569	252,513	0%
Reach 3	1,447,171	1,446,059	1,445,092	1,443,603	1,442,244	1,441,172	1,440,570	1,440,193	1,439,644	1,438,996	1,438,530	1,437,979	1,435,439	1,433,726	1,431,858	1%
Reach 4	173,937	173,252	172,370	171,221	169,675	168,614	167,852	166,950	165,744	164,491	163,567	162,820	161,694	160,831	159,269	8%
Reach 5	22,697	22,584	22,568	22,525	22,496	22,392	22,307	22,238	22,152	22,050	21,946	21,862	21,792	21,732	21,572	4%
Reach 6	273,959	273,892	273,863	273,780	273,661	273,539	273,446	273,392	273,368	273,343	273,319	273,304	273,255	273,117	272,866	0%
Reach 7	1,034,665	1,034,665	1,034,664	1,034,663	1,034,656	1,034,650	1,034,644	1,034,637	1,034,633	1,034,629	1,034,627	1,034,626	1,034,623	1,034,619	1,034,606	0%
Reach 8	1,294,190	1,293,486	1,293,207	1,292,347	1,290,378	1,288,211	1,286,801	1,286,114	1,285,485	1,284,733	1,284,037	1,283,531	1,283,168	1,282,867	1,282,335	1%
Reach 9	503,607	503,604	503,604	503,604	503,604	503,603	503,602	503,601	503,599	503,597	503,595	503,593	503,590	503,588	503,581	0%
Reach 10	544,843	544,873	544,865	544,859	544,854	544,852	544,851	544,849	544,849	544,848	544,847	544,846	544,846	544,845	544,844	0%
Reach 11	652,507	652,416	652,399	652,352	652,284	652,201	652,114	652,036	651,952	651,856	651,752	651,660	651,562	651,450	651,253	0%
Reach 12	1,022,097	1,022,088	1,022,086	1,022,084	1,022,078	1,022,065	1,022,042	1,022,019	1,022,000	1,021,979	1,021,955	1,021,928	1,021,903	1,021,878	1,021,833	0%
Reach 13	434,755	434,081	433,843	432,878	430,367	427,429	425,478	424,571	423,832	422,857	421,673	420,590	419,674	418,924	417,825	4%
Reach 14	916,425	916,320	916,305	916,224	915,984	915,536	915,028	914,666	914,454	914,304	914,153	913,982	913,809	913,654	913,413	0%
Reach 15	73,939	73,083	72,038	70,972	70,138	69,660	69,550	69,379	68,963	68,578	68,406	68,065	65,685	64,963	64,321	12%
Rea ch 16	654,374	568,495	510,029	464,586	403,326	377,175	374,623	368,565	356,218	345,269	343,403	342,724	333,292	329,456	324,900	50%

Figures

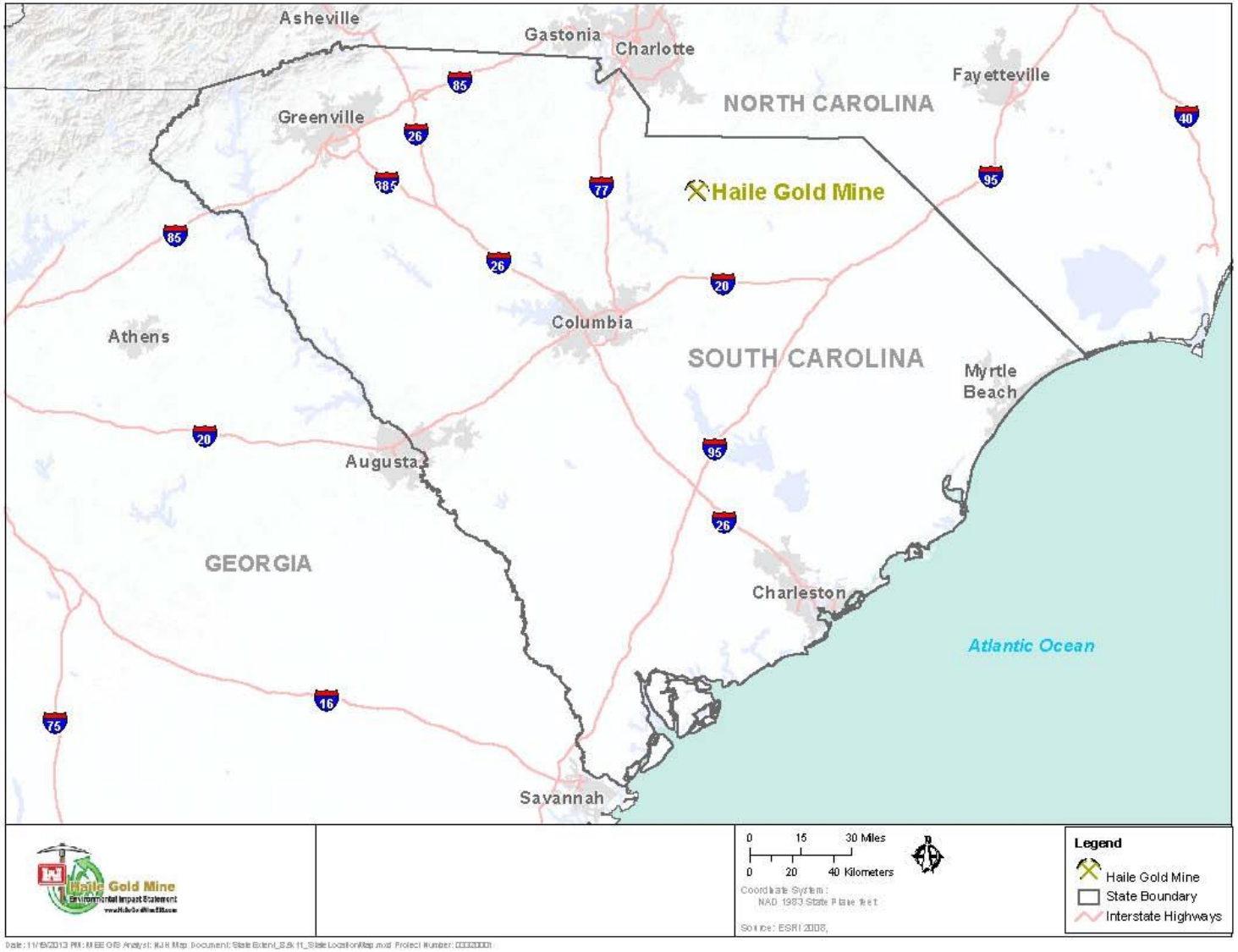

Figure 1-1 Location of the Proposed Haile Gold Mine Project

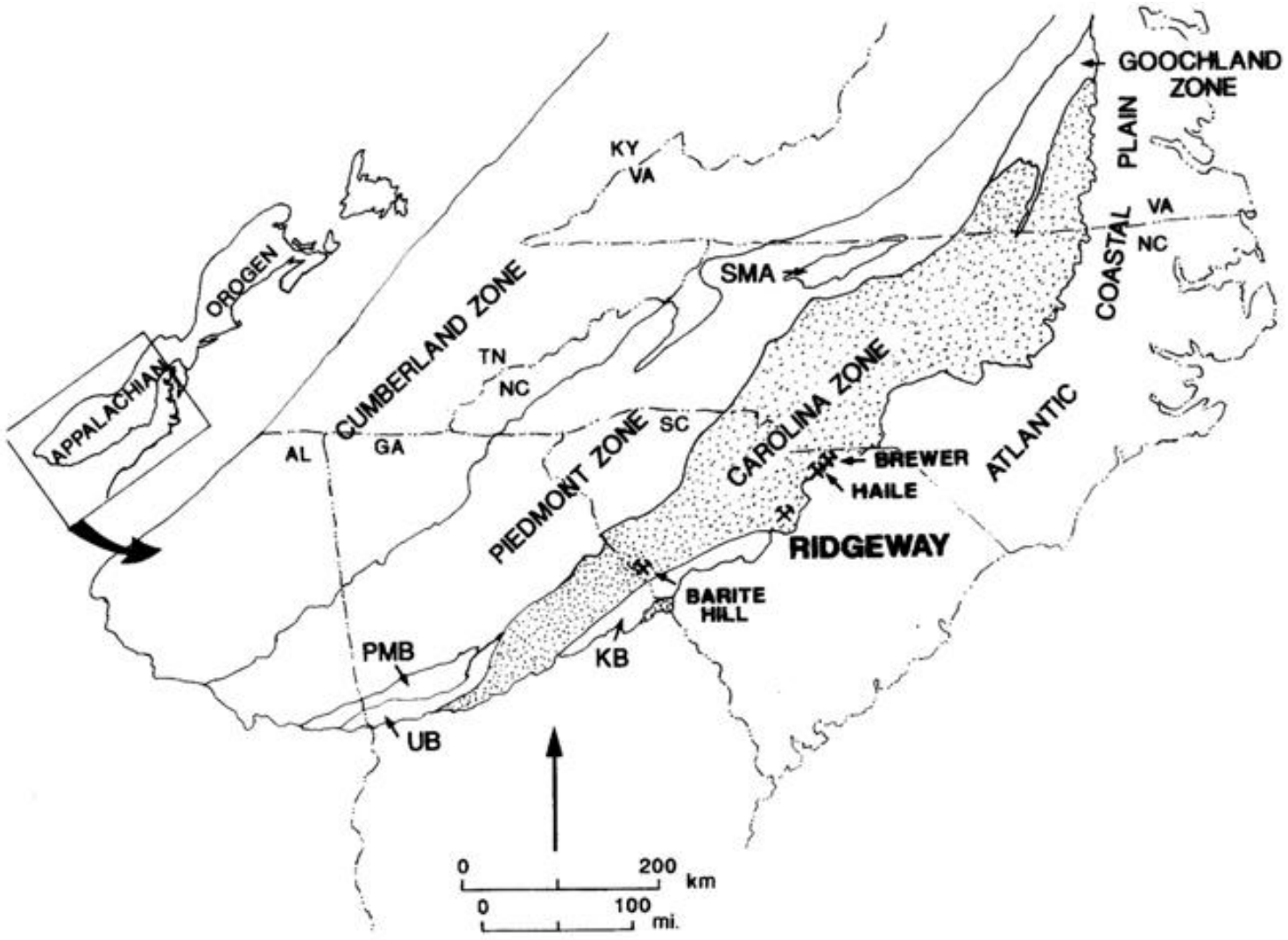

Figure 1-2 Location of the Proposed Haile Gold Mine Relative to the Ridgeway and Brewer Mines

Source: South Carolina Geology, Vol. 40, pg. 27.

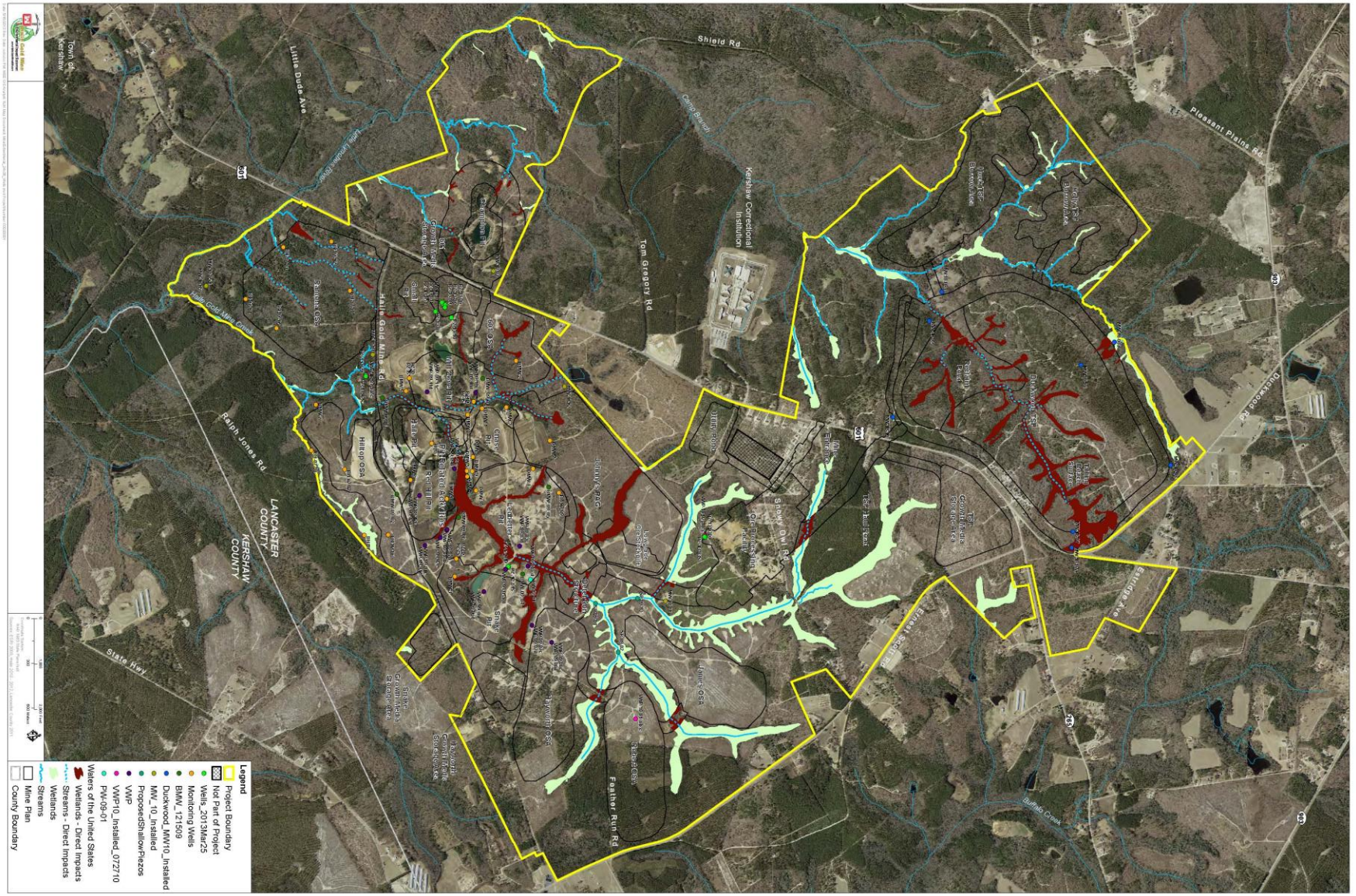

Figure 1-3 Aerial Photo of the Site (2009), with Proposed Facilities Highlighted

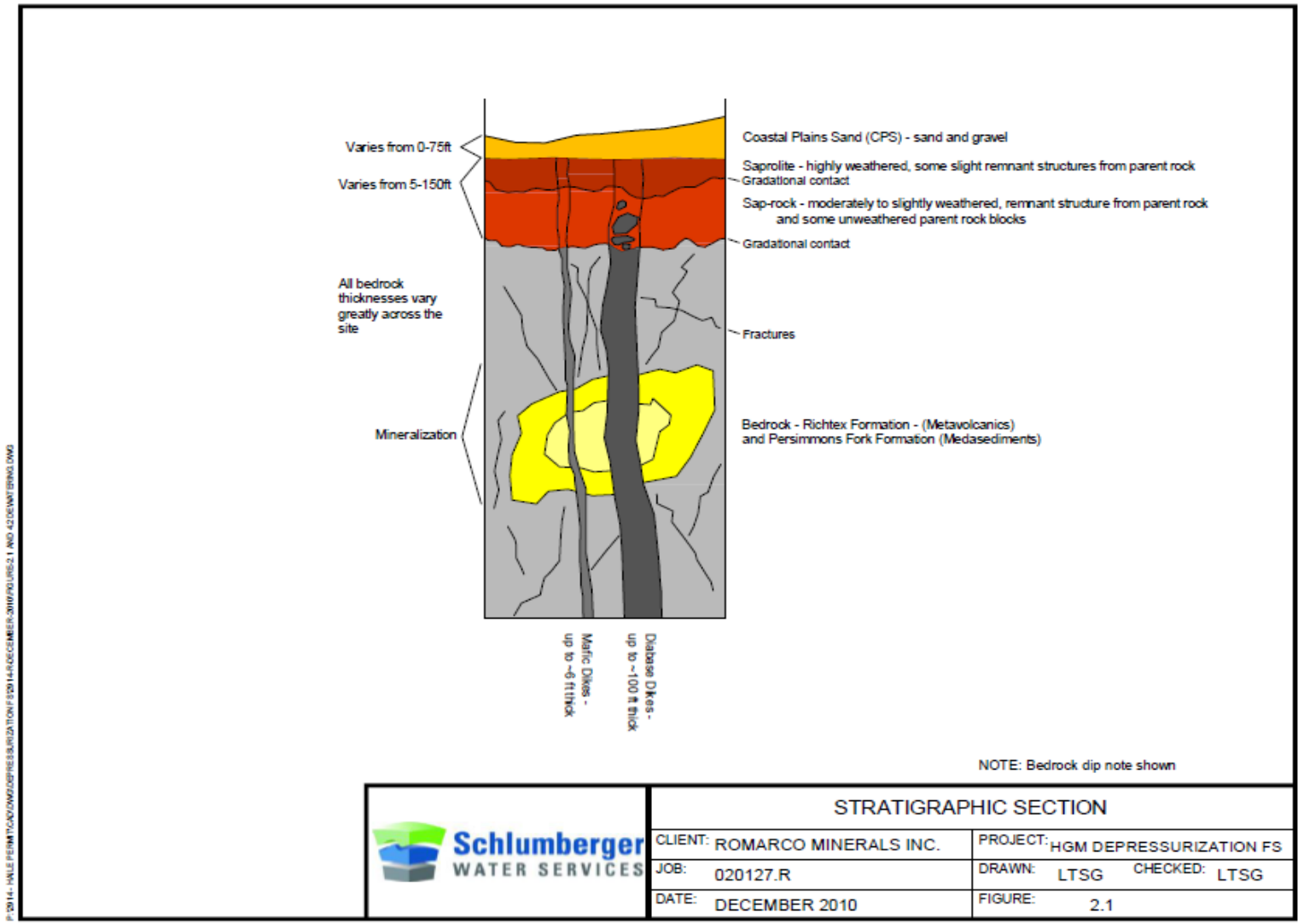

Figure 2-1 Generalized Stratigraphic Section Reflecting the Bedrock Pattern under the Coastal Plains Sand and Saprolite

Source: Schlumberger Water Services 2011.

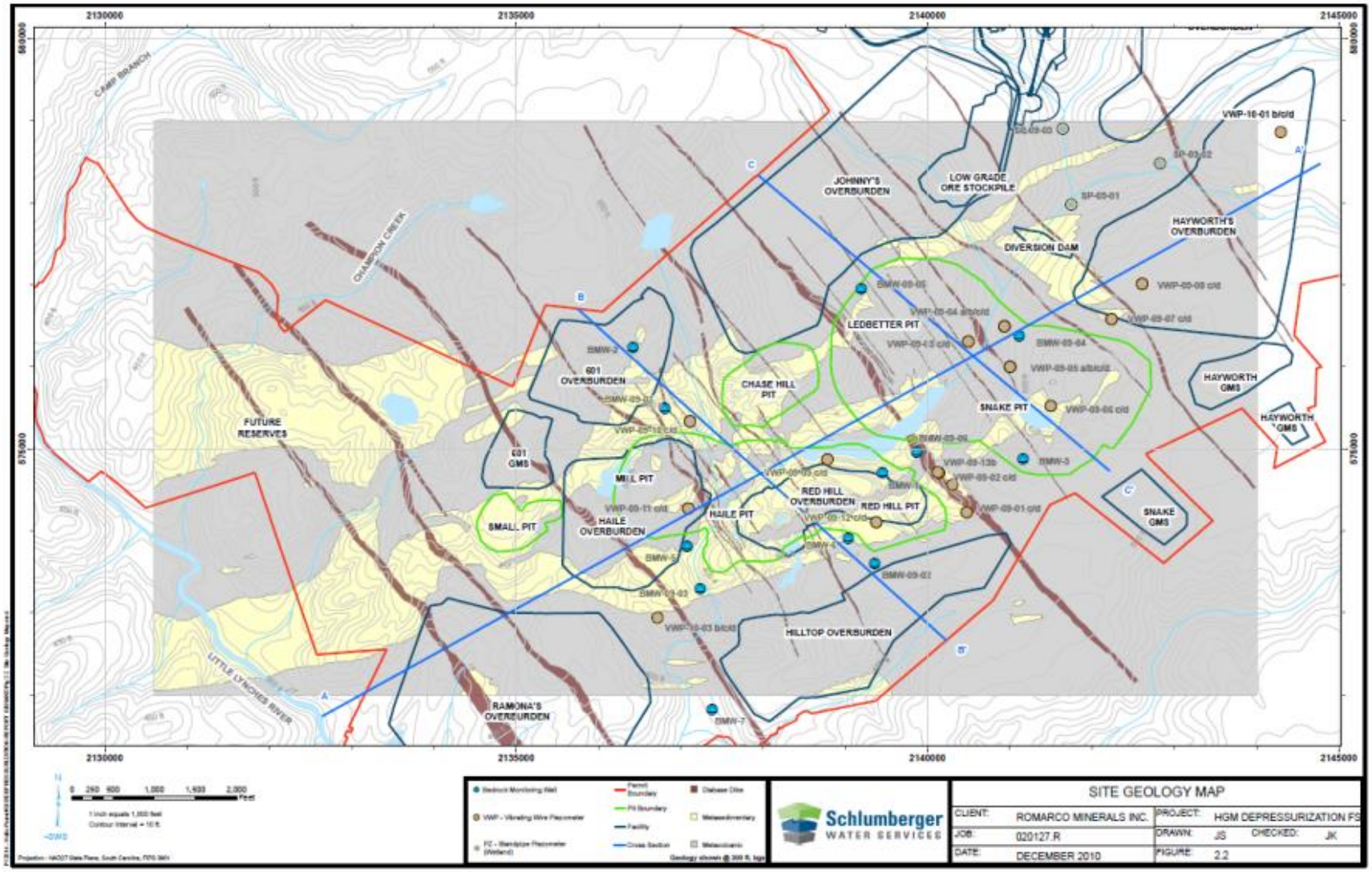

Figure 2-2 Site Geology Map Depicting the Geologic Interpretation at 300 Feet below Ground Surface

Source: Schlumberger Water Services 2011.

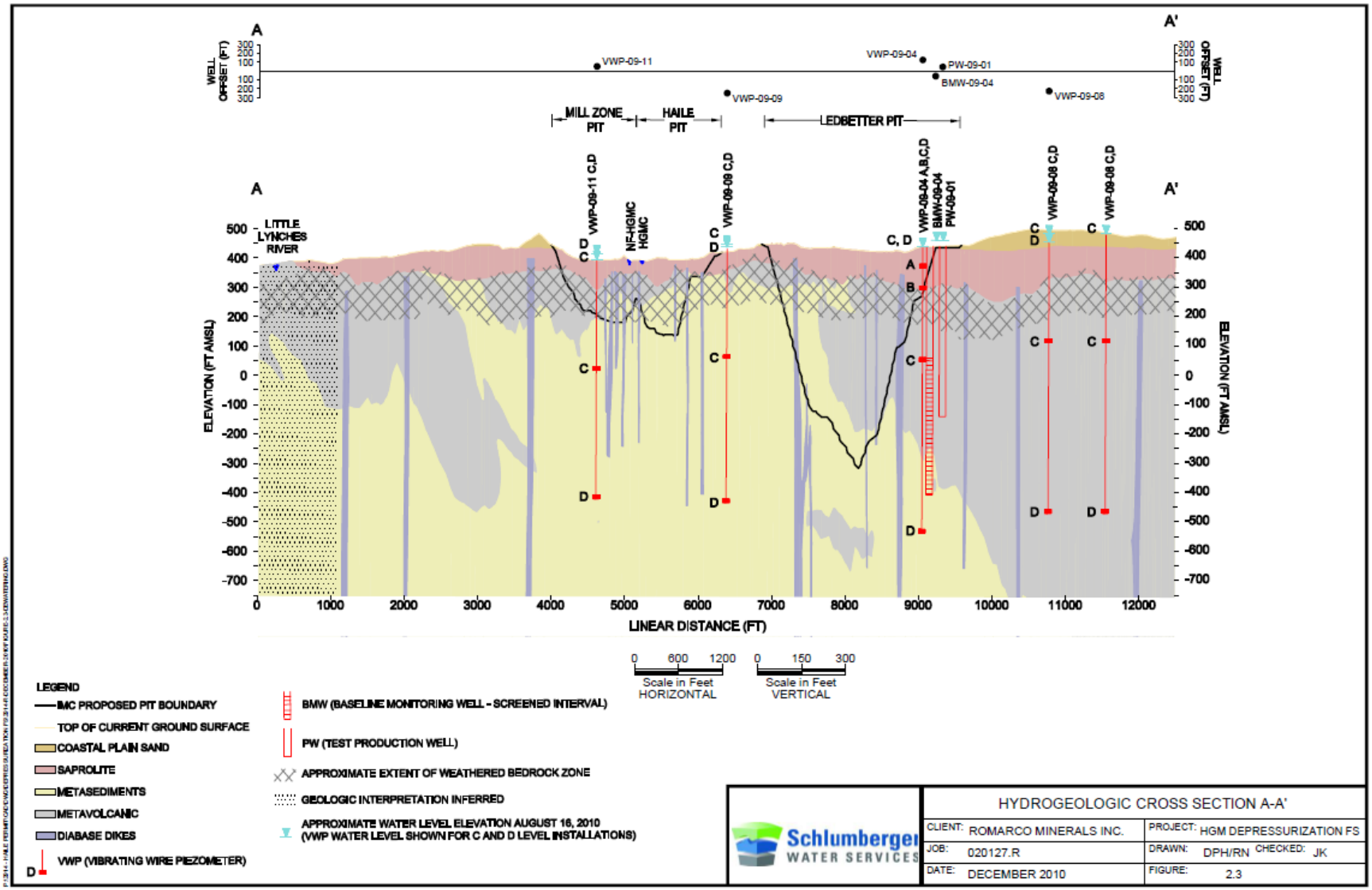

Figure 2-3 Hydrogeologic Cross Section A-A'

Source: Schlumberger Water Services 2011.

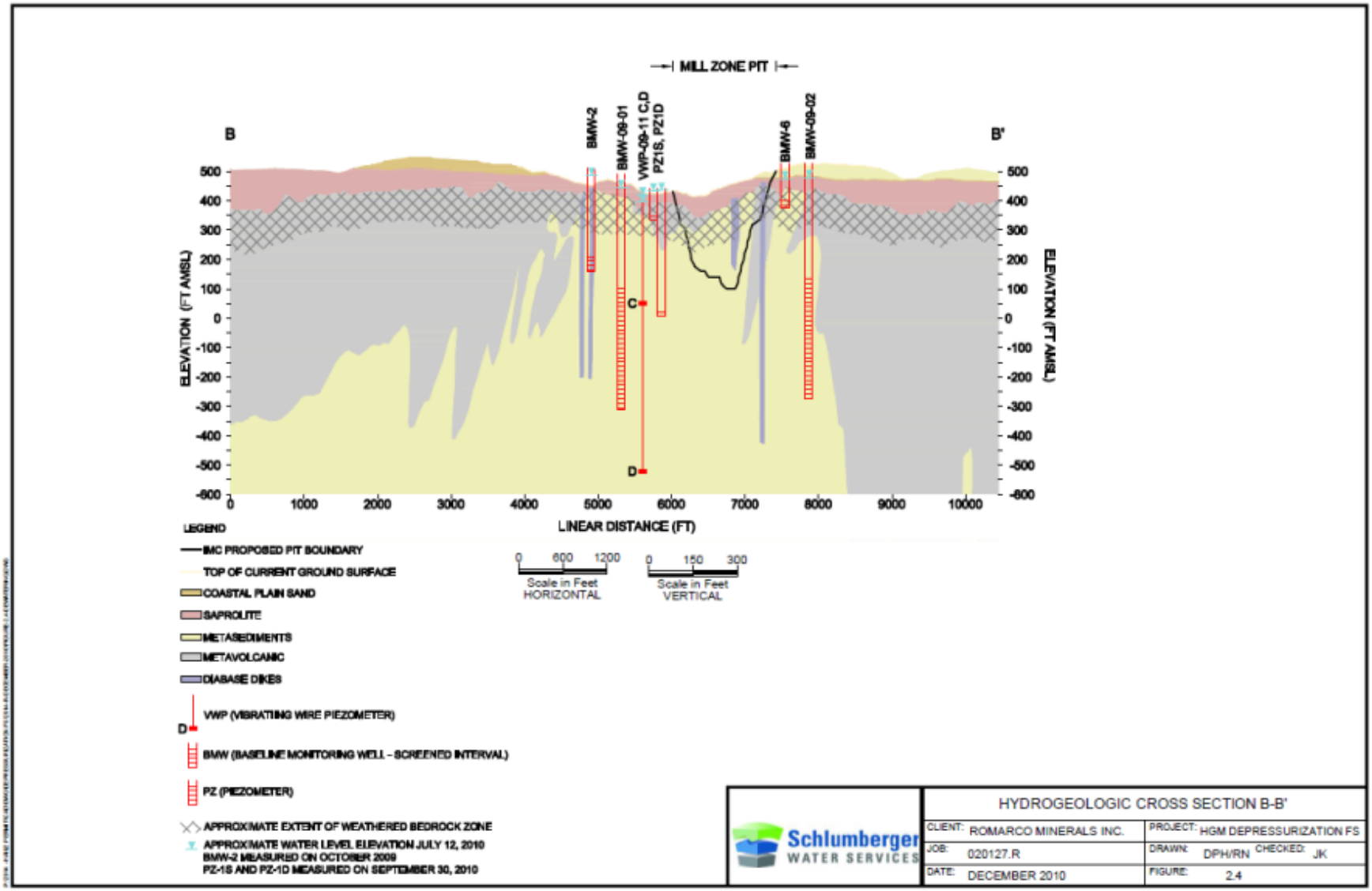

Figure 2-4 Hydrogeologic Cross Section B-B'

Source: Schlumberger Water Services 2011.

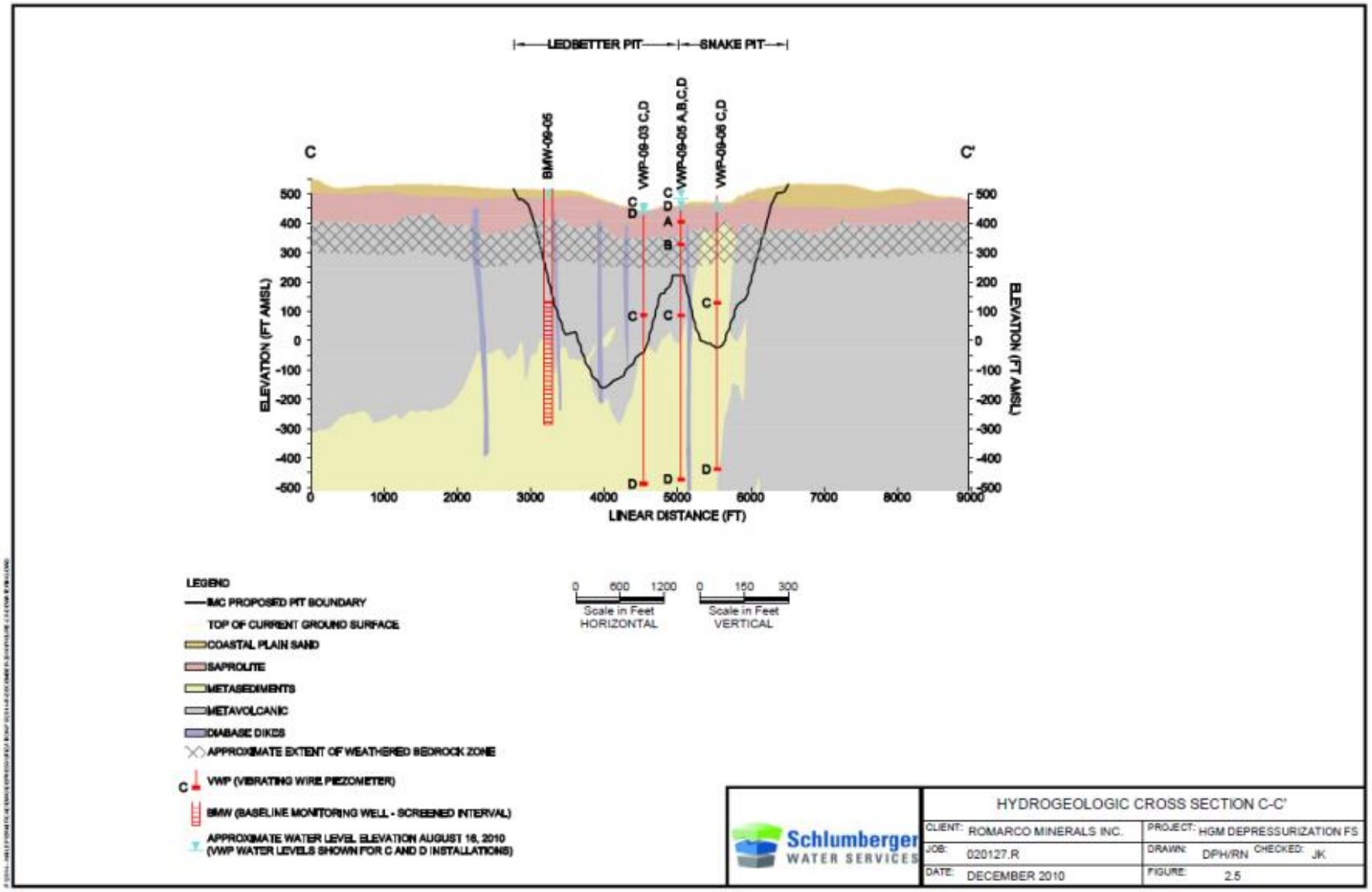

Figure 2-5 Hydrogeologic Cross Section C-C'

Source: Schlumberger Water Services 2011.

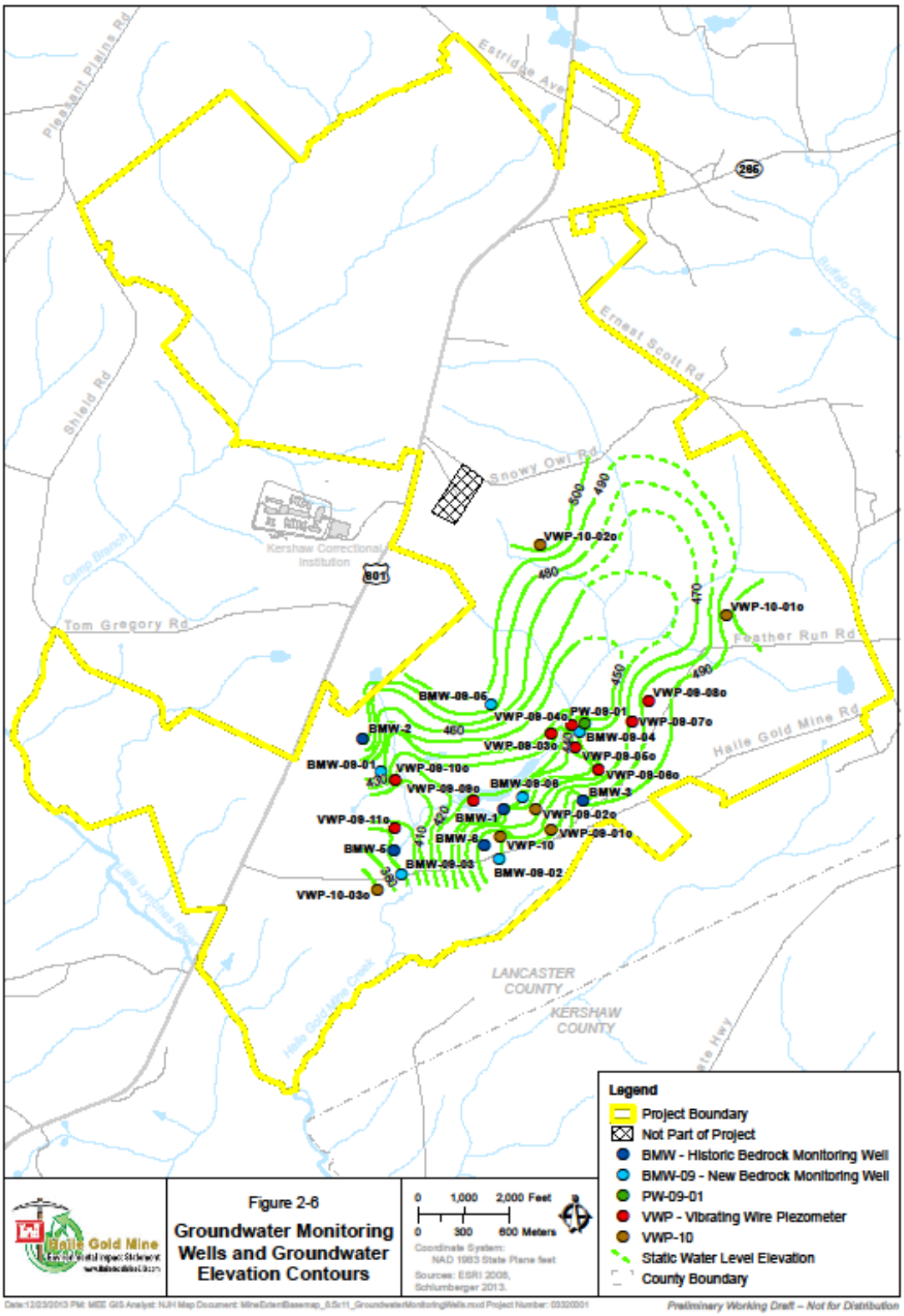

Figure 2-6 Groundwater Monitoring Wells and Groundwater Elevation Contours

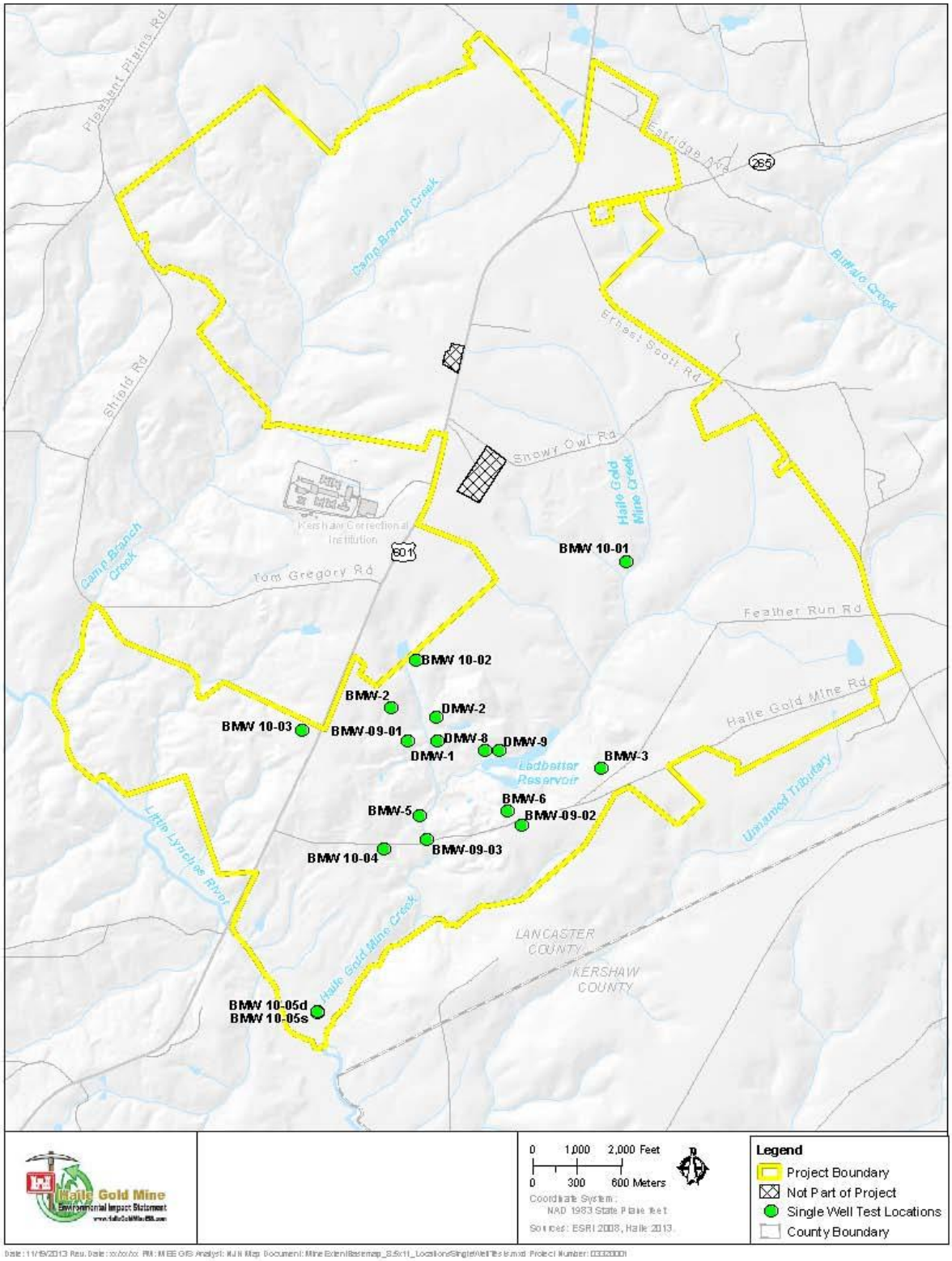

Figure 4-1 Location of Boreholes Where Single-Well Pumping Tests Were Conducted

Figure 4-2 Example of the Cross Sections Generated from the Vulcan Model

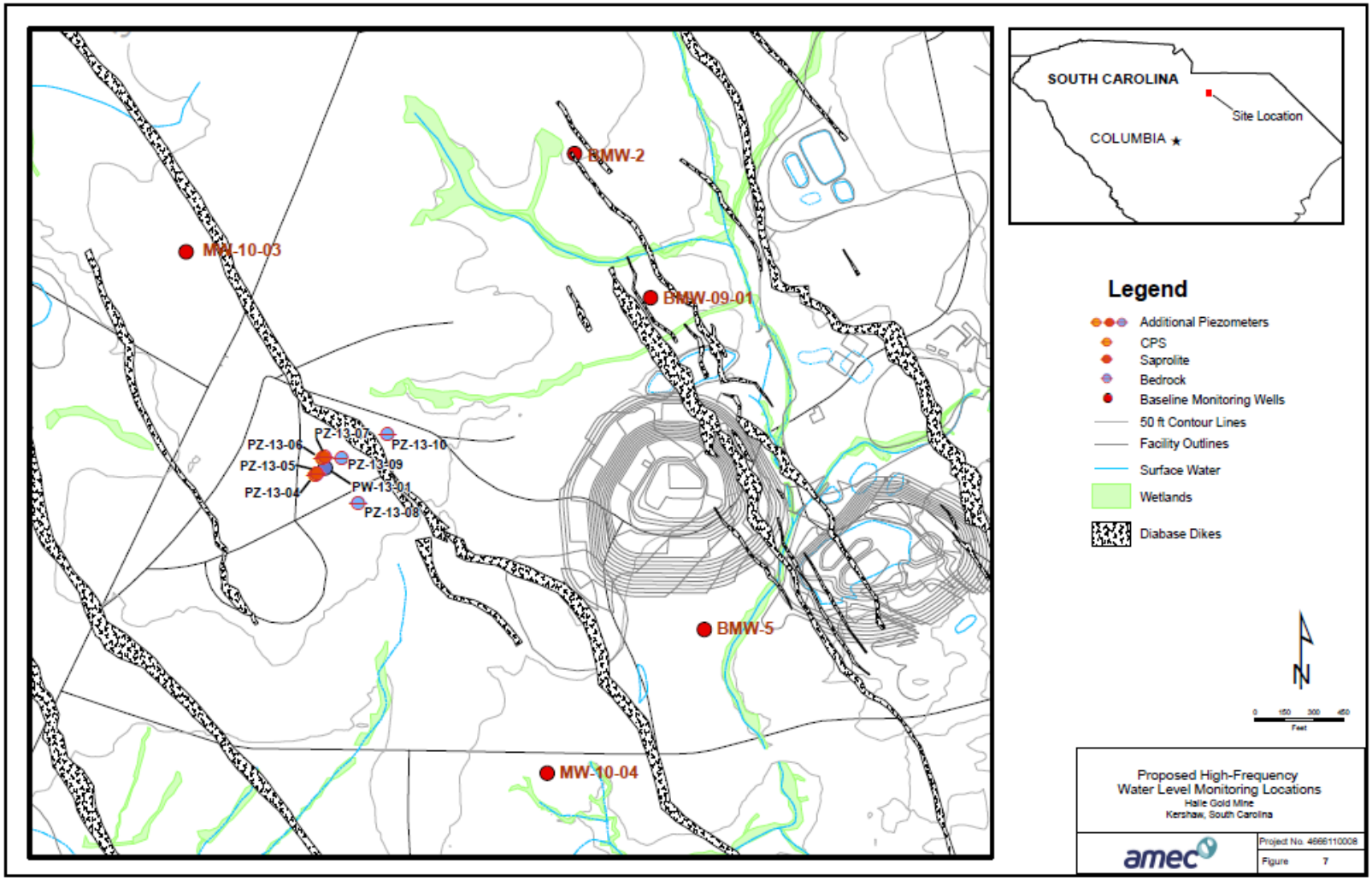

Figure 4-3 Locations of Piezometers Installed in 2013

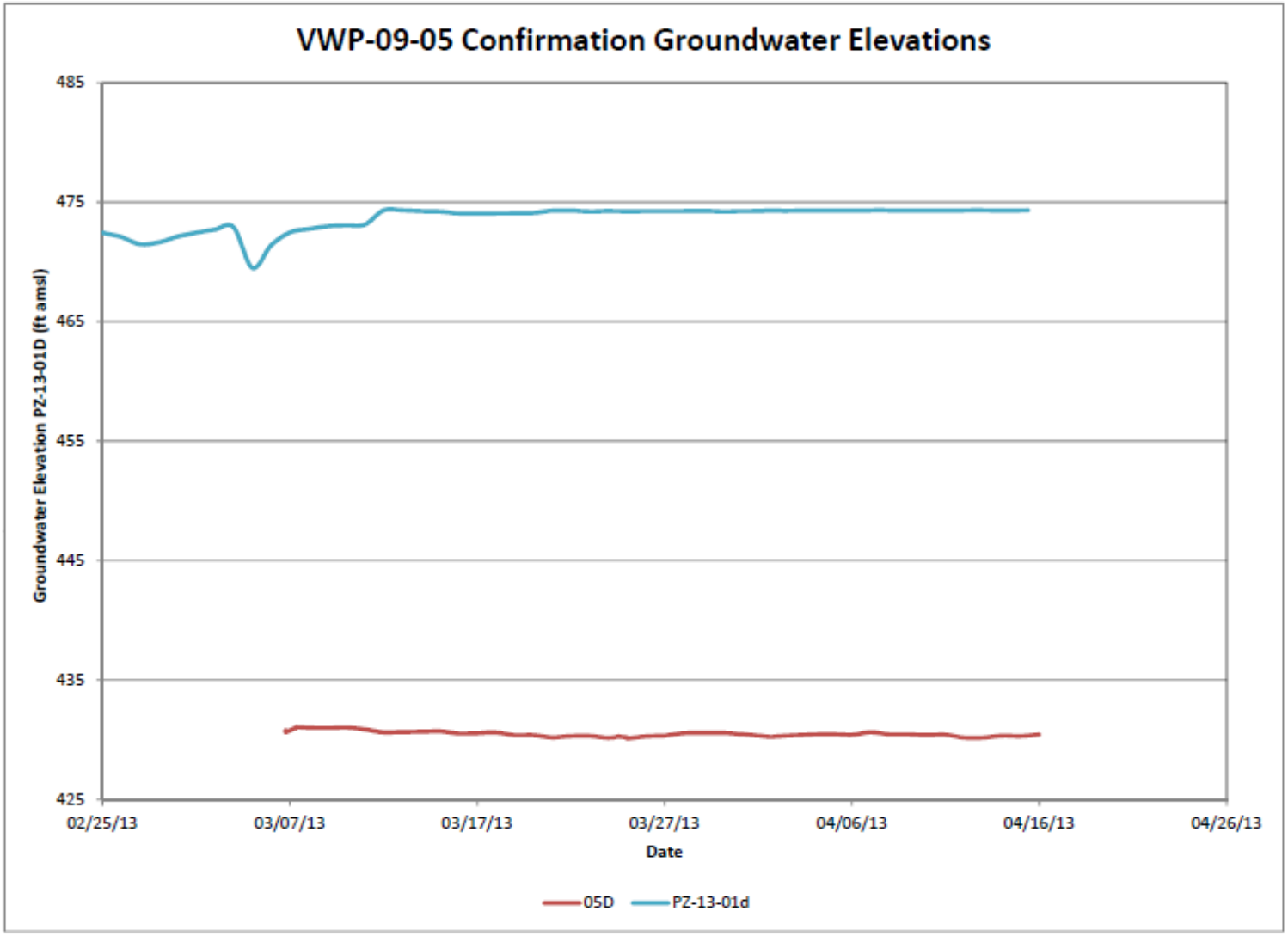

Figure 4-4 **Water Levels for One of the Piezometer/Vibrating Wire Piezometer Pairs that Illustrates the Magnitude of Variance in Water Levels**

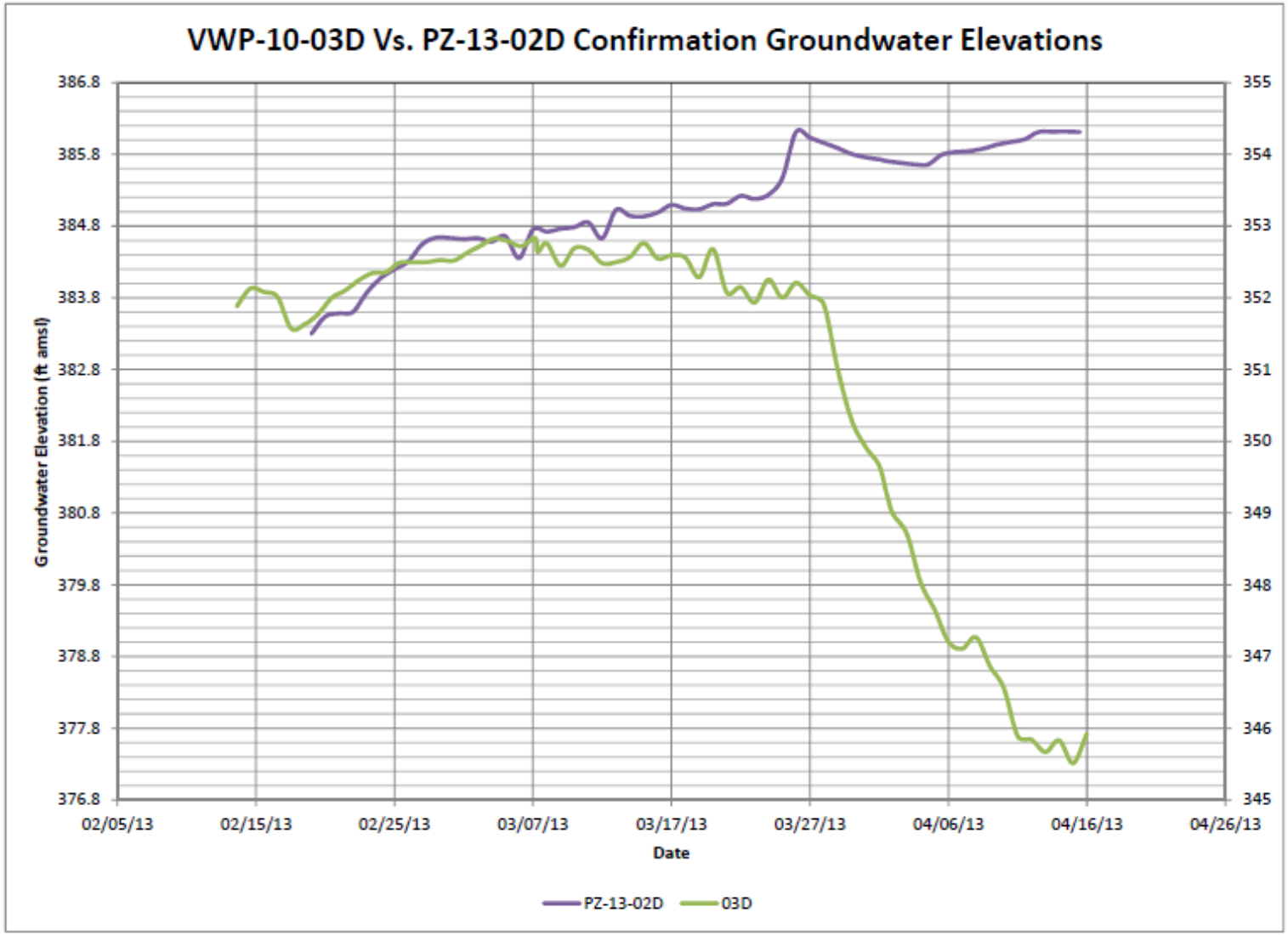

Figure 4-5 **Example of the Variance between the Vibrating Wire Piezometer and Piezometer Data after the Data were Shifted**

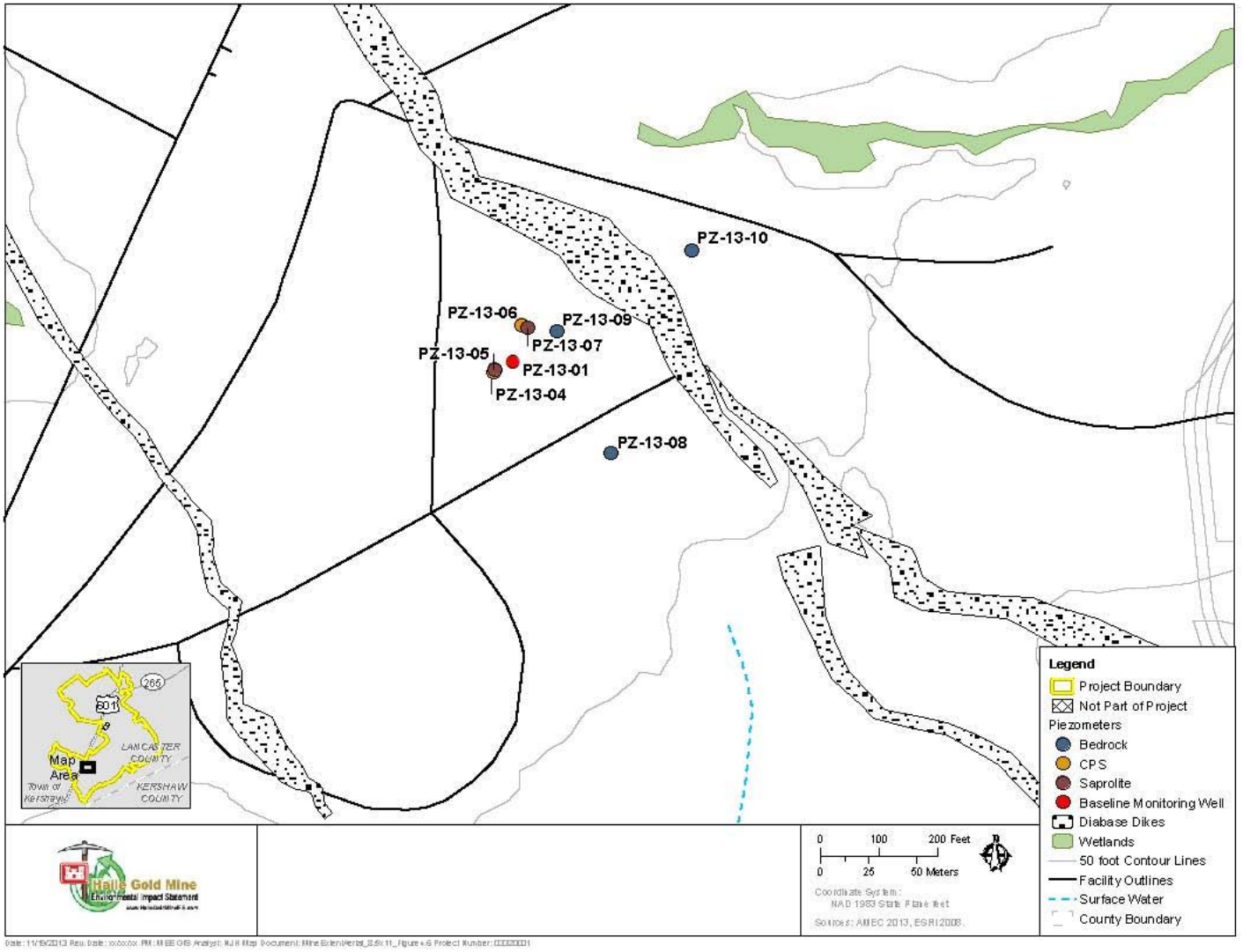

Figure 4-6 Layout of Piezometers for the 2013 Bedrock Aquifer Test

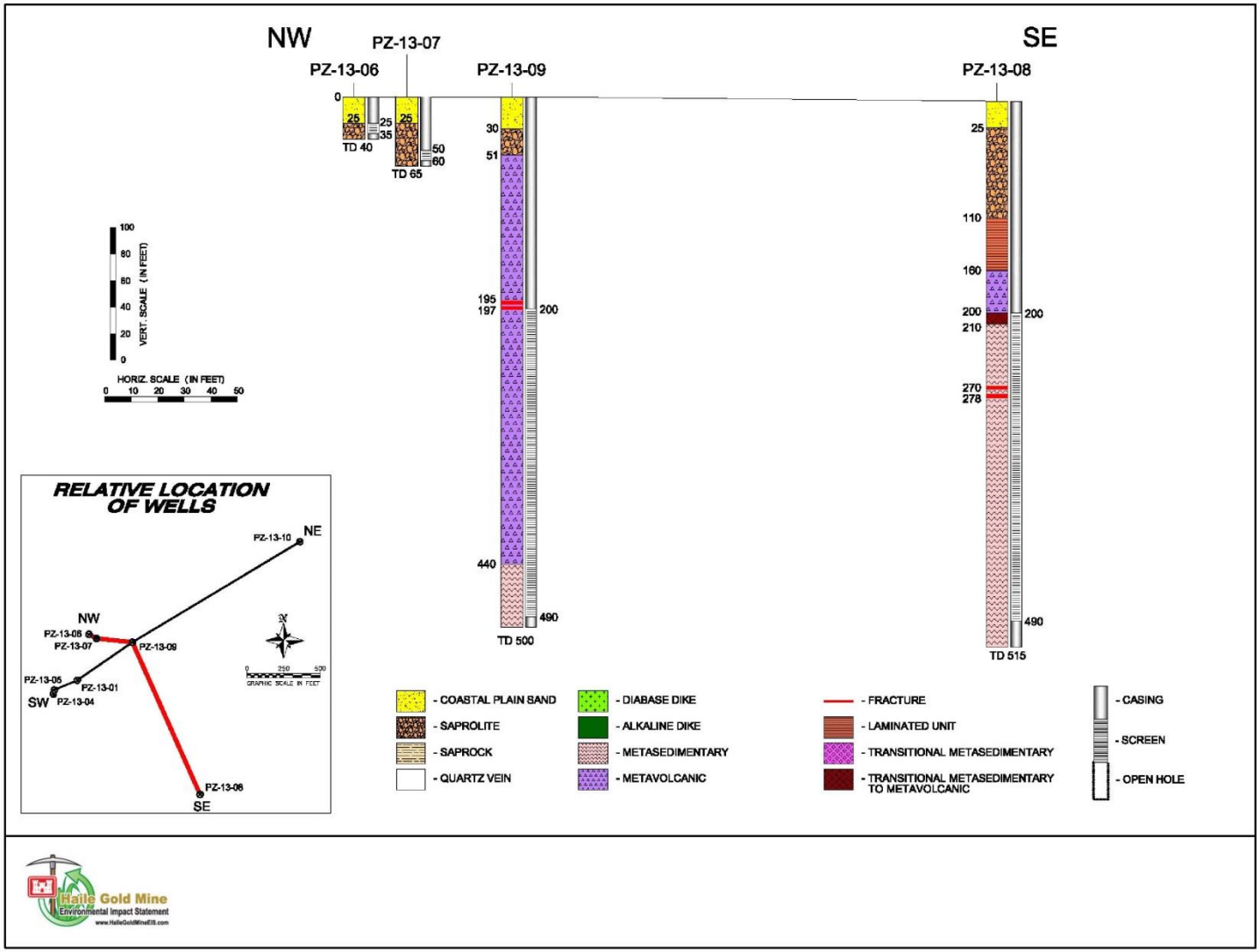

Figure 4-7 **Geologic Descriptions and Construction Details Compiled into a Graphical Representation along a Northwest-Southeast Cross Section**

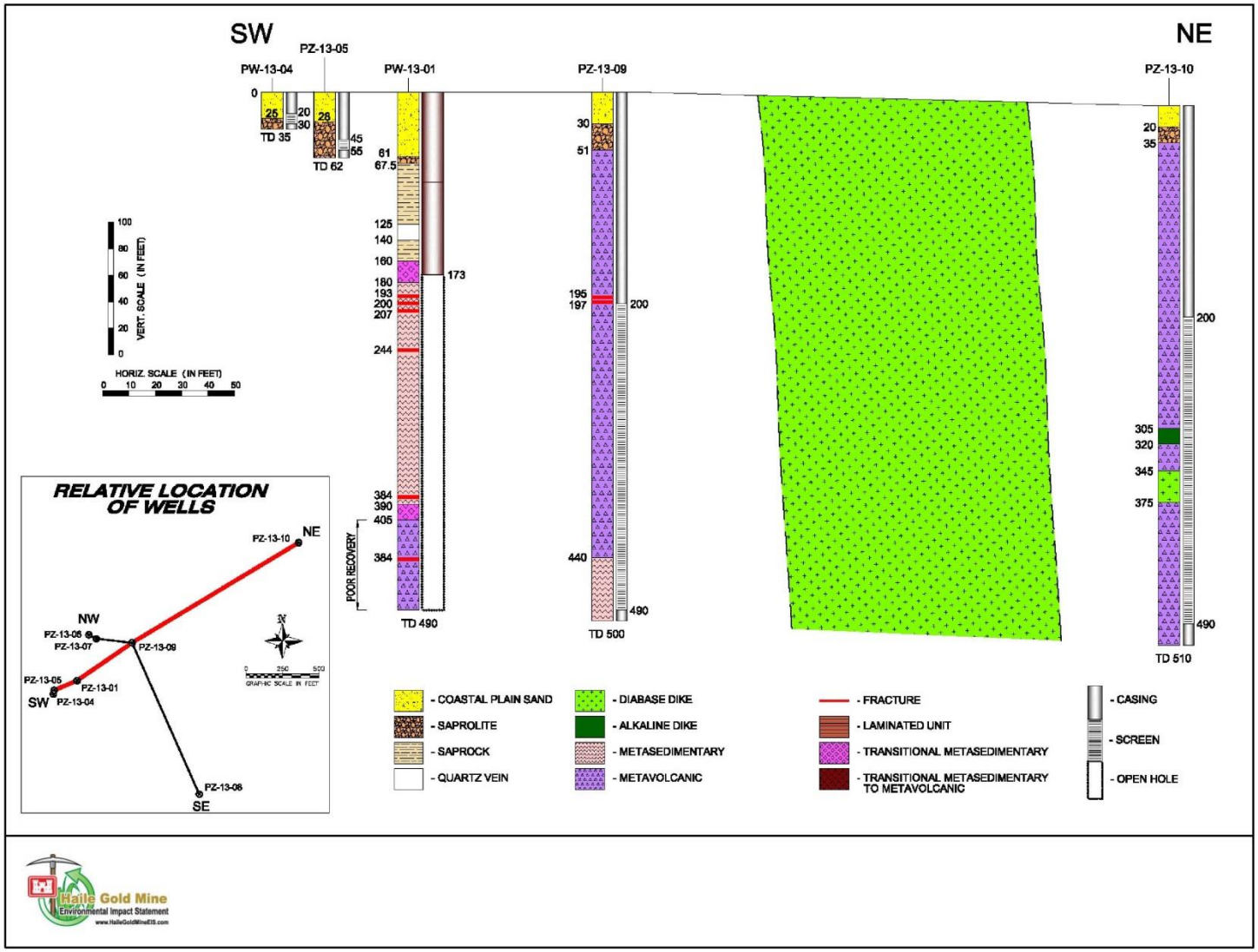

Figure 4-8 **Geologic Descriptions and Construction Details Compiled into a Graphical Representation along a Southwest-Northeast Cross Section**

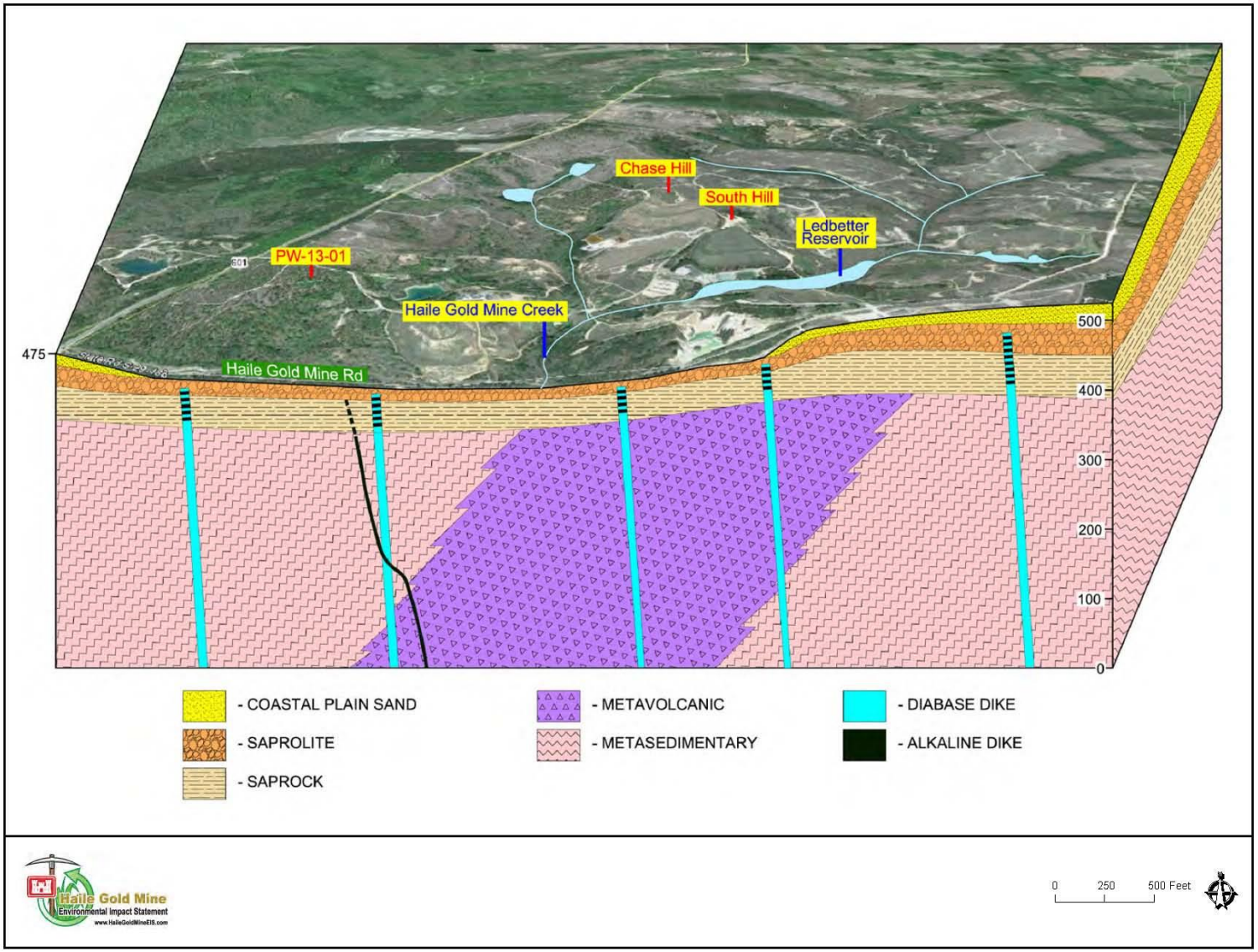

Figure 5-1 Cross-Sectional Representation of the Site Conceptual Model

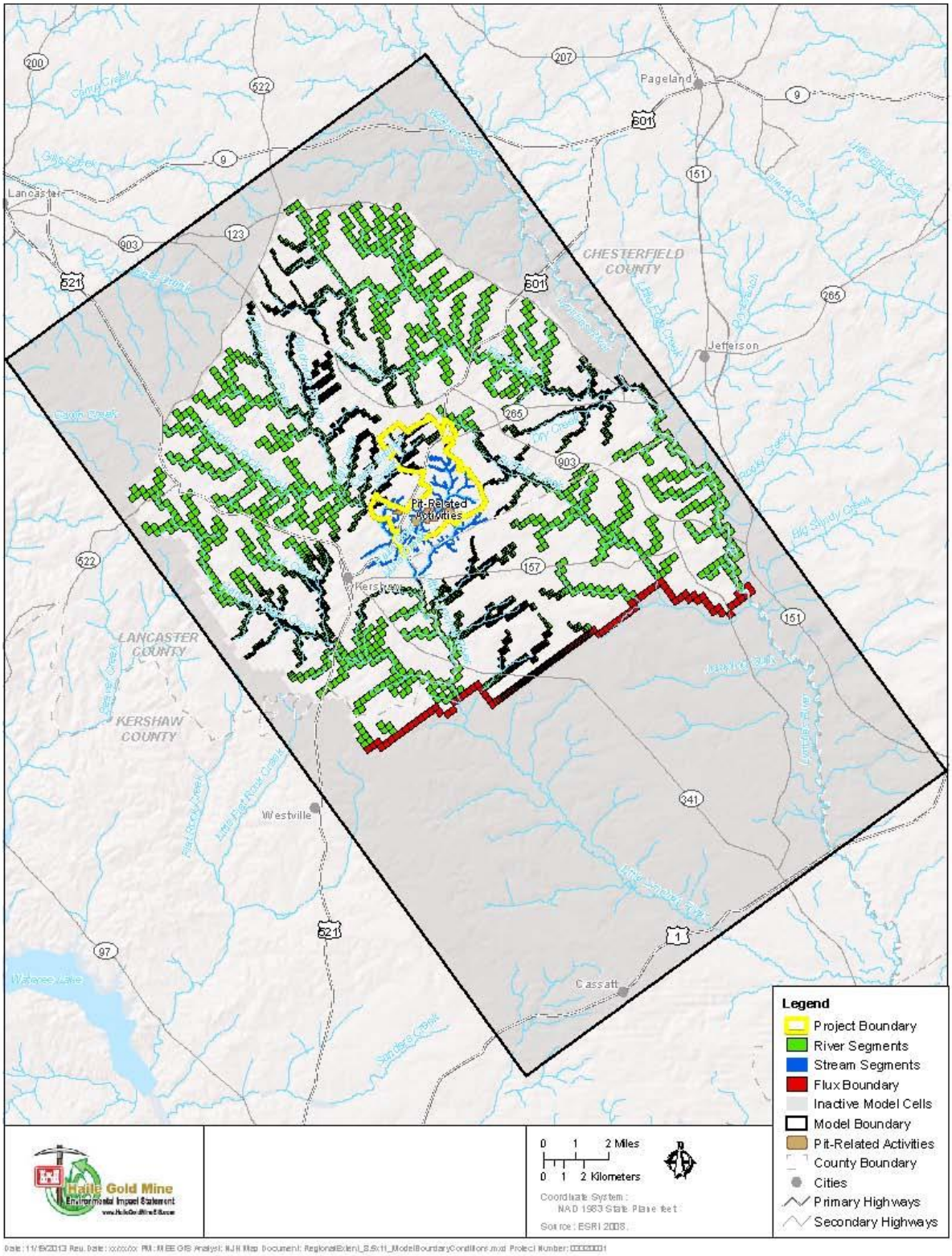

Figure 6-1 Domain and Boundary Conditions of the Cardno ENTRIX Model

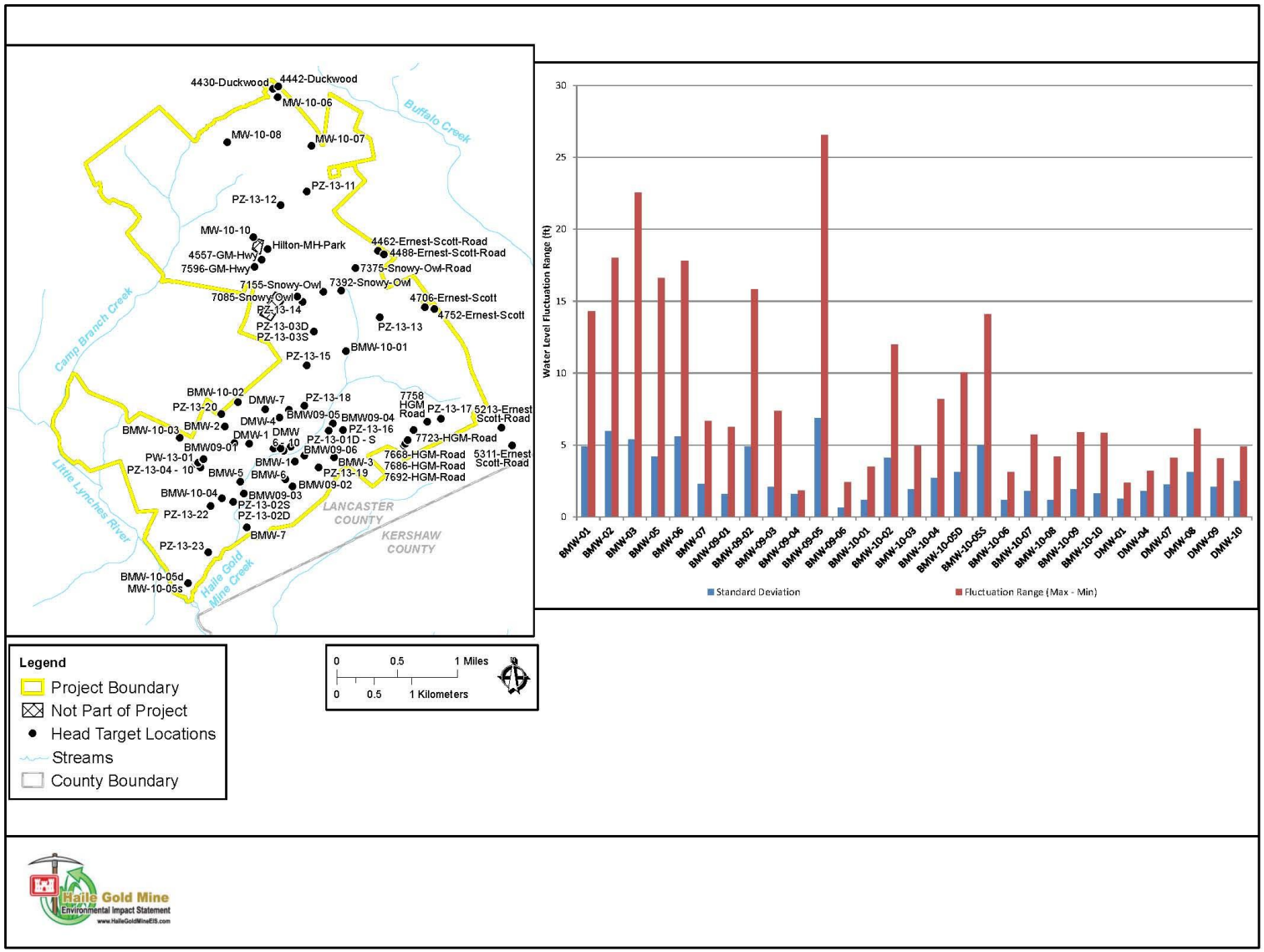

Figure 6-2 Observed Range in Heads of the Selected Target Wells

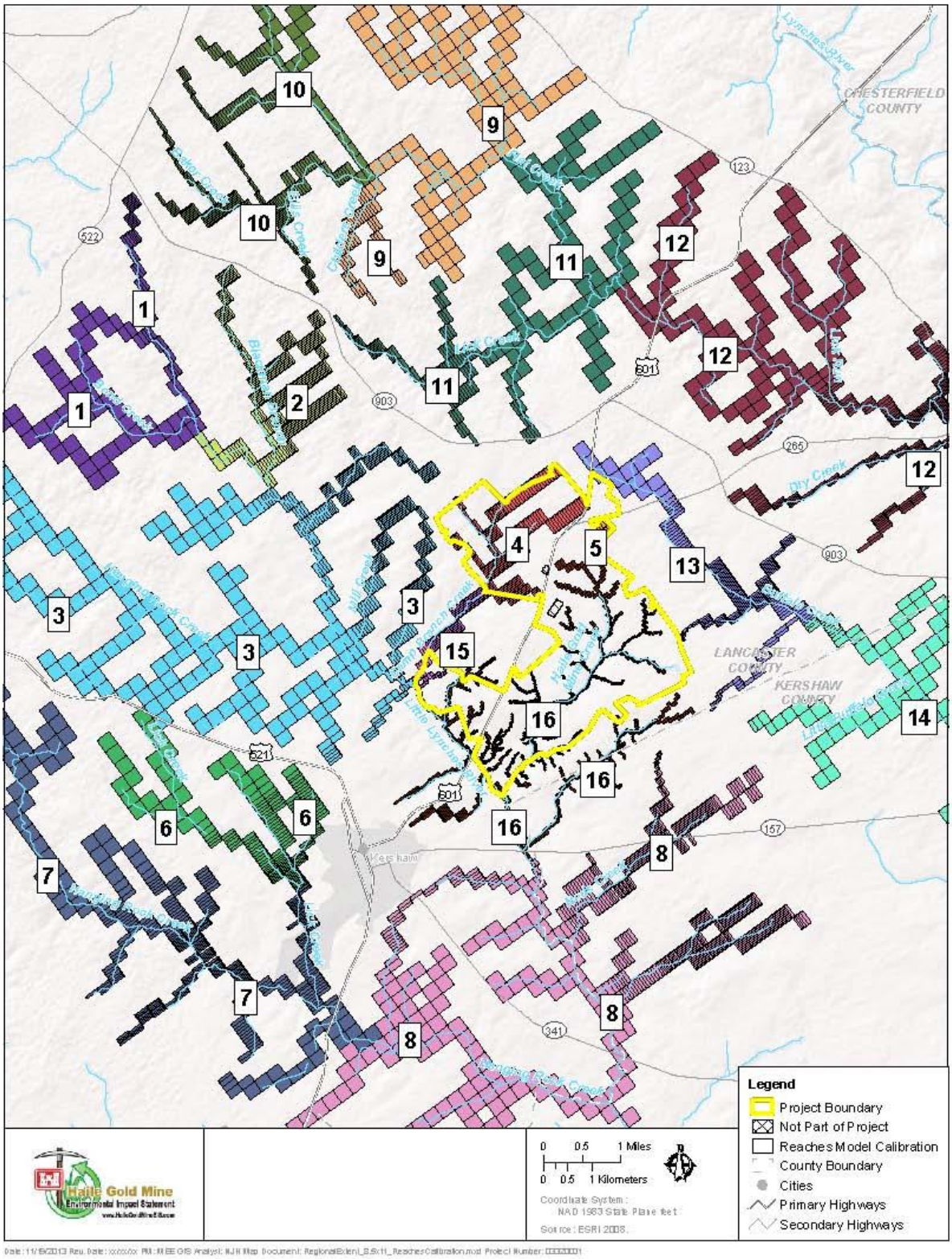

Figure 6-3 River and Stream Reach Designations Used in the Calibration Process for the Cardno ENTRIX Model

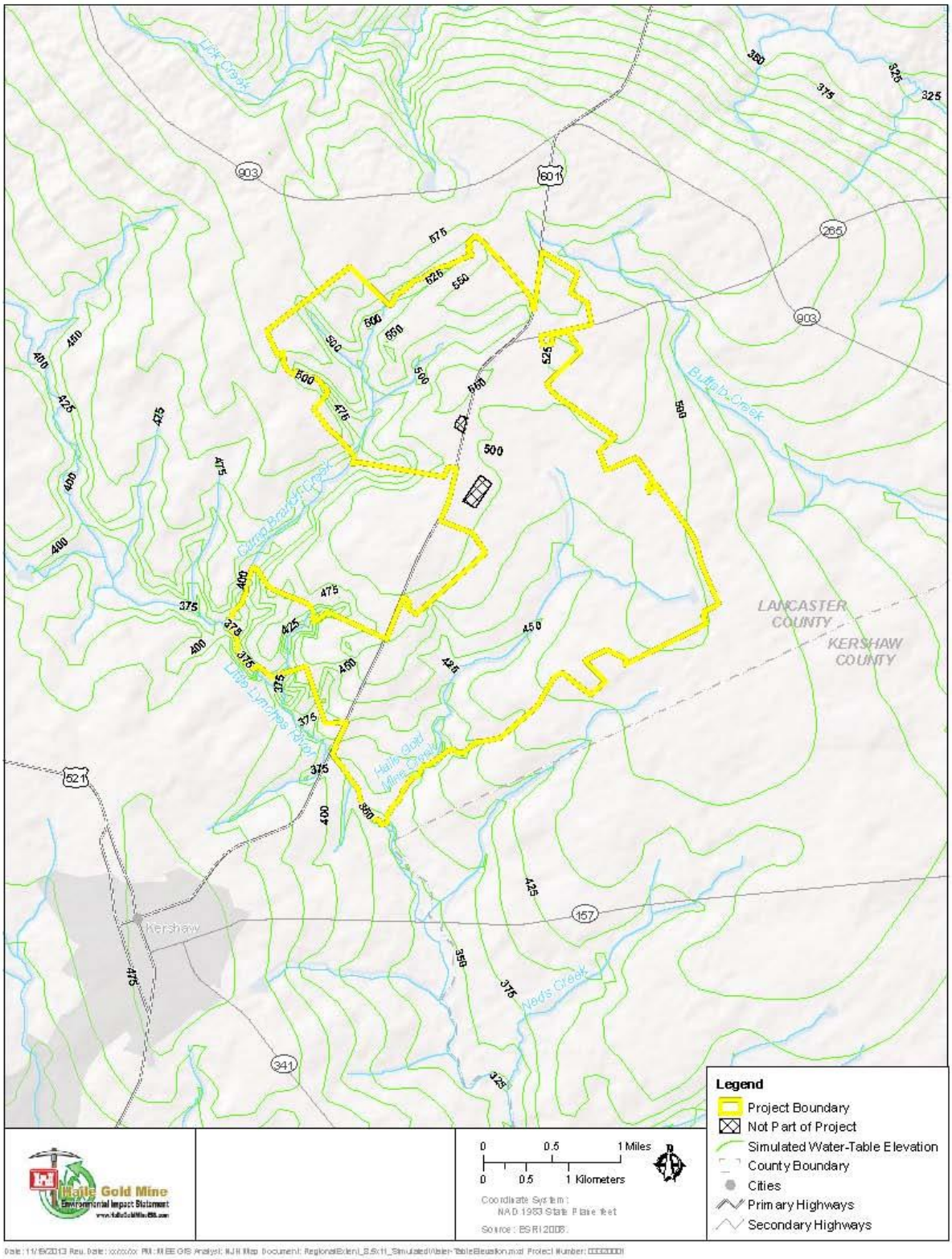

Figure 6-4 Water Table Elevation Simulated by the Cardno ENTRIX Model

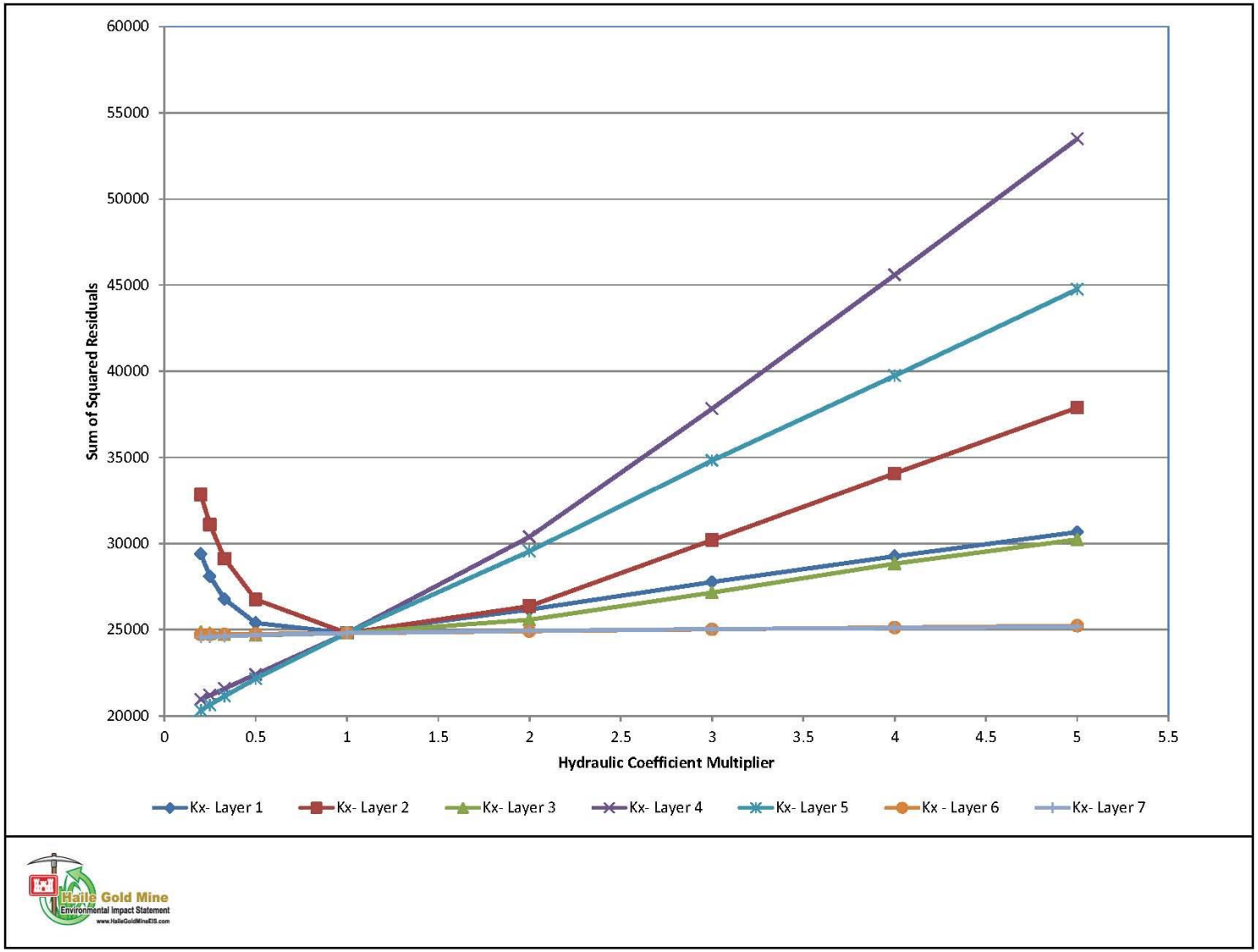

Figure 6-5 Sensitivity Analysis Results for Horizontal Hydraulic Conductivity (Kx)

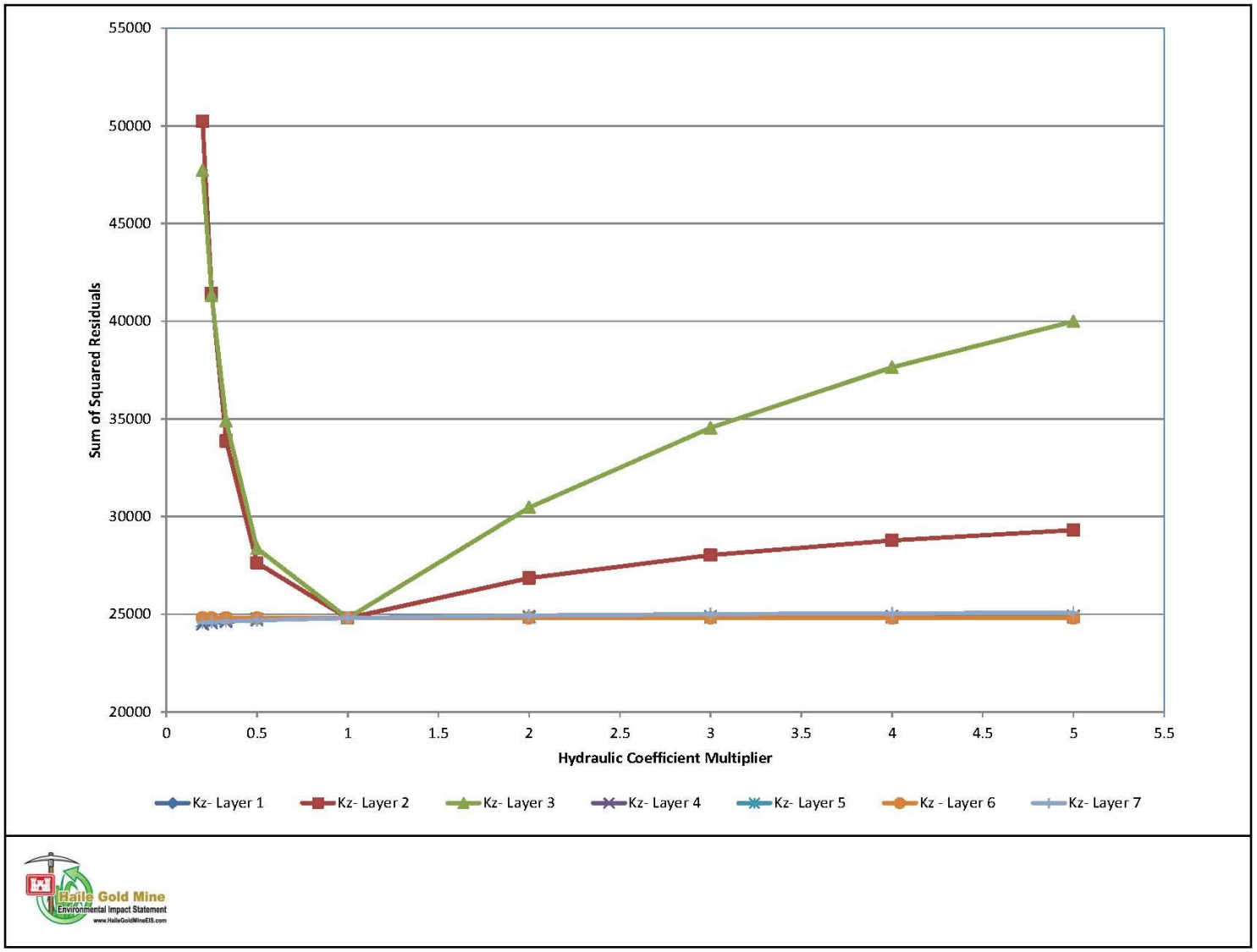

Figure 6-6 Sensitivity Analysis Results for Vertical Hydraulic Conductivity (Kz)

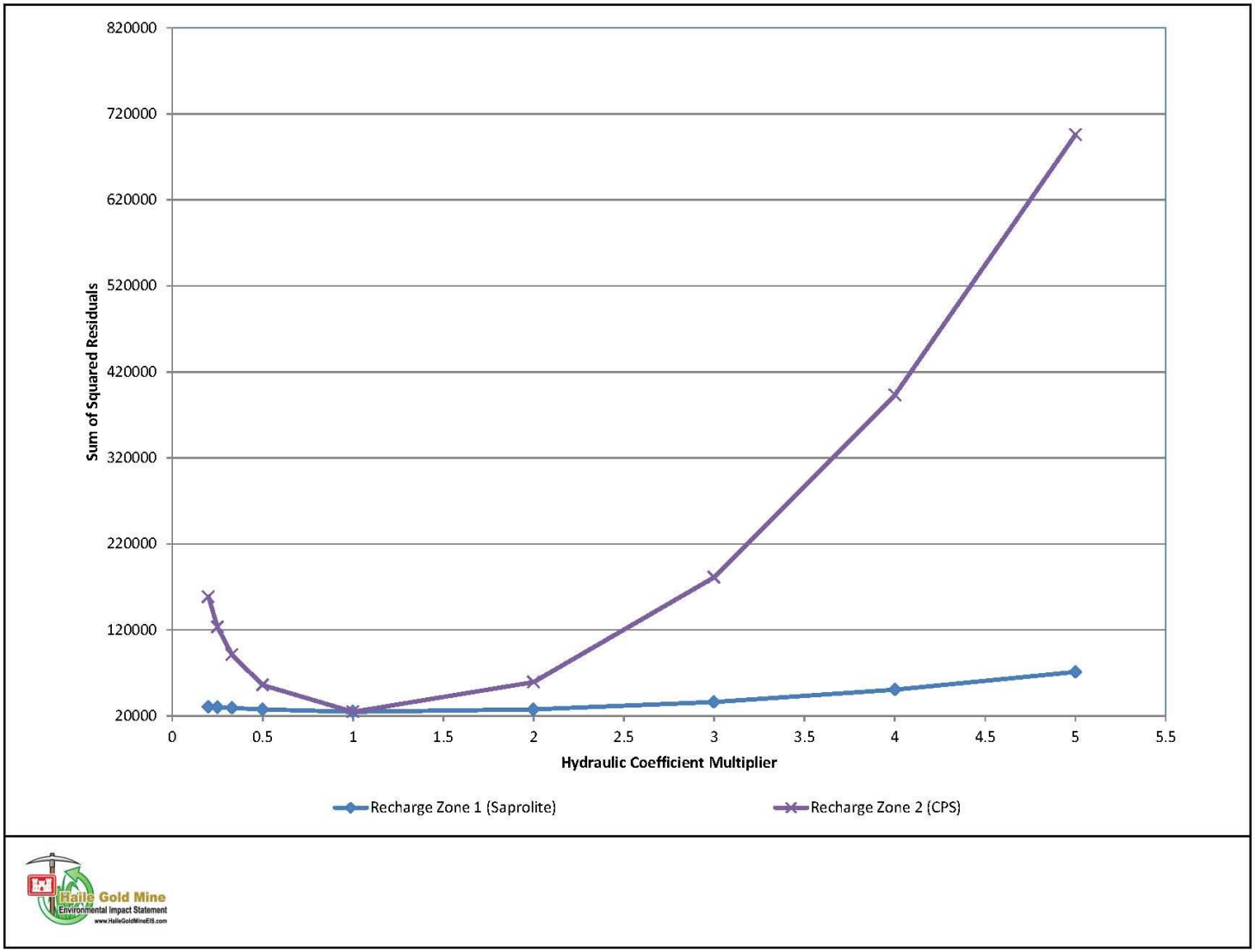

Figure 6-7 Sensitivity Analysis Results for Groundwater Recharge

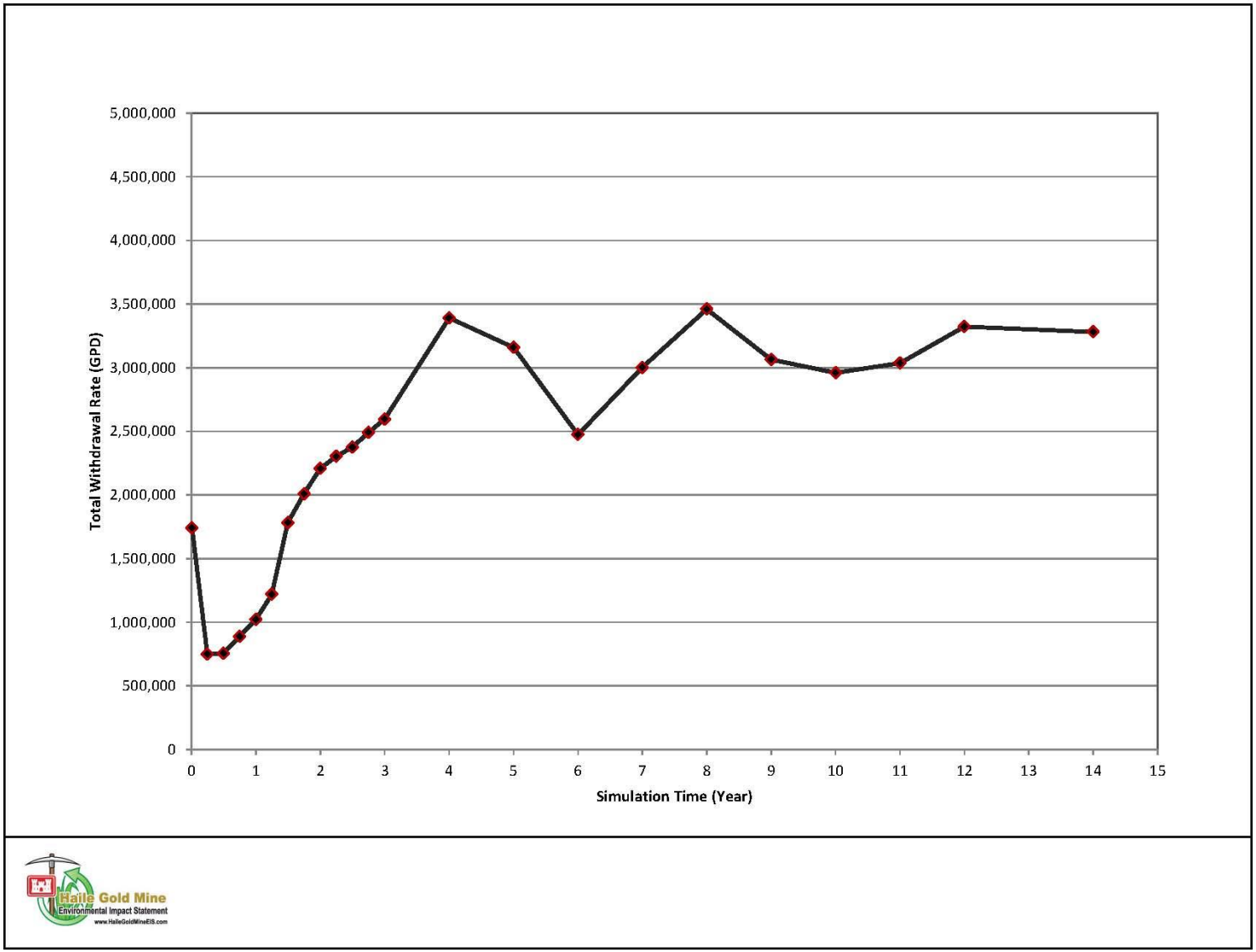

Figure 7-1 Simulated Cumulative Groundwater Withdrawal Rates from Mine Pits (Mine Years 0 through 12)

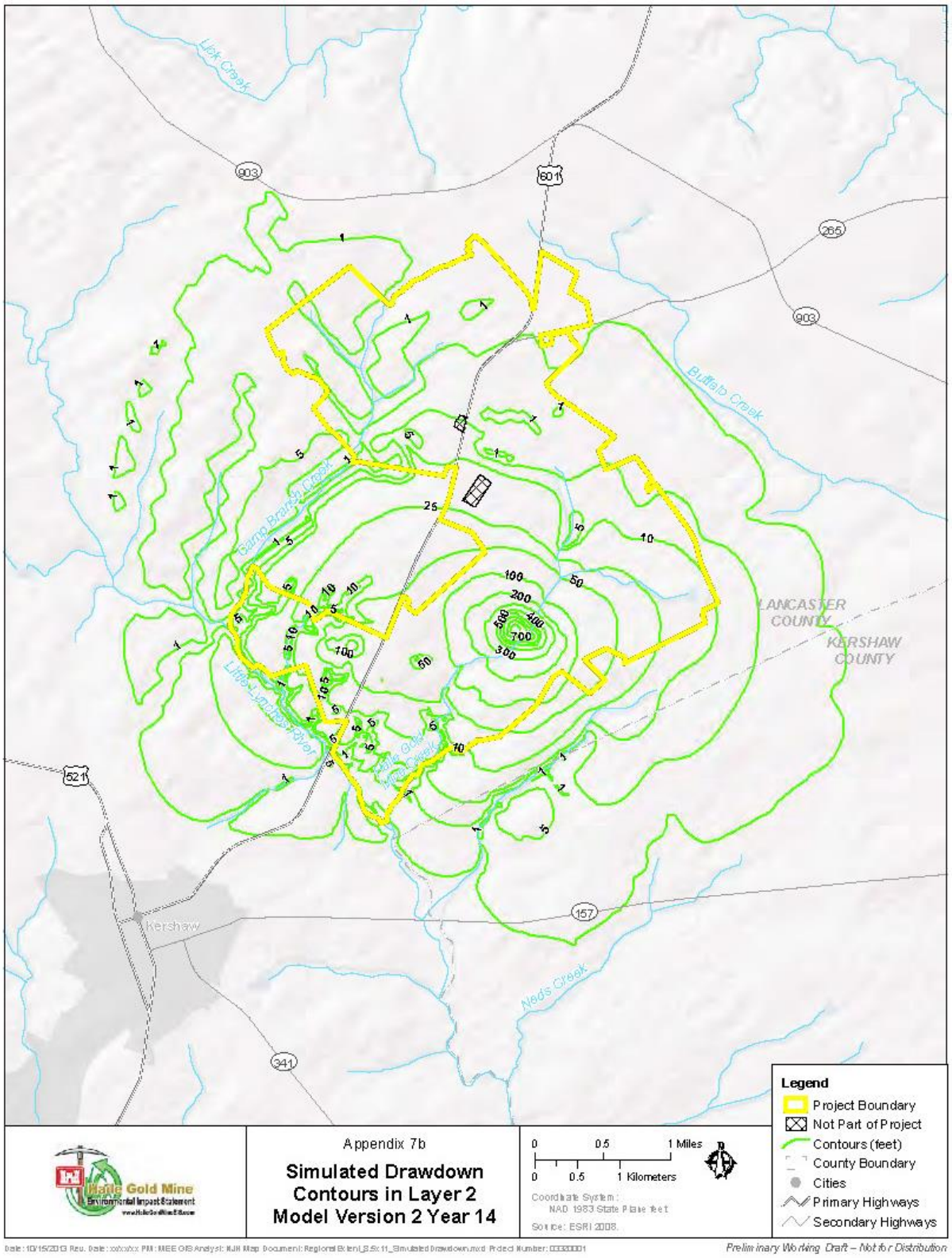

Figure 7-2 Maximum Simulated Drawdown in Layer 2 Model Version 2

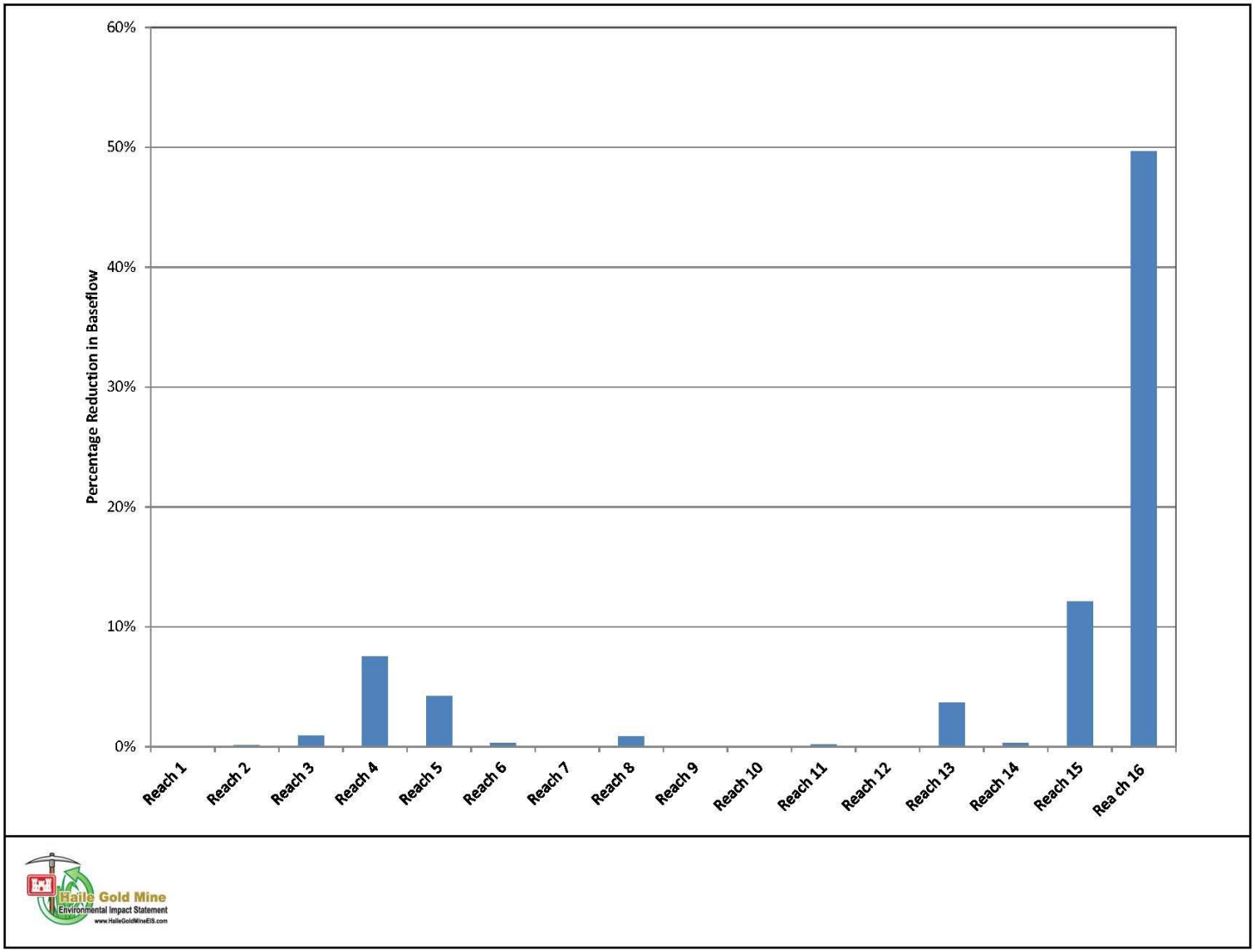

Figure 7-3 Simulated Reduction in Baseflow from Pre-Mining Conditions in Selected River and Stream Reaches